FUNMIG

Fundamental Processes of Radionuclide Migration in Salt Rock Far Field

A Natural Analogue Study

GRS - 255

Gesellschaft für Anlagen-
und Reaktorsicherheit
(GRS) mbH

FUNMIG

Fundamental Processes of Radionuclide Migration in Salt Rock Far Field

A Natural Analogue Study

Ulrich Noseck (ed.)

December 2009

Acknowledgement:

The underlying work of this report was supported by the Federal Ministry of Economics and Technology (BMWi) under the identification number 02 E 9995 titled „Grundlegende Prozesse zum Radionuklidtransport im Fernfeld eines Endlagers im Salz (Kurztitel FUNMIG-RTDC5)“.

The work was carried out under auspices of the Gesellschaft für Anlagen- und Reaktorsicherheit (GRS) mbH.

Resonsibility for the content of this publication lies solely with the authors.

GRS - 255
ISBN 978-3-939355-30-4

Keywords:
Geochemistry, Hydrogeology, Migration, Natural Analogue, Uranium

Table of contents

1 Introduction

The results presented in this report are mainly based on the work performed within the Research and Technology Development Component (RTDC) 5 “Processes and transport studies relevant for salt rock disposal concepts“ of the Integrated Project “Fundamental processes of radionuclide migration” (FUNMIG). This report firstly gives a brief overview on the whole integrated project FUNMIG and highlights some major results before describing in detail the work and results from RTDC 5.

The FUNMIG project in general dealt with all aspects of radionuclide migration from a deep geological radioactive waste repository to the biosphere and the application of the results to the safety case /BUC 10/. The project focussed on radionuclide migration processes in the far field of a nuclear waste repository. This included investigations on basic processes applicable to all types of host rock and disposal concepts as well as investigations on key issues for the three host-rock types clay, crystalline and salt presently investigated in Europe. In case of the salt-option the overburden of the salt formation itself is considered to represent the so-called far field. Hence migration processes in such sedimentary formations have been addressed.

Within the overall project, the spatial scales reached from nanometres to kilometres and the time-scales from short-term lab-investigations up to geological periods in natural systems. The project consisted of several Research and Technology Development Components and one additional component on training and knowledge transfer:

- RTDC 1: Well established processes.
- RTDC 2: Less established processes (ill defined).
- RTDC 3: Radionuclide migration in clay-rich host rock.
- RTDC 4: Processes and transport studies relevant for crystalline rock disposal concepts.
- RTDC 5: Processes and transport studies relevant for salt rock disposal concepts.
- RTDC 6: Integration of processes and abstraction to performance assessment.
- Component 7: Training, knowledge management and dissemination of knowledge.

The six RTDCs altogether covered basic processes common to all disposal concepts under consideration in Europe, through to studies of host-rock type specific processes and application of the results to the disposal safety case. RTDC 1 investigated the conceptually well established radionuclide migration processes with the aim to fill in critical data gaps while RTDC 2 was aimed at deepening the understanding of conceptually less understood fundamental processes driving radionuclide migration in the geosphere. The RTDCs 3 to 5 focussed on investigations of the far field of the three host-rock types clay granite and salt. RTDC 6 provides a forum for documenting the general aspects of the safety case developments integrating the outcome of the other RTDCs.

The integrated project FUNMIG consisted of more than 50 participating organisations and several associated groups. A various amount of results has been obtained and has been documented in many papers. In sections 2 and 3 the main overall results for the two host rock types clay (RTDC 3) and granite (RTDC 4) are briefly described. All details can be found in the final EUR report of FUNMIG /BUC 10/, the annual workshop proceedings /REI 06/, /BUC 07/, /BUC 09/, the results from the Euradwaste conference /DAV 09/ and various publications outside of FUNMIG reporting. Furthermore, a special issue of Applied Geochemistry is intended to be published in 2010.

In section 5 the results obtained in RTDC 5, where GRS acted as the RTDC leader, are described in more detail. All results of this RTDC have been documented in several publications, which are compiled in the annex of this report.

2 Clay host rock

RTDC 3 was lead by Scott Altmann (Andra). The work programme was construed to study the major phenomena expected to govern radionuclide migration in clay rock geological barrier systems /ALT 09/. Investigations have been carried out on anionic and cationic radionuclide diffusion and retention in compact clay rock over a wide range of space and time scales. Significant improvements in understanding of the distribution of total radionuclide mass between dissolved and sorbed species have been achieved. The results contributed to the consolidation of the conceptual models describing diffusion-driven transport of anionic radionuclides in clay rocks and produced credible strategies / methods for carrying out the up-scaling needed to obtain representative parameter values usable for performance assessment simulations of a clay rock geological barrier system, in particular taking into account the effects of spatial heterogeneity of rock physical-chemical properties.

One important question for the clay host rock was, if there is a sound theoretical basis for describing radionuclide speciation in the pores of highly compacted clay materials and clay rocks, in particular the distribution of total radionuclide mass between dissolved and sorbed species? The results obtained within FUNMIG showed similar equilibrium sorption states (K_d-values) in dispersed and compacted materials for moderately sorbing cations like Sr^{2+}, Cs^{+}, and Co^{2+} for all clay rocks investigated. This implies that the same sorption site populations are accessible in dispersed and compacted materials and that the corresponding mass action laws are valid. It was not possible to demonstrate this for highly sorbing radionuclides, e. g. actinides, because of extremely long times needed for appropriate experiments. Here, further research needs were identified.

3 Granite host rock

This RTDC was lead by Tiziana Missana (CIEMAT). With respect to granitic rocks the work comprised investigations of specific processes influencing radionuclide migration in crystalline rock formations, both at laboratory and in-situ scale /MIS 09/. Processes which are considered to be fundamental in performance assessment (e. g. fluid-flow system, matrix diffusion and sorption), were studied focusing on those aspects not yet completely understood, i. e. effects of heterogeneities, interaction mechanisms, transport model selection and up-scaling methodologies.

The studies on matrix diffusion were focused on the development of experimental and modelling methodology to account for the physical and mineralogical rock heterogeneity. Results obtained so far are promising to describe this mechanism more adequately. In a similar way, the quantification of sorption by determination of K_d in the intact rock, proposed in RTDC 4, provides more realistic data based on more in-depth knowledge of retention processes at the rock surface. The research on this issue should continue on these premises.

The studies allowed the development of up-scaling modelling methodologies. Additional studies focused on the combination of fluid and reactive transport in heterogeneous media. However, the application of these models to real conditions is still missing and needs further efforts.

A significant part of the RTDC 4 work was devoted to study the relevance of colloids originating from the compacted bentonite barrier on radionuclide migration in crystalline media. The main parameters affecting the generation and stability of colloids were identified; laboratory experiments provided data to update existing models on colloid generation and to quantify the “source term” more precisely.

Both strongly and slight sorbing elements showed, in the presence of colloids, a breakthrough peak related to colloid-driven transport. However, dynamic experiments demonstrated that bentonite colloid recovery decreases significantly as approaching the hydrodynamic conditions expected in a repository (i. e. very low water flow rates) even under conditions unfavourable to colloid attachment to rock surface. The retention of colloid on the rock surface was analysed and quantification studies were started, including the determination of bentonite colloids diffusion coefficients. Results obtained

so far, indicated that future experiments should be focused on the study of irreversibility of RN-colloids and rock-colloid interactions in dynamic conditions.

4 Application of the results to the safety case

Within the RTD Component 6, lead by Bernhard Schwyn (Nagra), the involved Waste Management Organisations (WMOs) and an Integration Monitoring Group coordinated the linking of the scientific work performed in the Components 1 to 5 to its use in performance assessment and monitored the improvements achieved within the project for the safety cases of the individual radioactive waste disposal programmes in Europe /SCH 09/. Boundary conditions for the near field of a radioactive waste repository, in particular radionuclide fluxes and concentrations but also repository induced perturbations of the geosphere, were defined based on the WMOs' safety cases and on the outcome of the European Project NF-PRO. A comprehensive catalogue providing concise information for each task performed in FUNMIG was compiled. It facilitates the retrieval of knowledge acquired within FUNMIG and was used to map these tasks to internationally accepted lists of Features, Events and Processes (FEPs) for clay-rich, crystalline and salt host rocks. The subsequent evaluation revealed issues important for future safety cases, namely the mechanistic understanding, quantification and up-scaling of radionuclide diffusion in clay-rich host rocks and, for crystalline host rocks, the influence of colloids on radionuclide transport and the up-scaling of reactive transport modelling in fractured systems. Finally, the scientific outcome of FUNMIG was synthesised for each of the three host rocks by collecting the individual tasks in "Super-FEPs". The transferability of knowledge between the host rocks is limited due to the host rock and site specificity of the research performed in FUNMIG.

5 RTDC5: Salt host rock – radionuclide migration in sedimentary formations

5.1 Introduction

In RTDC 5 lead by Ulrich Noseck (GRS) the far field of the host rock formation salt, i. e. the sedimentary layers in the overburden of a salt formation was subject of the investigations. In contrast to the two other host-rock specific components the investigations were focussed on a real system analyses at an analogue site. The study was performed at Ruprechtov Site in Czech Republic representing an analogue for potential migration processes in a similarly structured overburden of a salt dome but also of other geological formations, which are foreseen as potential host rocks for radioactive waste repositories.

Due to the uncertainties in the safety assessment within the very long geological time frame multiple lines of evidence, supporting the modelling results as well as the conclusions to be drawn, will be of increasing importance for a safety case. One category of supporting arguments can be derived from natural analogues. The main benefit of natural analogues in a safety case is to increase understanding of long-term processes in geological environment and scale. In this context the investigations at Ruprechtov have been performed.

The speciation of uranium is of high relevance for the safety case, since uranium is the major constituent of spent nuclear fuel. The migration behaviour of uranium released from a spent fuel repository can be very complex. Retardation and sorption parameters are strongly affected under varying geochemical conditions, i. e. sorption and precipitation processes strongly depend on the groundwater properties such as pH, Eh, pCO_2, complexing agents as carbonates and natural organic matter, which determine the chemical speciation and hence the equilibrium distribution of uranium. Particularly, the redox state of uranium is of high relevance, since U(IV) mineral phases are sparingly soluble in contrast to U(VI) phases. Moreover, U(VI) forms negative species in many geochemical environments compared to the dominating neutral tetravalent $U(OH)_4$ species, resulting in quite different sorption behaviour.

Uranium speciation and interaction with various mineral phases have been analysed in numerous studies. Further, there is knowledge available from several natural analogue

studies (e. g. /IWA 04/, /MIL 00/ and references therein) or investigations at potential repository sites indicating mobility and / or immobility of uranium. For example radiochemical studies on Boom Clay indicated that in general the Boom Clay is in state of secular equilibrium and no significant mobility of uranium has been effective during the last million years /CRA 04/. Otherwise, at Forsmark Site, quite high concentrations of uranium have been found in several groundwater samples in the depth of 200 - 650 m /LAA 06/. These findings are of interest for the siting and safety assessment programme as they indicate that uranium might be mobile in groundwaters at the Forsmark Site. Its impact on the site understanding need to be further investigated.

5.2 Approach and objectives of the work within FUNMIG

The Ruprechtov Site was selected, since the uranium deposit is shallow (close to the surface), and sedimentary layers, typical for the overburden of host rocks, with clay minerals, high organic content and partly sandy water bearing horizons exist at the site. Beside this a large data set had been already available before the FUNMIG work. The Ruprechtov Site, located in the north-western part of the Czech Republic, is geologically situated in a Tertiary basin filled with argillised pyroclastic sediments /NOS 04/. The geological situation of the investigation area is characterised by the occurrence of a granitic body, which partly crops out in the west and in the south and is widely kaolinised in varying thicknesses (up to several tens of metres) on its top in the central part. The horizon of major interest is the so-called clay/lignite layer, a layer of 1 - 3 m thickness at the interface of kaolin and overlaying plastic clay sediments in 20 to 50 m depth, with high content of SOC and areas of uranium enrichment.

Within the FUNMIG project specific questions have been addressed, to receive an in-depth understanding of the evolution of the natural system and the key processes involved in uranium mobilisation and immobilisation as well as the behaviour of organic matter. Emphasis was put into characterisation of the immobile uranium phases, their long-term stability, uranium speciation and the factors controlling mobility of uranium in the system. The second major issue comprised the behaviour of colloids and organic matter in the system, particularly focused on better understanding the interrelation between sedimentary organic carbon (SOC) and dissolved organic carbon (DOC), its impact on the mobility of uranium and generally the role of microbes involved in these processes. As described above the investigations represent a natural analogue study,

where specific questions are addressed, reflected by the following topics. The methodology for each topic is briefly described.

5.2.1 Characterisation of the uranium speciation

Different microscopic and macroscopic methods have been applied to selected samples to characterise the immobile uranium phases. These methods comprise µ-XRF and µ-XAFS spectroscopy, ASEM and electron microprobe, sequential extraction, U(IV)/U(VI) separation with $^{234}U/^{238}U$ ratio determination. Detailed information about the methods can be found in /NOS 08/. In addition, sorption experiments have been performed and exchangeable uranium determined by isotope exchange with ^{233}U, e. g. /HAV 06/, /VOP 08/. µ-XRD and µ-XAFS were applied the first time to natural samples and the method was further developed within the FUNMIG project. In addition several measurements of U(IV)/U(VI) speciation in the groundwater and accompanying geochemical calculations have been performed.

5.2.2 Characterisation of colloids and organic matter

Colloids: A borehole groundwater sampling system and a mobile laser-induced breakdown detection equipment (LIBD) for colloid detection, combined with a geo-monitoring unit has been further developed and applied to characterise the natural background colloid concentration in groundwaters of the Ruprechtov natural analogue site. To minimise artefacts during groundwater sampling the contact to atmospheric oxygen has been excluded by use of steel sampling cylinders to be opened and closed below groundwater level by remote control. The groundwater samples collected in this way have been transported to the laboratory where they were eluted from the cylinders under original hydrostatic pressure without contact to oxygen. Behind the LIBD detection cell the system consists of in-series connected detection cells for pH, Eh, electrical conductivity, and oxygen content. More details can be found in /HAU 07/.

Organic matter: Additional work was carried out on characterisation of DOC and SOC. Generally, humic substances as potential complexing agents that can be released into groundwater due to organic matter degradation were extracted and additionally characterised using elementary analysis, ash and moisture content, UV-Vis spectroscopy, FTIR spectroscopy, acidobasic titrations and MALDI-TOF. Humic acid complexation reaction with U(VI) as a potential interaction in groundwater was then studied /CER 08/.

Moreover, DOC in groundwater was characterised by MALDI-TOF spectroscopy. Details can be found in /CER 07/. This work comprised also analyses of specific environmental isotopes, in particular $\delta^{34}S$ in dissolved sulphates as well as $\delta^{13}C$ and ^{14}C in DIC and DOC. Inverse geochemical modelling using Netpath was performed to understand the changes in the isotope signatures and therewith contribute to the understanding of the carbon chemistry, in particular to identify microbial degradation of organic matter.

5.3 Results

5.3.1 Uranium in the sedimentary system

The application of macroscopic and microscopic methods mentioned above provided detailed insight into the U enrichment processes at the Ruprechtov Site /NOS 08/. The major results achieved are

- identification of uranium immobilisation reactions in the clay/lignite horizon,
- identification of primary and secondary U-bearing mineral phases in the clay/lignite horizon,
- identification of the long-term stability of these uranium (IV) mineral phases like UO_2 and ningyoite, and
- evaluation of the role of sorption reactions.

Detailed X-ray spectroscopic investigations with a micro-focussed beam identified U as a tetravalent phosphate or sulphate mineral phase, in good agreement with ASEM and electron-microprobe results. The high resolution made it possible for the first time to discern an As-rich boundary layer (arsenopyrite) surrounding a framboidal pyrite nodule. Furthermore, the spatial distribution of elements and element correlations, i. e. Fe with As(0) and U with As(V), have revealed one important immobilisation mechanism of U(VI) by reduction to U(IV) on these arsenopyrite layers /DEN 05/, /DEN 07/.

The results from the microscopic methods are supported by wet chemical U(IV)/U(VI) separation as well as by sequential extraction, which also indicate that U occurs in the tetravalent state. Sequential extraction identified major part of uranium in the respective steps for (reduced) U(IV) forms and the residual fraction /HAV 06/, /NOS 08/. By cluster analysis of sequential extraction results, performed to identify possible correlations be-

tween elements, a strong correlation of U with As and P was found, supporting the mechanism postulated above and the existence of uranium phosphate mineral ningyoite identified by SEM-EDX.

U-series analyses were used to obtain information of U mobility. The activities of ^{238}U, ^{234}U and ^{230}Th were analysed in the bulk samples from several boreholes from the U-enriched clay/lignite horizon. Furthermore, $^{234}U/^{238}U$ activity ratios (AR) were determined in the three phases U(IV), U(VI) and U(res) separated by the wet chemical method.

For the bulk analysis nearly all data indicated stable conditions with respect to bulk uranium /NOS 08/. This observation as well as the result that nearly all samples U(res) and U(IV) exhibit in nearly all samples an AR below one is a strong indicator for the long-term chemical stability of these U phases. In order to attain low AR values of app. 0.2 in the U(IV) and U(res) phase no significant release of bulk uranium must have occurred during a time period of several half-lives of ^{234}U, i. e. for at least one million years /NOS 08/. This is in good agreement with the hypothesis that the major uranium input into the clay/lignite horizon occurred during Tertiary, more than 10 My ago /NOS 06/. It further can be derivated that because several data points are found the bulk uranium addition area some uranium accumulation may be still in progress. This result is supported by the AR of the U(VI) fraction, which varies from 1.2 to 3.4 and in general reflects the AR observed in groundwater showing that at least part of it has recently formed. However, it is not fully clear, whether all U in this fraction is originally U(VI). There are indications that some oxidation of U(IV) occurs during sample storage /SUK 07/.

The thermodynamic evaluation of the aqueous speciation and solubility behaviour of uranium in the reducing clay/lignite horizon at Ruprechtov Site indicates that the uranium concentrations are controlled mainly by amorphous UO_2. Saturation indices of crystalline uraninite and coffinite as well as mixed oxides are greatly exceeded /NOS 09b/. Moreover, the U(IV) phosphate mineral ningyoite almost reaches saturation. These results underpin the experimental results that both minerals UO_2 and ningyoite have been observed in the clay/lignite horizon (see above). They are also in good agreement with results from other analogue studies, where similar geochemical conditions are met, and amorphous uraninite was identified as U-controlling mineral phase, e. g. at Tono Site /IWA 04/.

All results from thermodynamic calculations also indicate that U(IV) is the predominant redox state in the clay/lignite layers at Ruprechtov Site /NOS 09b/. However, due to the high CO_2 partial pressure in the system carbonato complexes can stabilise hexavalent uranium in solution, which might explain that uranium redox state analyses performed in one borehole showed only 20 % U(IV) in the groundwater.

However, although part of dissolved uranium exists in the U(VI) state, the uranium concentrations in solution are quite low with values below 1 µg/l in most boreholes in spite of high U contents of up to 600 ppm in the corresponding sediments. They are an additional indication for the high stability of the immobile uranium phases in the clay/lignite horizon.

5.3.2 Colloids in the natural system

As discussed above part of the work was dedicated to method-development and qualification. During the project a new mobile geomonitoring system including a system for the laser-induced breakdown detection of colloids (LIBD) was developed /HAU 07/. It was successfully applied to the detection of colloids in natural groundwater samples from Ruprechtov Site and other sites in Sweden.

It could be shown that colloid concentrations down to µg/l can be detected with the special sampling technique. By comparison with in-situ probe measurements in several boreholes it was also demonstrated that reducing conditions with minimal access of atmosphere oxygen are maintained. In-situ experiments in granite demonstrated that colloid generating processes like redox changes (e. g. in the EDZ) and/or mechanical erosion can increase the natural colloid background by up to several orders of magnitude.

The natural background colloid concentrations LIBD determined at Ruprechtov were compared with data of studies performed in Äspö (Sweden) and Grimsel (Switzerland). A comprehensive representation of colloid concentrations in different water samples as determined by LIBD as a function of the respective ionic strength is given in /HAU 07/. Increasing ionic strength usually forces colloid aggregation which is reflected in lower colloid concentration in the respective groundwater.

In the Ruprechtov groundwater samples the ionic strength varies in the range of $2 \cdot 10^{-3}$ to $1.1 \cdot 10^{-2}$ mol/l without any significant influence on the measured colloid concentration.

The broad bandwidth of detected colloid concentrations in groundwater of ionic strength <100 mmol/l (Grimsel, Ruprechtov) suggests that different parameters besides ionic strength as e. g. pH and/or groundwater velocity may control the actual colloid concentrations. However, the studies suggest that an ionic strength of 100 mmol/l represents some kind of upper limit: colloids may persist in groundwater with ionic strengths below this value for considerable time scales and variable colloid concentrations. At ionic strengths above 100 mmol/l natural aquatic colloid stability is effectively decreasing. As a consequence, for groundwater samples from Äspö and simulated NaCl solutions a clear dependency of the maximum colloid concentrations with the salinity of the solution is found.

5.3.3 Carbon chemistry and role of organic matter in the sedimentary system

One part of the work comprised the re-evaluation of existing, and the evaluation of new hydrological, geochemical and environmental isotope data from groundwater wells at Ruprechtov Site to characterise the hydrogeological flow regime and the carbon chemistry in the system. The existing idea about the flow system in the tertiary sediments was confirmed and the complexity of the system was demonstrated /NOS 09a/. Differences in stable isotope signatures in the northern part of the site indicate very local connections of the flow system in the underlying granite with that in the tertiary sediments via fault zones.

In order to understand the carbon chemistry and the interrelation between SOC and DOC isotopes of carbon in DIC, DOC and SOC were evaluated. This work is described in detail in /NOS 09a/. The observed increase of $\delta^{13}C$ values and decrease of ^{14}C activities in dissolved inorganic C during evolution of the groundwater from the infiltration area to the clay/lignite horizon was modelled using simple open- and closed-system models as well as an inverse geochemical model, which included changes in other geochemical parameters. The general result is that additional CO_2 input from microbial degradation of dissolved and sedimentary organic C (DOC and SOC) into the system is evident and can explain the development of $\delta^{13}C$ and ^{14}C isotopes in DIC in the clay/lignite horizon. There is also some indication for input of endogenous CO_2, which is known from other locations in the Eger Rift nearby. The occurrence of microbial degradation of SOC in the clay/lignite layers is underpinned by the increase of biogenic DIC, DOC, and phosphate concentrations. The impact of microbial SO_4^{2-} reduction on

this process is confirmed by an increase of $\delta^{34}S$ values in dissolved SO_4^{2-} from the infiltration area to the clay/lignite horizon with an enrichment factor of 11 ‰.

The very low DOC concentrations of 1 to 5 mg C/l in the clay/lignite horizon (compared to other sites with SOC-bearing sediments /BUC 00/) with an organic matter content up to 50 % C is probably caused by very low availability of organic matter to the processes of degradation and DOC release, demonstrated by extraction experiments with SOC.

The integration of all results showed that organic matter did not play such an important role by direct interaction with uranium, but SOC contributed and still contributes to maintain reducing conditions in the clay/lignite layers. This result is supported by the finding that the highest accumulations of uranium are located slightly below the parts, which are highly enriched in organic matter. It can be concluded that SOC within the sedimentary layers was (and to some extent still is) microbially degraded. By this process DOC is released, providing protons to additionally dissolve SIC. Moreover SO_4^{2-} is reduced leading (and has lead in the geological past) to the formation of iron sulphides, especially pyrite. Reducing conditions, being maintained amongst others by sulphate reducing bacteria, caused the reduction of As, which sorbed onto pyrite surfaces, forming thin layers of arsenopyrite. Uranium U(VI), originally being released from the outcropping/underlying granite, was reduced to U(IV) on arsenopyrite surfaces. UO_2 and uranium phosphates were formed by reaction of U(IV) with phosphates PO_4^{3-}, released by microbial SOC degradation. These U(IV) minerals have been stable and immobile over geological time frames.

5.4 Conclusions and outlook for the Ruprechtov analogue

This natural analogue study contributed to the safety case regarding the far-field transport of radionuclides in sedimentary layers in different ways. A very important part was the aspect of method development and testing, e. g. colloid sampling under undisturbed conditions with detection limit in the µ-molar range, and further development of µ-XRF and µ-XANES with first application to natural samples as well as application of modern isotope analyses like $\delta^{34}S$ signatures to identify relevant processes in the field. All these methods are important for characterisation of a potential repository site including lab and field experiments.

The Ruprechtov natural analogue study serves as an example of a strong long-term barrier function of a sedimentary layer. The system provides evidence that uranium is

and was effectively immobilised in a sedimentary layer of a formation, which was exposed to surface erosion in the geological past. All results indicate that uranium was efficiently immobilised in a reducing environment (controlled by the SO_4^{2-}/S^{2-} couple) over millions of years and no significant release of immobilised uranium occurred within that time. Although part of dissolved uranium exists in the U(VI) state, probably stabilised by carbonate complexes, the uranium concentrations in solution are kept quite low with values typically below 1 µg/l in the uranium-enriched horizon. The key processes involved in uranium immobilisation were identified. The observation of a strong impact of microbial processes contributing directly and indirectly to the uranium immobilisation is one further important result from the Ruprechtov study.

The importance of an appropriate handling of the redox-sensitive samples became evident. The samples have to be carefully stored under inert argon atmosphere directly after drilling. However, in some of the samples, an alteration after long storage times, partly even under argon atmosphere, could be observed, which might have affected the U(IV)/U(VI) ratio in the sediment sample concerned. Another challenge was the determination of Eh-values under low flow conditions at the site. The projected kaolin mining at Ruprechtov Site might provide the opportunity to investigate the effect of disturbed geochemical conditions in the clay/lignite horizon and its impact on the uranium behaviour. These issues will be tackled in a specific follow-on investigation.

6 FUNMIG - Outlook

The IP FUNMIG contributed to a deeper understanding in several fields of radionuclide migration. It also contributed to increase the exchange between research groups and performance assessment, particularly by the integration work organised in RTDC6. In a final panel discussion at the Euradwaste conference issues for further R&D work on far-field processes have been raised.

Since several programmes are approaching the implementation of repositories within a decade, the main work here will be in the fields of site characterisation and monitoring of the far field. However, scientific investigations will continue and accompany the implementation process. The goal of such investigations is to enhance the understanding of far-field processes and to help to reduce uncertainties, contribute on optimisation, and eventually help reducing costs. During the panel discussion several possible issues for future research have been raised, like:

- Sorption on crystalline rock and, although less important, on overburden of salt formations: By moving to a more advanced stage of the disposal programme the justification of the safety case becomes more important. Such a justified case needs to build up on the demonstration of an acceptable level of process understanding in order to ensure that the data used are void of unacceptable experimental artefacts. It need to be shown that they represent the assumed system, and can be used for reliable predictions for up-scaling with respect to time and space. The latter is especially important because in the safety case the system evolution has to be considered, where geochemical conditions might change. In order to determine the impact of these changes on the radionuclide retention behaviour the underlying sorption processes need to be known.
- In-depth interpretation of existing data, above all from FUNMIG: It was discussed that it might be valuable to evaluate the outcome of the four IP's ESDRED, NF-PRO, FUNMIG and PAMINA in an integrated way. On the basis of an overview of the advances in the state of knowledge for European national programmes at their different levels of development, further open issues can be identified and prioritised, and conclusions and recommendations for future Euratom disposal programme can be given, which can be fed into the disposal technology platform, presently under development.

- Geochemical in-situ experiments, micro analytics: In several performance assessment studies, geochemical effects, particularly the speciation of radionuclides play a central role. Since the migration modelling of radionuclides in the near field and far-field rely on thermodynamic databases, which are based on compilations and mainly laboratory experiments, a verification of the radionuclide speciation through in situ measurements would contribute to increase confidence in the performance assessment of nuclear waste disposal. Taking advantage of existing underground laboratory facilities and the progress in analytical chemistry, it is a real challenge to be able to compare measurements and predictions.

- Retardation processes for mobile radionuclides, mineral reactions influencing radionuclide migration and isotopic dilution and exchange: Recent safety cases for disposal concepts in clay rock formations showed that the principal radionuclides migrating through the geological barrier are ^{129}I, ^{36}Cl, ^{79}Se, ^{14}C ^{99}Tc. In all cases this is a result of neglecting sorption for them, i. e. attributing them retardation values of 1. However, these radionuclides might be slightly (but potentially significantly) retarded by mechanisms like Se immobilization by ferrous iron sorbed on clay, or Se(II) sorption onto pyrite, or isotopic dilution processes especially for ^{14}C, ^{36}Cl and ^{129}I. Theoretical studies, together with laboratory studies and field studies are necessary to document such processes. While safety assessment results from existing safety cases for different radioactive waste disposal concepts show, remain well within the required safety limits, additional safety margins, and increased confidence in the safety demonstration would be gained in case research would be able to show the capacity of such processes to retard migration of these radionuclides.

For all these issues it was also stated that the host-rock specifity has to be taken into account for potential projects and might restrict the co-operation to some extent.

7 References

/ALT 09/ Altmann, S.; Tournassat, C.; Goutelard, F.; Parneix, J.C.; Gimmi, Th.; Maes, N.; Reiller, P.: Radionuclide migration in clay-rich host formations: Process understanding, integration and up-scaling for safety case use. - In: "Proceedings of Seventh European Commission Conference on the Management and Disposal of Radioactive Waste. Euradwaste '08". EUR 24040. Brussels, 2009.

/BUC 00/ Buckau, G.; Artinger, R.; Geyer, S.; Wolf, M.; Fritz, P.; Kim, J.I.: Groundwater in-situ generation of aquatic humic and fulvic acids and the mineralization of sedimentary organic carbon. - Appl. Geochem. 15, 819-832, 2000.

/BUC 07/ Buckau, G.; Kienzler, B.; Dura, L.; Montoya, V.: 2nd Annual Workshop Proceedings of the Integrated Project "Fundamental Processes of Radionuclide Migration" (6th EC FP IP FUNMIG). - SKB Technical Report TR-07-05, June 2007.

/BUC 09/ Buckau, G.; Dura, L.; Kienzler, B.; Montoya, V.; Delos, A.: 4th Annual Workshop Proceedings of the Integrated Project "Fundamental Processes of Radionuclide Migration" (6th EC FP IP FUNMIG). - FZKA 7461, July 2009.

/BUC 10/ Buckau, G. et al.: Fundamental Processes of Radionuclide Migration (6th EC FP IP FUNMIG). - EUR report. To be published.

/CER 07/ Cervinka, R.; Havlova, V.; Noseck, U.; Brasser, Th.; Stamberg, K.: Characterisation of organic matter and natural humic substances extracted from real clay environment. - Annual Workshop Proceedings of the IP Project FUNMIG. Edinburgh 26.-29. November, 2007.

/CRA 04/ De Craen, M.; Wang, L.; Weetjens, E.: Natural evidence on the long-term behaviour of trace elements and radionuclides in Boom Clay. - Final report of DS2.9 for the period 2000-2003, R-3926, SCK-CEN, Mol, Belgium, 2004.

/DAV 09/ Davies, C. (ed.): Euradwaste ’08. Seventh European Commission Conference on the Management and Disposal of Radioactive Waste. - EUR 24040. Brussels, 2009.

/DEN 05/ Denecke, M.A.; Janssens, K.; Proost, K.; Rothe, J.; Noseck, U.: Confocal micro-XRF and micro-XAFS studies of uranium speciation in a Tertiary sediment from a waste disposal natural analogue site. - Environ. Sci. Technol. 39(7), 2049-2058, 2005.

/HAU 07 Hauser, W.; Geckeis, H.; Götz, R.; Noseck, U.; Laciok, A.: Colloid Detection in Natural Ground Water from Ruprechtov by Laser-Induced Breakdown Detection. - In: „Annual Workshop Proceedings of the IP Project FUNMIG”. SKB Technical Report TR-07-05, June 2007.

/HAV 06/ Havlová, V.; Laciok, A.; Vopálka, D.; Andrlík, M.: Geochemical Study of Uranium Mobility in Tertiary Argillaceous System at Ruprechtov Site, Czech Republic. - Czechoslovak Journal of Physics, Vol. 56, Suppl. D, 1-6, 2006.

/IWA 04/ Iwatsuki, T.; Arthur, R.; Ota, K.; Metcalfe, R.: Solubility constraints on uranium concentrations in groundwaters of the Tono uranium deposit, Japan. - Radiochim. Acta 92, 789-796, 2004.

/LAA 06/ Laaksoharju, M.; Smellie, J.; Tullborg, E.; Gimeno, M.; Gómez, J.; Gurban, I.; Hallbeck, L.; Auqué, L.; Buckau, G.; Gascoyne, M.; Raposo, J.: Hydrogeochemical evaluation of the Forsmark site, modelling stage 2.1. - SKB-R06-69, Stockholm, 2006.

/MIL 00/ Miller, W.; Alexander, R.; Chapman, N.; McKinley, I.; Smellie, J.: Geological disposal of radioactive wastes & natural analogues. - Waste Management Series, Vol.2, Pergamon, Amsterdam 2000.

/MIS 09/ Missana, T.; Gomez, P.; Pérez-Estaún, A.; Geckeis, H.; Samper, J.; Laaksoharju, M.; Dentz, M.; Alonso, U.; Buíl, B.; Siitari-Kauppi, M.; Montoto, M.; Suso, J.; Carretero, G.: Laboratory and In Situ Investigations on Radionuclide Migration in Crystalline Host Rock. FUNMIG Project. - In: "Proceedings of Seventh European Commission Conference on the Management and Disposal of Radioactive Waste. Euradwaste '08". EUR 24040. Brussels, 2009.

/NOS 04/ Noseck, U.; Brasser, Th.; Rajlich, P.; Laciok, A.; Hercik, M.: Mobility of uranium in Tertiary argillaceous sediments - a natural analogue study. - Radiochim. Acta 92, 797-803, 2004.

/NOS 06/ Noseck, U.; Brasser, Th.: Radionuclide transport and retention in natural rock formations – Ruprechtov site. - Gesellschaft für Anlagen- und Reaktorsicherheit, GRS-218, Köln, 2006.

/NOS 08/ Noseck, U; Brasser, Th.; Suksi, J.; Havlova, V.; Hercik, M.; Denecke, M.A.; Förster, H.J.: Identification of Uranium Enrichment Scenarios by Multi-Method Characterization of Immobile Uranium phases. - Phys. Chem. Earth, 33, 969-977, 2008.

/NOS 09a/ Noseck, U.; Rozanski, K.; Dulinski, M.; Havlova, V.; Sracek, O.; Brasser, Th.; Hercik, M.; Buckau, G.: Characterisation of hydrogeology and carbon chemistry by use of natural isotopes – Ruprechtov site, Czech Republic. - Appl. Geochem. 24, 1765-1776, 2009.

/NOS 09b/ Noseck, U.; Suksi, J.; Havlova, V.; Cervinka, R.: Uranium Geochemistry at Ruprechtov site. - In: „4th Annual Workshop Proceedings of the Integrated Project Fundamental Processes of Radionuclide Migration (6th EC FP IP FUNMIG). Forschungszentrum Karlsruhe, FZKA 7461, July 2009.

/REI 06/ Reiller, P.; Buckau, G.; Kienzler, B.; Duro, L.; Martell, M.: 1st Annual Workshop Proceedings of Integrated Project Fundamental Processes of Radionuclide Migration IP FUNMIG. - CEA-R-6122, September 2006.

/SCH 09/ Schwyn, B.; Schneider, J.; Rüedi, J.; Alonso, J.; Altmann, S.; Brassinnes, S.; Cormenzana, J.L.; Hautojärvi, A.; Marivoet, J.; Puigdomenech, I.; Rübel, A.; Tweed, C.; Missana, T.; Noseck, U.; Reiller, P.; Schäfer, Th.: Radionuclid migration in the far field. The use of research results in safety cases. - In: “Proceedings of Seventh European Commission Conference on the Management and Disposal of Radioactive Waste. Euradwaste ’08”, EUR 24040, Brussels, 2009.

/SUK 07/ Suksi, J.; Noseck, U.; Fachinger, J.; Salminen, S.: Uranium redox state and $^{234}U/^{238}U$ activity ratio analysis in uranium-rich samples from Ruprechtov site. - In: „Annual Workshop Proceedings of the IP Project FUNMIG”, SKB Technical Report TR-07-05, June 2007.

/VOP 08/ Vopalka, D.; Havlova, V.; Andrlik, M.: Characterization of U(VI) behaviour in the Ruprechtov site (CZ). - Proc. of the International Conference Uranium Mining and Hydrogeology V, Freiberg, September 14.-18., 2008.

A Annex: Publications of RTDC

A.1 A new confocal µ-XRF set-up for measuring 3D elemental distributions with spatial resolution on the micrometer scale

M. A. Denecke
Forschungszentrum Karlsruhe (FZK), Institut für Nukleare Entsorgung, PO Box 3640, 76021 Karlsruhe, Germany

* Corresponding author: Melissa@ine.fzk.de

Abstract

A confocal system was tested for the measurement of trace element distributions in tomographic cross-sections at different depths below a uranium-rich sediment sample surface. The primary focusing optic used was a new planar compound refractive lens array generating X-ray microbeams for high resolution three-dimensional elemental analysis. The focus beam spot-size achieved was 2 x 5 μm^2 (VxH) and the system performs with a 16 µm depth resolution. Experiments were performed at the Fluoro-Topo-Beamline at ANKA. Spatially resolved measurements of three dimensional distributions of elements in a uranium-rich sediment bore core samples from the Ruprechtov site were made with the set-up. Uranium hot-spots were observed to be located near but not on grain boundaries of Fe(II) minerals in the sediment. Arsenic is found enriched directly at the surface of framboidal Fe(II) minerals, indicating an arsenopyrite-mineral coating is present on pyrite. These results show that the confocal set-up using new planar CRL allows elemental mapping below the surface of heterogeneous, natural samples with a spatial resolution in the micrometer range.

Introduction

Successful understanding of the processes determining radioactive contaminant behavior in the environment, as part of performance assessment (PA) for proposed nuclear waste disposal strategies, increasingly requires structure information and characterization of radioactive contaminants on a molecular-scale. Due to the heterogeneity of natural systems, different hard X-ray microprobe techniques with high sensitivity and high spatial resolution are indispensable to such speciation studies. For this reason, we have for the first time tested a confocal μ-XRF set-up for recording three dimensional trace element distributions in bulky samples.

Objectives

The objective of the first phase of this project was to test a system for measurement of three dimensional trace element distributions, with a spatial resolution in the micrometer range, applicable to bulky samples.

Results and discussion

We tested new planar compound refractive lens (CRL) array generated X-ray microbeams for three dimensional elemental analysis with high resolution at the Fluoro-Topo-Beamline at ANKA. Three dimensional distributions are measurable by using a confocal μ-XRF set-up. This set-up allows probing the local composition of specified volumes, thereby enabling measurement of the distribution of trace elements in tomographic cross-sections situated at different depths below the surface. This has the great advantage that tomographic cross-sections can be recorded without reverting to classical tomographic data acquisition and processing methods of rotating the sample during measurement and subsequent mathematical reconstruction. This allows recording stacks of tomograms of relatively large samples, such as the sediment bore-core (about 20 mm in diameter and nearly 10mm thick) used for these tests.

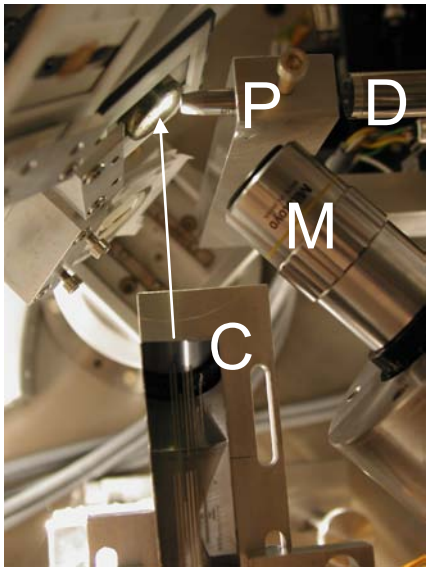

Fig. 1. Photograph of the confocal CRL/polycapillary set-up. Arrow marks the focused beam path to the sample. See text for labelling explanation.

The confocal set-up was constructed by positioning a polycapillary X-ray half-lens (X-ray Optics systems, Albany, NY, US) in front of the Si(Li) detector and using a new planar SU8 polymer CRL, fabricated by the Insitut für Microstrukturtechnik-FZK, as

focusing optic for the incident synchrotron radiation [1]. The polycapillary half-lens serves as depth-selective collimation and radiation-collection device. The CRL array primary focusing optic used can be seen mounted on an Al-plate in the photograph of the confocal set-up in Fig. 1 (indicated with "C"). The array consist of 10 sets of SU8 polymer resist material cross-lenses with parabolic profiles on a rectangular Si wafer, all having identical focal distances of 15 cm, and each set designed for different energies from 5 keV to 30 keV. The relatively long focal distance for the CRLs makes them applicable for experiments where the focusing optic cannot be placed directly next to the sample, e.g, in radioactive samples requiring containment or shielding.

A photograph of the set-up is shown in Fig. 1, detailing the relative position of a sediment sample, microscope (M), SU8 CRL array (C), polycapillary lens (P), and X-ray detector (D). After alignment of the foci of both lenses relative to one another, a cube-shaped analysis volume is defined from which fluorescent radiation can reach the detector [2].

The footprint on the sample of the beam generated by the CRL lens is measured from

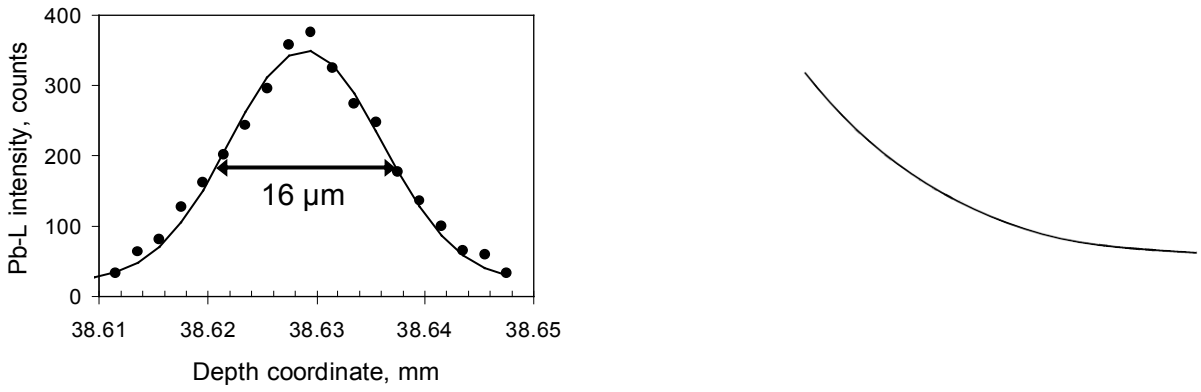

Fig. 2 (left) Depth-resolution and (right) MDL values obtained with the confocal set-up (1000 s counting time) for transition elements from the NIST SRM 613, trace elements in a glass standard.

knife-edge scans to be 2 x 5 μm^2 (VxH) in cross-section. The depth resolution is estimated by scanning a thin glass standard foil (National Institute of Standards and Technology, NIST) through the analysis volume (Fig. 2, left) to be around 16 µm in the energy-range 10-15 keV. The relative minimum detection limits (MDL) for elements Ti-Mo in a silicate-rich matrix are also shown in Fig. 2 (right, collection time = 1000 s). The MDL lie in the 0.3-30 ppm range, indicating that trace element mapping in confocal mode is feasible within reasonable acquisition times.

This new set-up was tested on a uranium-rich sediment sample from Ruprechtov site. This sample stems from argillaceous sediments, with high of kaolin, quartz, and organic matter content and containing pyrite minerals. Work package RTDC5 comprises

characterization of the immobile uranium phases in these sediments by application of microscopic methods with high spatial resolution accompanied by bulk analyses such as U(IV)/U(VI)-separation, sequential extraction, and sorption/desorption measurements. The aim is to identify the immobile uranium phases and to understand the mechanisms leading to immobilization of uranium during diagenesis in the sedimentary system at Ruprechtov site, which is similar to sediments found in covering rocks of salt formations in northern Germany.

Fig. 3 shows the Fe, As, U distributions recorded for the uranium-rich sediment bore core sample from the Ruprechtov site [3] investigated. The cross sections were measured at a 60µm depth below the sediment sample surface. The sample surface photograph is shown at the lower left of Fig. 3. The high lateral resolution available using the CRL array makes it possible to discern an As-rich boundary layer surrounding Fe(II)-nodules in the sample, not yet observed [4]. This suggests that an arsenopyrite mineral coating of framboidal pyrite nodules is present in the sediment. Uranium occurs in direct vicinity of the As-rich boundary layers.

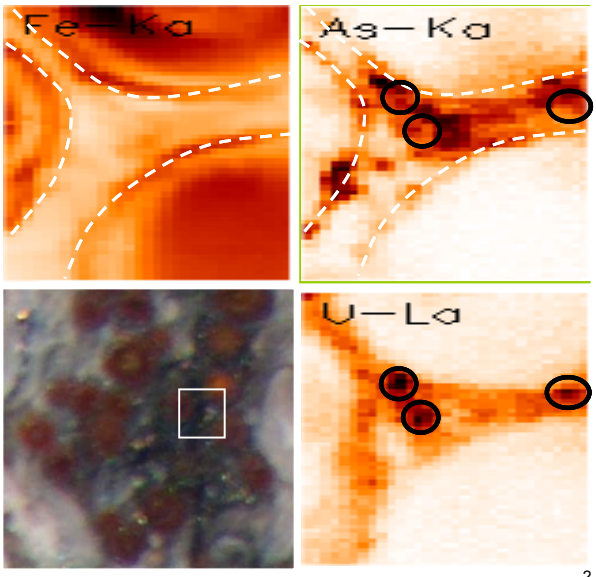

Fig. 3. Confocal µ-XRF maps of a 120 x 120 µm^2 section (2 x 4 µm^2 step size) from 60 µm below the surface. Circles indicate U hot-spots. Dashed lines indicate As-rich rim around Fe(II)-nodule.

Application to PA

The confocal set-up tested allows measurement of trace elemental maps in heterogeneous, natural mineral systems. This technique is especially suited for the study of natural analogues in a bottom-up approach to understanding immobilization reactions responsible for creating hot-spots in such samples.

Ruprechtov site is an example of such an analogue for radionuclide transport in the far field of a repository, where the uranium transport and subsequent enrichment in tertiary argillaceous sediment layers occurred on a geological pastime-scale. In the long term, understanding of the dominant immobilization reactions may provide information that will aid in increasing confidence in PA and/or help develop more intelligent technical barriers. Measurements of other samples from Ruprechtov site are intended to check if similar uranium speciation and element correlations are found which confirm the proposed mechanism for uranium immobilization [4], or if also other uranium species can be detected. Furthermore, upcoming tests of the confocal set-up to secure microscopic information on the distribution of sorbed radionuclides in cores from field studies (specifically Äspö) are planned. This will provide insight into radionuclide retention

processes on a molecular scale necessary for either justifying bulk distribution/retention coefficients used in PA or for adjustment of the coefficients to increase PA reliability.

Summary and conclusions

A confocal set-up using a planar CRL to focus the incident synchrotron X-ray beam to the micrometer range has been successfully used for characterization of the distribution analysis of trace elements in a natural analogue sample.

Acknowledgements

The vast expertise and experimental assistance of Koen Janssens, Department of Chemistry, University of Antwerp, is acknowledged with gratitude. We thank ANKA for beamtime allotment and the Fluoro-Topo-Beamline scientist, Rolf Simon, for his help.

References

[1] V.Nazmov, E.Reznikova, A.Somogyi, J.Mohr, V.Saile. Planar sets of cross X-ray refractive lenses from SU-8 polymer. Proceedings of SPIE 2004, Vol. 5539, pp. 235-242.

[2] K. Janssens, K. Proost and G. Falkenberg, “Confocal microscopic X-ray fluorescence at the HASYLAB Microfocus beamline: Characteristics and possibilities", Spectrochim. Acta B, (2004) *59*, 1637-1645.

[3] U. Noseck, T. Brasser, W. Pohl, *Tertiäre Sedimente als Barriere für die U-/Th-Migration im Fernfeld von Endlagern,* Gesellschaft für Anlagen- und Reaktorsicherheit (GRS) mbH, GRS-176, Braunschweig (2002).

[4] M.A. Denecke, K. Janssens, K. Proost, J. Rothe, U. Noseck, “Confocal micro-XRF and micro-XAFS studies of uranium speciation in a tertiary sediment from a waste disposal natural analogue site”, Environ. Sci. Technol. (2005) *39*(7), 2049-2058.

A.2 Elemental correlations observed in Ruprechtov tertiary sediment: micro-focus fluorescence mapping and sequential extraction

Melissa A. Denecke[1*], Václava Havlová[2]

[1] Forschungszentrum Karlsruhe, Institut für Nukleare Entsorgung, P.O. Box 3640, D-76021 Karlsruhe, Germany. Corresponding author.
[2]Nuclear Research Institute Řež plc, Waste and Environmental Management Department, Husinec- Řež, PSČ 250 68, Czech Republic

Abstract

Sequential extraction (SE) is used for determination of U and other elements in a U-rich sediment from the Natural Analogue Site Ruprechtov. In Tertiary clayey samples U is found to be bound onto organic matter and/or be present in reduced form. In granitic samples carbonates/alumosilicates play a more important role in the U distribution.

Extended element analyses (Na, K, S, Fe, As, P) of SE leachates were completed. Cluster analyses of these results are used for identifying possible correlations between elements and for comparing these to previous correlations derived from µ-XRF and µ-XAFS investigations. According to the SE cluster analysis P, As and P can be assigned into one group. Fe and S are separated from U, i.e. we find no direct dependence of U on Fe and S. K and Na are mainly associated with residual minerals. Agreement with micro-scale measurements is observed: U in the sediment is associated with As and is present as phosphate in reduced U(IV) form.

Introduction

The Natural Analogue Study at the Ruprechtov site aims at understanding behaviour of natural radioelements in plastic clay formations. This system is chosen as an analogue for sedimentary overburden of radioactive waste repository host rocks (salt, granite, clay). The most similar proposed repository systems studied are Gorleben (Germany) and Mol (Belgium).

Objectives

The main objective of the Ruprechtov site study is to find and describe the main mobilisation/immobilisation processes for performance assessment (PA)-relevant elements, namely uranium, thorium and radium. The system consisting of U – argillized clay – organic matter – granite – groundwater is studied both in-situ and in the laboratory in both a macro- and microscale. The investigations include drilling, field tests, geochemical and hydrogeological modelling, as well as monitoring, sampling, both in situ and laboratory characterisation of sediment and groundwater. In this report we compare results from investigations using micro x-ray fluorescence (µ-XRF) and micro x-ray absorption fine structure (µ-XAFS) on core sections of Tertiary clay samples with the results from sequential extraction (SE) of the same material type.

µ-XRF / µ-XAFS is performed in order to assess mechanisms leading to immobilization of the uranium during diagenesis (Denecke et al., 2005). SE is a widely used tool for speciation of selected elements (in this study, U) bound onto different fractions of sediment (see, e.g., Tessier et al., 1979; Percival 1990, Havlová and Laciok, 2006).

Results and discussion

µ-XRF and µ-XAFS results show uranium to be present as a tetravalent phosphate/sulfate in the regions studied and that U(IV) is associated with As(V) (Denecke, et al., 2006). Arsenic is present in the sediment as either As(V) or As(0);we did not find any evidence for As(III). The As(0) is observed to be intimately associated with the surface of Fe(II) nodules and likely arsenopyrite.

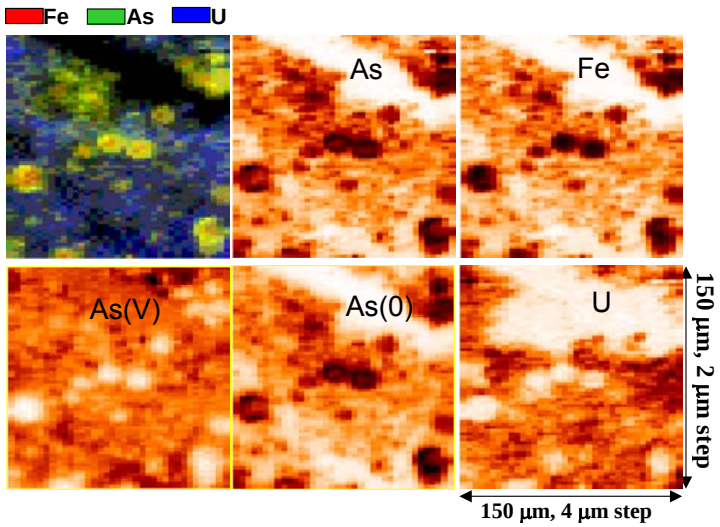

Fig.1: µ-XRF distribution maps for a 150*150 µm^2 area of a thin section of a sample from NA5. The distribution of the total As, Fe and U measured with E_{excite} = 18 keV and its corresponding Red-Blue-Green (Fe, As, and U, respectively) image , as well as the arsenic chemical state distributions for As(V) and As(0) are shown. As(0) is obtained from the As Kα fluorescence recorded using E_{excite} =11.861 keV; As(V) distribution is the difference between As Kα fluorescence recorded using E_{excite} = 11.870 keV and E_{excite} 11.861 keV, i.e. map at 11.87 keV minus the As(0) map

Numerous correlation functions between As and U are determined from measured fluorescence intensities of elemental distribution maps recorded for samples NA4 and NA5. An example of distribution maps measured for a 150*150 µm^2 area of a thin section of a sample from borehole NA5 is shown in Fig. 1. In this case it is possible to selectively differentiate between As(0) and As(V) in the maps by tuning the incoming incident photon energy (E_{excite}) to the corresponding ionisation energy. The correlation between U and As(V) and between As (total As, As(0) and As(V)) and Fe is shown in Fig. 2. We observe a correlation between As(V) and U. The linear correlation between As(0) and Fe shows that these are in the same phase, which is another indication of arsenopyrite presence in the sample. The difference between the correlation between As(0) and Fe and between the total As and Fe is hardly different, indicating that As(V) is a minority species.

The sequential extraction (SE) scheme is applied to Ruprechtov samples of different origin (6 boreholes, different depths, different rock types – kaolinized granite/Tertiary argillized clay). Samples are leached using different extractants in order to quantify various forms of U present in the sediment. The SE scheme consists of the following steps:

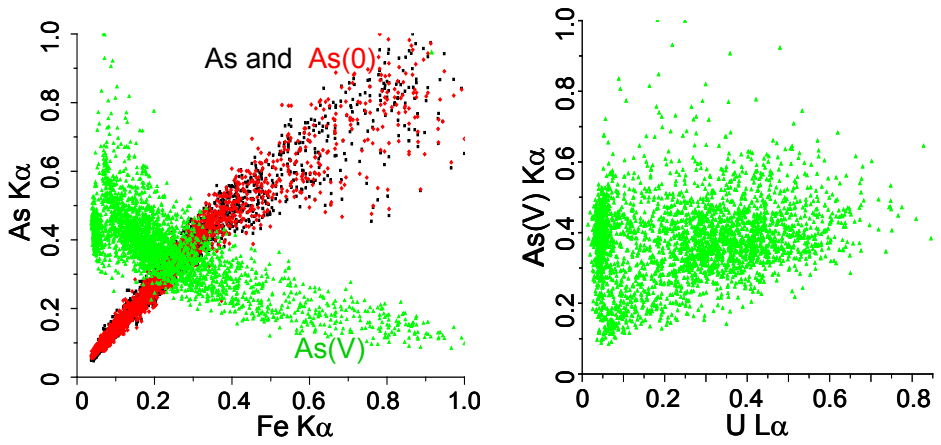

Fig 2: Correlation plots between Fe and As(0) [◆], As(V) [▲], and total As [□] (left) and between U and As(V) (right).

1. U bound on exchangeable sites (leaching with $MgCl_2$)
2. U bound on carbonates (leaching with ammonium acetate with acetic acid)
3. U bound to Fe/Mn oxides (leaching with hydroxylaminehydrochloride in acetic acid)
4. U bound onto organic matter/in reduced form (using H_2O_2 and HNO_3)
5. U in residuum (using boiling with HNO_3)

SE results of the uranium associated with the various fractions, expressed as percent of total U content are shown on Fig 3.

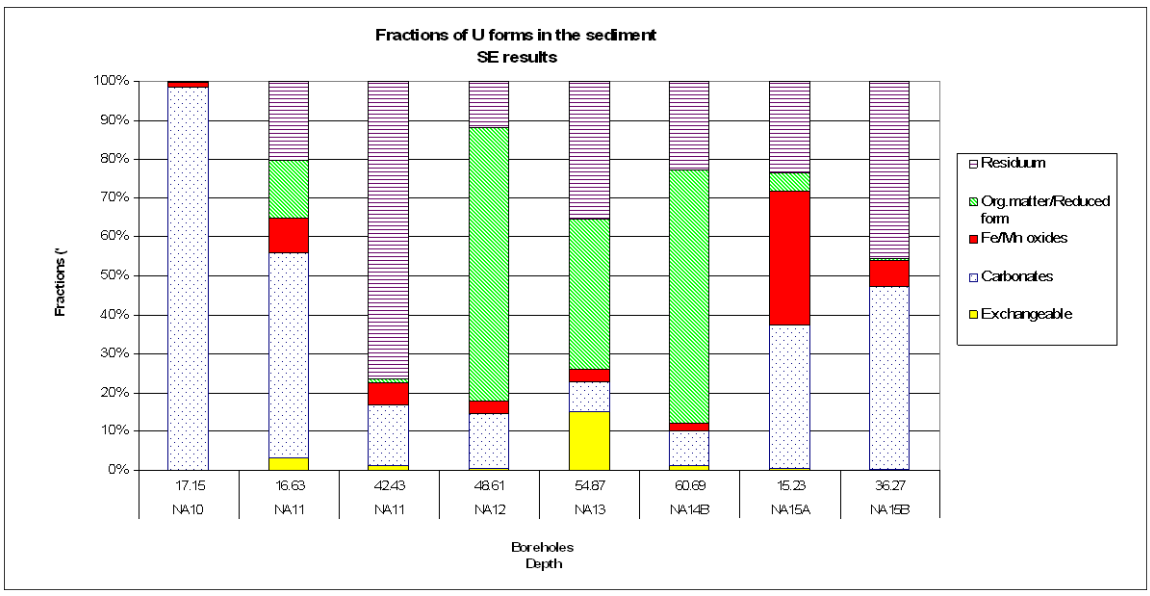

Fig. 3: Fractions (in %) of U in the sediment samples (SE results). NA10&NA15A – kaolinized granite, the rest of the samples – argillized Tertiary clay.

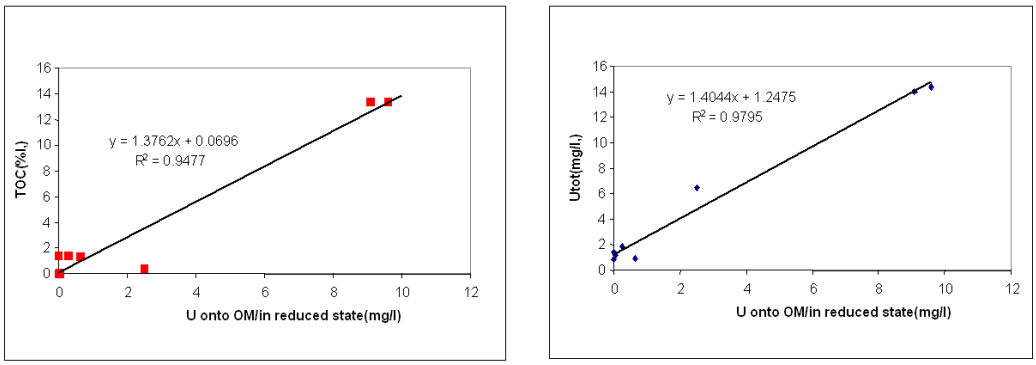

Fig. 4: Dependency of the U fraction bound onto organic matter(OM)/in reduced form in mg/l on TOC in percent (left) and on Utot in mg/l (right). Lines depict linear regression results, both yielding a slope of around 1.4.

In Tertiary clay samples (all samples except NA10 and NA15B) we find U bound onto organic matter and/or in reduced form to be proportional to the total U content (Utot) and on total organic carbon content (TOC). In other words, observed increases in Utot and TOC are associated with increasing content of U bound to organic matter and/or in reduced form (see Fig. 4). In granitic samples (NA10, NA15B) we find that carbonates/alumosilicates play a more important role in U binding.

Extended element analyses (Na, K, S, Fe, As, P) of SE leachates are completed for two samples in order to define phases dissolving in each extraction step. Cluster analyses are then used in order to identify possible correlations between elements (see Fig. 5). P, As and U can be assigned into one group. This is in agreement with observations derived from the µ-XRF and µ-XAFS measurements. Fe and S are not correlated with U, i.e. there is no direct evidence of U dependence on Fe and S. The elements K and Na are mainly associated with residual minerals. As a vast amount of K is leached in step 2, we can assume that alumosilicates or carbonate complexes are more responsible for U distribution than carbonate minerals themselves.

Cluster analyses

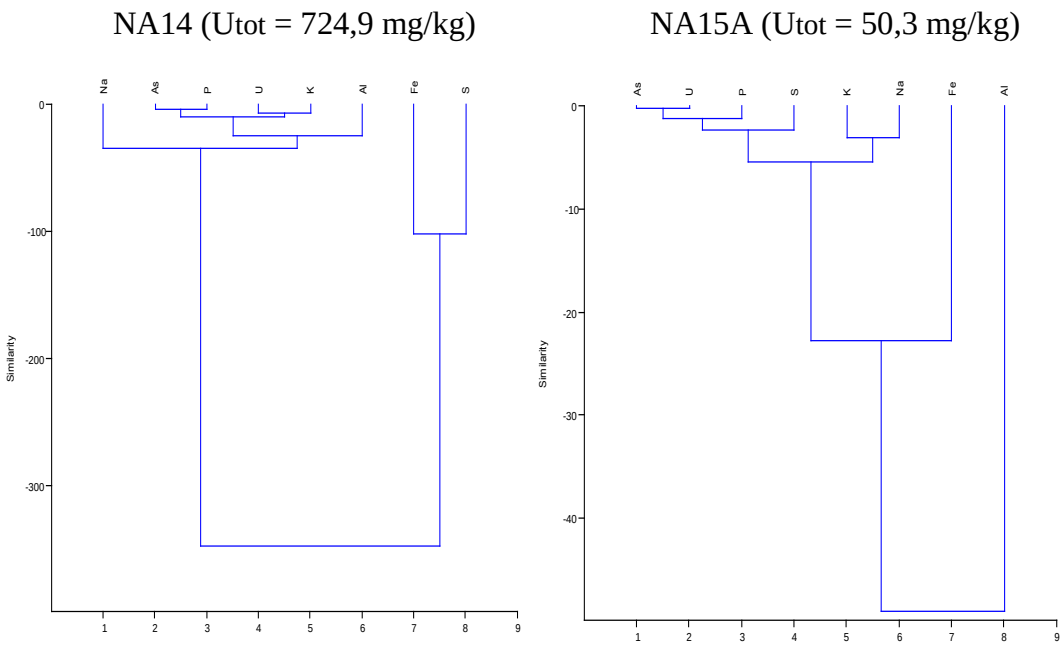

Fig. 5: Cluster analyses for extended SE results for two samples of Tertiary clay from the Ruprechtov site.

Conclusions

Both micro-focus fluorescence mapping and sequential extraction of Ruprechtov clay samples showed that U accumulation in the sediment is associated with As. Analysis of µ-XAFS reveals the presence of U-phosphate phases in the sediment, corroborated by the cluster analysis showing a correlation between U and P. Cluster analysis further shows that there was no direct dependence between U and Fe and S. This is in agreement with the observation in the elemental distributions for Fe and U. U is observed to be located in sample areas void of Fe. In this comparative study the application of independent methods, i.e. SE and µ-XRF/µ-XAFS, yields complementary results. This is important as we find similar elemental correlation results using the x-ray based methods as in SE. This indicates that SE results are not erroneously fraught with artefacts caused by speciation changes during the extraction processes.

References

Denecke, M.A., Janssens, K., Proost, K., Rothe, J., Noseck, U. (2005) *Environ. Sci. Technol.* **39**(7), 2049-2058.

Denecke, M.A., Somogyi, A., Janssens, K., Simon, R., Dardenne, K., Noseck, U. (2006) *Microscopy Microanal.* (invited contribution; accepted)

Havlová V., Laciok A. (2006): Geochemical study of uranium mobility in Tertiary argillaceous system at Ruprechtov site, Czech Republic. *Czech Journal of Physics*, Vol. 56, Suppl. D. (in press).

Percival J. B. (1990): Clay mineralogy, geochemistry and partitioning of uranium within the alternative halo of Cigar Lake uranium deposit, Saskatchewan, Canada. Carleton University, Ottawa, PhD thesis.

Tessier A., Campbell P.G.C. and Bosson M.(1979): Sequential extraction procedure for the speciation of particulate trace metals. *Anal. Chemistry* **51** 844-851.

A.3 Uranium redox state and $^{234}U/^{238}U$ ratio analyses in uranium rich samples from Ruprechtov Site

Juhani, Suksi[1]; Ulrich Noseck[2*], Johannes Fachinger and Susanna Salminen[1]
[1] University of Helsinki, Laboratory of Radiochemistry, P.O. Box 55, FI-00014 Helsinki, Finland
[2] Gesellschaft für Anlagen- und Reaktorsicherheit, Theodor-Heuss- Str. 4, 38118 Braunschweig, Germany
[3] Forschungszentrum Jülich – Institut für Sicherheitsforschung und Reaktortechnik, 52425 Jülich, Germany
* Corresponding author; ulrich.noseck@grs.de

Abstract

A method for separation of uranium (IV) and uranium (VI) has been further developed for application to natural samples from uranium-rich tertiary clay horizon at Ruprechtov site, Czech Republic. It has been applied to four samples with different uranium content from different boreholes. The $^{234}U/^{238}U$ activity ratio in each phase was determined.

The results show, that both forms U(IV) and U(VI) exist in the tertiary clay horizon. The $^{234}U/^{238}U$ ratio significantly differs between the forms with values below unity between 0.45 and 0.91 in the U(IV) phase and values above unity between 1.26 and 3.37 in the U(VI) phase. On one hand it clearly shows the impact of α-recoil process on the U(IV) phase, indicating its low mobility in this horizon. On the other hand the finding of clear U(VI) phases and their high $^{234}U/^{238}U$ ratio indicate that at least part of the U(VI) phase was recently formed. Results are discussed with regard to uranium enrichment scenarios at the site.

Introduction

Analyses of enrichment processes of radionuclides under natural conditions can contribute to the understanding of the long-term behaviour of geological formations as part of the barrier system of a repository for radioactive waste. At Ruprechtov site, uranium occurs in concentrations up to 400 ppm in lignite-rich argillaceous sedimentary layers. Previous results showed that uranium accumulation occurred by a multi phase process. Secondary U(IV) phases uraninite and ningyoite as well as uranium bearing primary minerals monazite, xenotime and zircon were detected (Noseck et al. 2006). The secondary U(IV) minerals were shown to be at least partly accumulated by transport of U(VI) and subsequent reduction to U(IV) by oxidation of As(0) in FeAsS surface layers on pyrite nodules to As(V) (Denecke et al. 2004 and 2006). Application of the U(IV)/U(VI) separation method with analyses of the $^{234}U/^{238}U$-activity ratios can help to better understand the enrichment processes and give information about the stability of the respective phases.

Objectives

Major objective of the study is the further development of the method with respect to its application to the uranium-rich sedimentary samples from Ruprechtov site. After confirmation of its applicability the aim is to quantify U(IV) and U(VI) fractions in these sediments and receive further information about time scales and processes associated with the different phases.

Experimental

Uranium dissolution was performed by extracting the sample material with the mixture of 4 M HCl and 0.03 M HF in Ar-atmosphere. Solid to solution ratio was ~ 0.1. Uranium dissolution was intensified performing extraction in ultrasonic bath and at the same time mixing the solution with Ar-bubbling. Uranium could not be dissolved quantitatively. Dissolution yield varied between 50% and 90%. Insoluble U was thought to represent U(IV) minerals.

Oxidation states U(IV) and U(VI) were determined using a slightly modified method from the one presented in Ervanne and Suksi (1996). U(IV) and U(VI) were separated from each others in anion exchange column regenerated with the extraction solution; U(IV) was collected in the first 20 ml and U(VI) was eluted with 20 ml of 0.1 M HCl. Separation is quantitative and no overlapping of U(IV) and U(VI) has been observed in the tracer experiments. Both fractions were purified from the daughters by another anion exchange step. Purified U was mounted on a plastic plate with “massless” CeF_3 precipitate for measurement. U concentration was determined using α-spectrometry. Alpha activities were measured by PIPS-detectors of 450 mm^2 area with a nominal resolution of 20 keV. A counting time varied between one and five days.

.

Results and discussion

The U(IV)/U(VI) separation was performed on four samples from three different boreholes in the so-called clay/lignite sand horizon, where uranium enrichment up to 500 ppm occurs in distinct layers of approx. 3 m thickness. Two samples were taken from borehole NA6, one from the major U-peak at 35 m and one from a second, smaller peak at 37 m. The other two samples were taken from

the highest uranium peaks in borehole NA13 and NA14. The distance between each borehole is approx. 50 m.

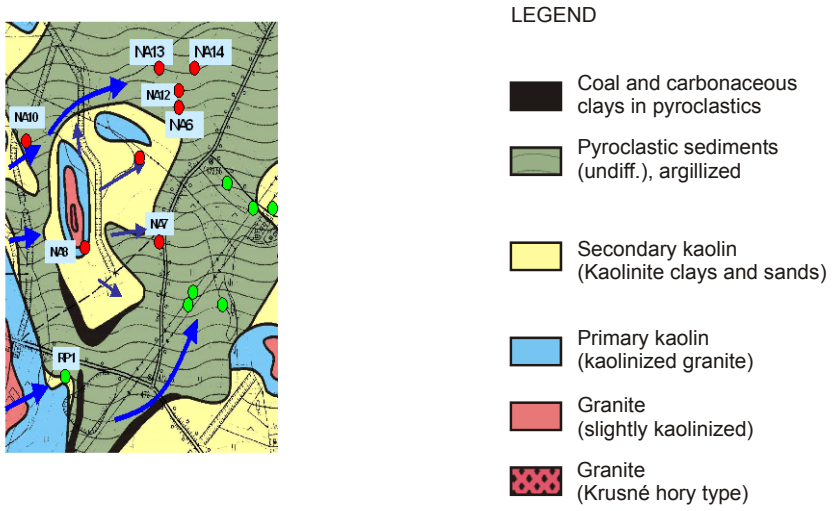

Fig. 1: Location of the boreholes analysed for $^{234}U/^{238}U$ AR in groundwater and for U(IV)/U(VI) separation of immobile uranium phase (NA6, NA13, NA14)

The results of all measurements are listed in Tab. 1. Total uranium content in the samples varies between 35 and 468 ppm with lowest uranium content in sample NA6, from 37 m depth (35 to 48 ppm). In the other samples uranium content is significantly higher with highest values of 468 ppm in NA6 from 35 m depth.

Tab. 1: Amount of uranium and $^{234}U/^{238}U$-activity ratios in the different phases from uranium separation

sample	U [ppm]	U(IV)		U(VI)		U(res, IV)		U(IV) total
		[%]	$^{234}U/^{238}U$	[%]	$^{234}U/^{238}U$	[%]	$^{234}U/^{238}U$	[%]
NA6 35a	356±7	28.7	0.54 ± 0.01	41.9	1.42 ± 0.02	29.5	0.65± 0.01	58.1
NA6 35b	468±9	45.9	0.56± 0.01	33.3	1.69 ± 0.03	20.7	0.64± 0.02	66.7
NA6 35c	369±8	23.3	0.47± 0.01	47.4	1.16± 0.02	29.3	0.67± 0.01	52.6
NA6 37a	37.3±2	73.7	0.79 ± 0.03	15.7	2.66± 0.07	10.6	0.73± 0.01	84.3
NA6 37b	47.5±1, 5	66.2	0.52± 0.01	9.0	3.37± 0.15	24.8	0.86± 0.02	91.0
NA6 37c	35.7±2	51.3	0.58± 0.01	19.8	2.56 ±0.08	28.9	0.71± 0.04	80.2
NA13 46	208±5	5.8	0.76± 0.07	43.9	1.23± 0.03	40.3		56.1
NA14 51	341±9	17.0	0.91± 0.04	41.5	1.27± 0.03	41.5		58.5

The first main observation is that immobile uranium consists of both U(IV) and U(VI). A second observation is that during the extraction procedure not all uranium is mobilized. The content of uranium in this residual phase is denoted as U(res).

The weight fraction of uranium in the different phases is graphically presented in Fig. 2 (left) and the corresponding $^{234}U/^{238}U$-activitiy ratios (denoted as AR) are shown in Fig. 2 (right). AR differs significantly in the U(IV) and U(VI) phases with ratios <1 in the U(IV) phase and ratios >1 in the U(VI) phase. The AR

of the residual phase is very similar to that observed in the U(IV) phase. Taking into account the higher stability of U(IV) phases we assume that residual uranium exists in oxidation state IV. Based on this assumption in all samples U(IV) represents the major uranium fraction with contents between 52 to max. 90 wt-%. The highest U(IV) fraction is found in sample NA6-37 which comprises the lowest total U content.

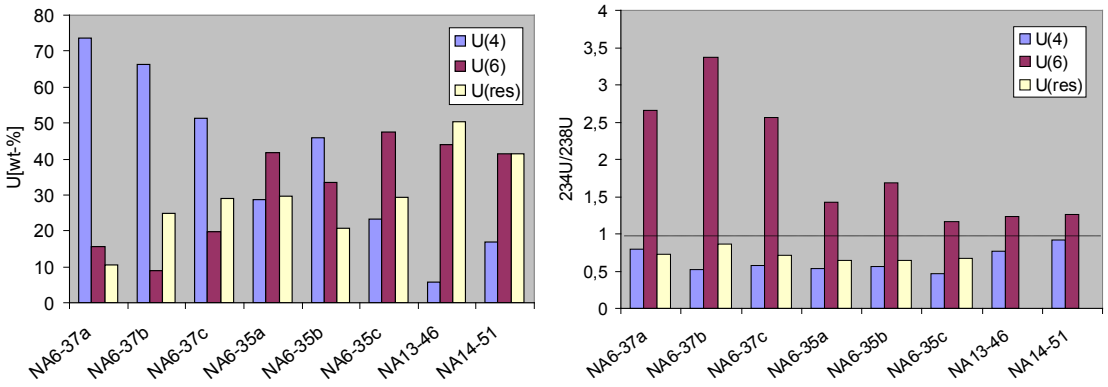

Fig. 2: Fraction of uranium in U(IV), U(VI) and U(res) phase (left) and corresponding $^{234}U/^{238}U$ isotope ratios (right). The line has been drawn to show radioactive equilibrium.

The $^{234}U/^{238}U$-activity ratios are strong indicators for the stability of the immobile uranium phases. Ratios significantly below unity are caused by the preferential release of ^{234}U. This is due to the α-recoil process and a correlated selective oxidation of the ^{234}U (e.g. Suksi et al., 2006). In order to obtain low ratios of approx. 0.5 as observed in the U(IV) phase it must have been stable for sufficiently long time, i.e. no significant release of bulk U has occurred during at least the last several 100 kys. This is in agreement with the scenario assumed for the major uranium input into the clay/lignite horizon, which occurred during Tertiary, more than 10 Mio years ago (Noseck et al. 2006). This stability of the U(IV) phases is also supported by geochemical calculations based on groundwater conditions with low Eh values especially in NA6 in the clay-lignite horizon indicating stability of uraninite and ningyoite under the today conditions.

The $^{234}U/^{238}U$ activity ratio in the groundwater generally reflects the nature of water-rock interaction and is therefore sensitive to groundwater conditions (see Suksi et al. 2006): in oxidising conditions both isotopes release in the groundwater in the ratio they occur in the rock and in anoxic conditions the release of ^{234}U is favoured. The low $^{234}U/^{238}U$ ratios in the U(IV) phase as observed in this study goes together with AR values >1 in porewater and groundwater from the clay/lignite horizon, which is shown in Fig. 3. This is expected because of the anoxic sediment conditions and preferred mobilisation of ^{234}U.

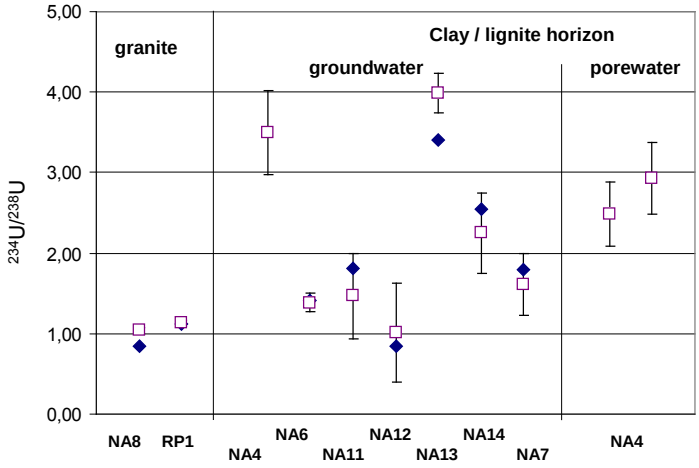

Fig. 3: $^{234}U/^{238}U$ activity ratios in groundwater from outcropping granite boreholes with high water flow and groundwater /porewater from clay lignite horizon measured by α-spectrometry (open squares) and ICP-MS (filled)

The variation of $^{234}U/^{238}U$ activity ratios in the groundwater of the different boreholes could be caused by differences in water flow conditions. In order to check this all available AR data of the different groundwaters are plotted versus the hydraulic conductivity of the corresponding water bearing horizons. At least for the clay/lignite horizon the hydraulic conductivity is considered as a suitable measure for water flow. Fig. 4 shows a clear trend, i.e. a decrease of $^{234}U/^{238}U$-activity ratio with increasing hydraulic conductivity.

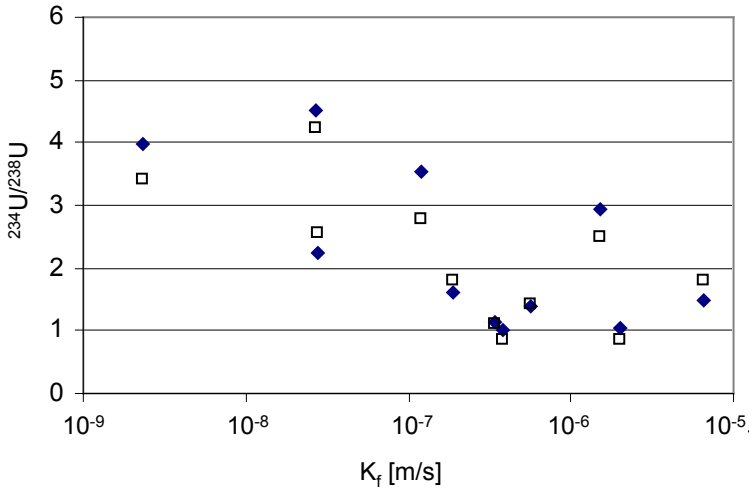

Fig. 4: $^{234}U/^{238}U$ activity ratios in groundwater from granite and clay lignite horizon versus hydraulic conductivity

For interpretation of activity ratios in the sedimentary U(VI) phase, we compare the data with the groundwater of corresponding horizons. The AR >1 indicates a recently formed (during the last several 100 ky) uranium phase. Therefore, it might be expected that this phase is more easily accessible and reflects a similar AR as the groundwater.

However, for the two samples from NA6 (35a and 35b) we recognize different values for the U(VI) phase. The value in the upper layer is about 1.2 to 1.7

and the value in the lower layer is in the range of 2.5 and 3.4. The value of the corresponding groundwater is about 1.4, i.e. similar to the value in the upper layer where also more U(VI) can be found. An explanation for different ARs in the U(VI) phase in the layers can be found in the spatially limited water flow in these horizons. The water transport mainly occurs on small fractures in the clay lignite or small sandy layers. For NA6 the water bearing layer overlaps with the area of the upper peak. The lower peak is approx. in 1 m distance of the water bearing layer. Therefore, the water exchange between pore water of the lower layer with smaller uranium peak is much slower than water exchange with the upper layer preventing U accumulation in the lower layer. As a result total U content in the lower layer remains smaller and the transfer process of ^{234}U from U(IV) phase to U(VI) phase is not as masked as in the upper layer, leading to observed ^{234}U enrichment in the U(VI) phase and in the porewater.

The AR in the U(VI) phases for NA13 and NA14 lies between 1.2 and 1.3. A comparison with groundwater is only possible for NA13, since NA14 water stems from the underlying granite horizon. The AR of groundwater from NA13 is 3.4 to 4, i.e. significantly higher than the value of the U(VI) phase in the sediment. This can be explained, if the major part of the U(VI) phase was not formed recently but over very long time scales. In this case one would expect to see much higher AR in the U(VI) phase, however. Another explanation for lower AR in the sedimentary phases than in the groundwater is that part of U(IV) is oxidised subsequently after sampling, either during U(IV)/U(VI) separation or during the time of sample storage. Partial oxidation of U(IV) with AR <1 after sampling would result in reduced AR for U(IV). Possible oxidation of U(IV) during the chemical separation procedure can be studied using U(IV) tracer in the procedure. In experiments with the ^{232}U(IV) tracer oxidation could not be observed.

The examination, whether oxidation occurred during sample storage is not done until now. It is planned to compare the results with those from a five step sequential extraction procedure and if possible to measure ARs of fractions from different steps. Furthermore it is planned to apply the method on samples, which have been stored under reducing conditions in a glove box directly after sample distribution.

Conclusions

The results from U(IV)/U(VI) separation identified the existence of both U(IV) and U(VI) phases in the uranium enriched clay/lignite horizon at Ruprechtov site. The major part of uranium is U(IV) and its fraction varies from 55 to 90 % in the investigated samples. This agrees well with results from SEM-EDX and µ-XANES and µ-EXAFS, which identified uraninite and phosphate (or sulphate) U(IV) minerals like ningyoite in hot spots found in the same horizon. The generally low $^{234}U/^{238}U$-activity ratios (<1) in the U(IV) fraction gives evidence that this phase is rather stable and immobile at Ruprechtov site because if water-sediment interaction had affected bulk U such activity ratios would not be possible.

.

The results for the U(VI) fraction are not so clear yet. At least part of U(VI) is recently formed. The AR in this fraction varies from 1.2 to 3.4 and is not in all cases similar to the fraction observed in groundwater. This can be explained, if part

of U(VI) is formed more than several 100 ky ago. But a decrease of AR might also be caused by oxidation subsequent to sampling. A disturbance of the originally reducing conditions and therewith oxidation of U(IV) to U(VI) could occur either by the separation procedure or during storage of the sample material. However, oxidation of low $^{34}U/^{238}U$-activity ratio U(IV) fraction by the separation procedure can be excluded, since experiments with ^{232}U tracers do not show any oxidation of U(IV) to U(VI). Concerning possible oxidation during storage, further experiments are planned with sample material stored from the beginning in a glove box under reducing atmosphere. These experiments will focus on the direct comparison of µ-XRF and µ-XAFS on the one hand and U(IV)/U(VI) separation on the other hand on the same sample.

Acknowledgements

This work has been / is financed by the European Commission, the German Federal Minstry of Economics and Technology (BMWi) under contract no. 02 E 9551 and no. 02 E 9995.

References

Denecke, M.A.; Janssens, K.; Proost, K.; Rothe, J.; Noseck, U. (2005) Confocal micro-XRF and micro-XAFS studies of uranium speciation in a tertiary sediment from a waste disposal natural analogue site, Env. Sci. Technol. 39, 2049-2058.

Denecke, Havlova, (2006) Element correlations observed in Ruprechtov sediments from micro-focus fluorescence mapping and cluster analysis of sequential extraction results, Proceedings of the 2. Annual FUNMIG workshop, Stockholm, 21.-23. November 2006.

Ervanne, H. and Suksi, J., (1996): Comparison of Ion-Exchange and Coprecipitation Methods in Determining Uranium Oxidation States in Solid Phases. Radiochemistry, Vol. 38, 324-327.

Noseck, U.; Brasser, Th. (2006) Application of transport models on radionuclide migration in natural rock formations - Ruprechtov site, Gesellschaft für Anlagen- und Reaktorsicherheit (GRS) mbH, GRS-218, Braunschweig, March 2006.

Suksi, J.; Rasilainen, K.; Pitkänen, P. (2006) Variations in the $^{234}U/^{238}U$ activity ratio in groundwater – A key to characterise flow system? *Physics and Chemistry of the earth*, Volume 31 (10-14), 556-571.

A.4 Evaluation of isotope data from Ruprechtov Site

Ulrich Noseck[1*], Thomas Brasser[1], Ales Laciok[2], Mirek Hercik[2], Václavá Havlová[2], Gunnar Buckau[3], Kazimierz Rozanski[4], Marek Dulinski[4]

[1] Gesellschaft für Anlagen- und Reaktorsicherheit, Theodor-Heuss- Str. 4, 38122 Braunschweig, Germany

[2] Nuclear Research Institute Řež plc, Waste and Environmental Management Department, Husinec- Řež, PSČ 250 68, Czech Republic

[3] Forschungszentrum Karlsruhe, Institut für Nukleare Entsorgung, P.O. Box 3640, 76021 Karlsruhe, Germany

[4] AGH – University of Science and Technology, Faculty of Physics and Applied Computer Science, al Mickiewicza 30, 30-059 Krakow, Poland

* Corresponding author: ulrich.noseck@grs.de

Abstract

All available natural isotope data from groundwater wells at Ruprechtov site are evaluated with respect to the hydrogeological flow regime in the tertiary sediments close to the clay/lignite layers and the behaviour of carbon in the system. Differences in stable isotope data indicate two different infiltration areas in the outcropping granites in the south-western part as source for water in clay/lignite layers in the middle and north and another in the southern part as source for the clay lignite layers in the eastern part of the investigation area. Differences in signatures in the northern part indicate very local connections probably via fault zones of the water system in the underlying granite and the tertiary sediments.

Based on the conceptual model for the hydrogeological flow regime, data for $\delta^{13}C$ and ^{14}C in DIC and DOC as well as $\delta^{34}S$ in dissolved sulphate are evaluated. The increase of biogenic DIC with increasing DOC concentration and the increase of $\delta^{34}S$ in water from the clay/lignite layers compared to water from granite in the infiltration areas give rise for microbial reduction of SOC and generation of DIC and DOC in the clay lignite layers. A more detailed paper about the results presented here is in preparation (Noseck et al. 2007).

Introduction

Ruprechtov site in Czech Republic is studied as an analogue for the behaviour of natural radionuclides in the overburden of salt domes because its geological conditions are similar to sedimentary sequences covering potential salt host rocks. The investigation area is a tertiary basin bordered in the west and south by outcropping granite. Main features of the investigation area are the crystalline basement covered by kaolin layers with varying thickness (few up to several tens of metres). The basin is mainly filled with tertiary argillized pyroclastic sediments. The interface between kaolin and pyroclastic sediments is characterized by a strong morphology. The horizon of major interest is the so-called clay/lignite layer at the interface of kaolin and pyroclastic sediments, with high content of sedimentary organic carbon (SOC), zones of uranium enrichment and partly aquiferous horizons (Noseck et al. 2006). An important instrument to understand the hydrogeological flow regime and the interrelation of sedimentary organic carbon with dissolved inorganic (DIC) and dissolved organic carbon (DOC) is the investigation of natural isotopes in groundwater. The work presented here shows results from the evaluation of natural isotope data sampled in groundwater wells at Ruprechtov site. It mainly focuses on aspects of the carbon chemistry at Ruprechtov site.

Objectives

Based on the evaluation of stable isotope data a conceptual model for the current hydrogeological situation at Ruprechtov site was proposed in (Noseck et al. 2006). Major objective of the work in FUNMIG is the evaluation and understanding of processes connected with changes in carbon chemistry, i.e. the development of DIC and DOC contents including changes in their ^{13}C and ^{14}C isotope signatures during water flow through the system.

Experimental

Natural isotope analyses of distinct groundwaters have been performed to characterise the hydrogeological flow regime at the site and especially the evolution of DOC and DIC during transport through the clay/lignite formation in more detail. $^{2}H/^{1}H$ and $^{18}O/^{16}O$ – isotope ratios have been analysed at near surface waters to identify typical local infiltration waters. Additionally ^{3}H, ^{14}C concentrations as well as $^{13}C/^{12}C$ and $^{34}S/^{32}S$-isotope ratios have been determined in the deeper groundwaters from several wells. The isotope ratios of $^{2}H/^{1}H$, $^{18}O/^{16}O$, $^{13}C/^{12}C$ and $^{34}S/^{32}S$ are given as per mille deviation $\delta^{2}H$, $\delta^{18}O$, $\delta^{13}C$, or $\delta^{34}S$. A detailed description of the experimental procedure can be found in (Noseck et al. 2006).

Results and discussion

Altogether 18 wells from recent drilling campaigns are available to sample and characterize undisturbed groundwater from aquiferous horizons. The position of boreholes is shown in Fig. 1. The blue font characterises water from either outcropping granite (NA8, NA10, RP1) or underlying granite (NA14, HR4).

Hydrogeological situation

Laboratory experiments at selected drill cores and on-site (pumping tests) measurements of hydraulic conductivities show that only distinct aquiferous horizons exist with kf-values of 10^{-5} to 10^{-8} m/s and thicknesses of about 1-2 meter only, mainly close to the clay/lignite layers (Noseck et al. 2006). They do not represent a continuous aquifer but areas with increased water flow. Compared with

this, the pyroclastic sediments and the underlying kaolin are low permeable with typical kf-values of 10^{-10} to 10^{-11} m/s. Additionally, fracture zones and areas with very low thickness of the underlying kaolin might represent hydraulic connections between clay/lignite layers and granite.

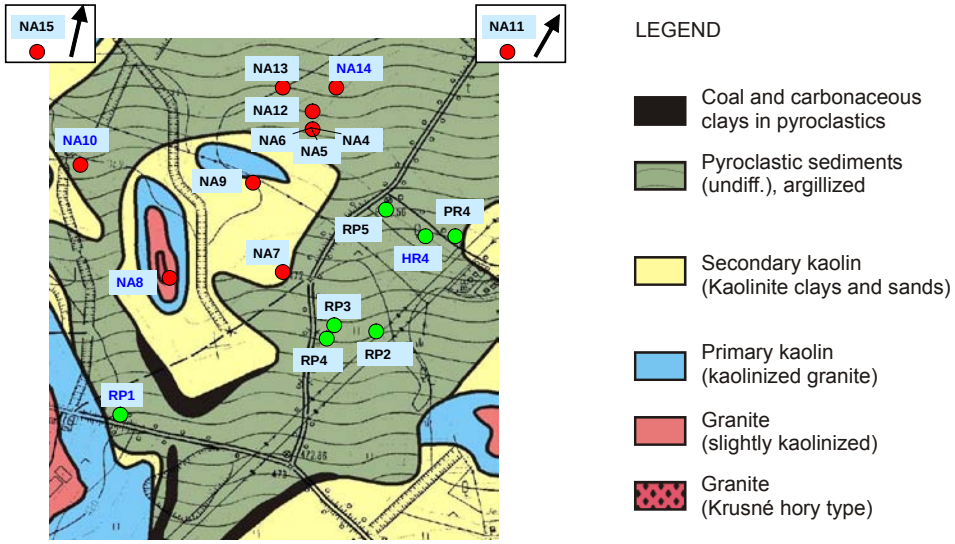

Fig. 1: Detailed view of location of boreholes at Ruprechtov site correlated to geologic map. Boreholes in granite in blue font

All isotope data including concentrations of DIC, DOC and dissolved sulphate are listed in Tab. 1. The results of the stable isotope analyses are shown in Fig. 2. From the figure on the left it is apparent that stable isotope composition varies in a rather broad range with $\delta^{18}O$ values from -9.8 to -8.8 ‰. In general the isotope signatures follow the world meteoric water line (WMWL). The data range of recent local infiltration waters is marked by the bold grey line.

Measurements of water levels confirm a hydraulic gradient from south west to north east (Noseck et al. 2006). Therefore, infiltration is expected in the outcropping granite areas in the western and southern part of the investigation area. Water with typical signature of local infiltration are found in granite well NA10, assumed to be representative for infiltration area in the western part. On the other hand isotopically light water is found in granite well RP1 in the south and in the boreholes in clay/lignite layers in the south-eastern part, indicating a second infiltration area in the South with major flow direction to north east. The wells in the kaolin and clay lignite layers in the middle and north show similar values as NA10, indicating that their water originates from the western infiltration area. However, some wells NA6, NA13, NA14 and HR4 occupy intermediate positions in the $\delta^{18}O$ - $\delta^{2}H$ diagram. An explanation is that they represent mixing waters of isotopically light and heavy waters. This might be the case for water from HR4 and NA14, which originates from the underlying granite and shows $\delta^{18}O$-values of approx -9.3. Similar isotope values in NA6 and NA13 might be caused by hydraulic pathways to underlying granite consisting of small fracture networks, which are only very locally connected.

Table 1: Depth of filter horizons, lithological units, natural isotope data and concentrations of DIC, DOC and dissolved sulphate in boreholes from Ruprechtov site

Well No.	Filtered horizon [m]	Lithology	$\delta^{18}O$ [‰]	$\delta^{2}H$ [‰]	Tritium [TU]	^{14}C DIC [pMC]	^{14}C DOC [pmc]	$\delta^{13}C$ DIC [‰]	$\delta^{13}C$ DOC [‰]	$\delta^{34}S$ SO_4^{2-} (‰)	DIC [mg/l]	DOC [mg/l]	SO_4^{2-} [mg/l]
NA-4	34.5 - 36.5	clay/lignite, U	-9.78	-68.0	0.0	3.2	39.96	-11.0	-26.6	24.63	74.2	4.22	19.8
NA-5	19.3 - 21.3	U	-8.98	-61.9	0.0	5.3		-10.9	-25		90.8		31.5
NA-6	33.4 - 37.4	clay/lignite, U	-9.27	-64.6	0.6	13.1		-12.4	-26.8	23.5	60	3.27	49.5
NA-7/1	15.5 - 19.5	kaolin	-8.96	-61.5	0.2					20.4	61.7	3.88	28.2
NA-7/2	10.5 - 11	clay/lignite, U	-9.00	-61.1	0.0	39.4		-16.1	-27.3		60.8		12.3
NA-8	8.5 - 24	granite	-9.22	-62.9	1.1	71.9	64.6	-21.9	-27.8	-8.5	14.5	3.01	59.1
NA-9	4.4 - 10	kaolin	-8.95	-60.8	0.0	72.1		-20.5	-27.1		37.1		11.8
NA-10	19.5 - 27.5	granite	-8.89	-61.5	1.6	54.6	193.67	-16.2	-26.4	0.2	33.8	1.99	40.8
NA-11	33.2 - 39	clay/lignite, U	-9.00	-65.5	1.5	7.8		-9.6			82.4		178.6
NA-12	36.5 - 39.3	clay/lignite, U	-8.87	-61.9	0.3	26.5	70.0	-16.0	-25.6	20.11	67	3.69	22.9
NA-13	42.2 - 48	clay/lignite, U	-9.24	-65.9	1.5		44.33		-27.2		68.8	2.32	22.9
NA-14	67.6 - 77.6	granite	-9.33	-64.9	0.6	9.8		-12.8		16.43	69.1		30.8
NA-15	28.8 - 31.6	granite	-9.88	-70.9	0.2	11.8		-13.7			39.4		40.1
RP-1	5 - 18	granite	-9.52	-66.9	0.2	21.0		-16.8		3.48	33.4	1.36	19.8
RP-2	25 - 43	clay/lignite, U	-9.81	-69.0	1.1	16.8		-13.2	-26.6		52.4	1.83	55.0
RP-3	25 - 48	clay/lignite, U (28 m)	-9.60	-68.2	1.0	13.3		-15.3	-26.6		59.7		24.6
RP-5	30 - 58	clay/lignite, U	-9.75	-68.4	0.0	6.4		-11.7			58.1		14.8
HR-4	46.5 - 95	granite	-9.31	-64.3	1.2	29.9		-14.5	-26.2				

Behaviour of carbon in the system

Carbon isotopes are measured in order to identify water ages, and/or to characterise water mixing processes as well as reactions within the carbon cycle. The ages of the waters calculated with ^{14}C values of DIC are in a range of 1,000 to more than 20,000 years. These ages are unexpectedly high. They are calculated without taking into account changes by chemical reactions of carbon compounds, i.e. it is necessary to look at the behaviour of carbon in more detail.

The most important reactions influencing ^{14}C and $\delta^{13}C$ ratios in dissolved inorganic carbon (DIC) are

Dissolution of sedimentary inorganic carbon (SIC) leads to a decrease in ^{14}C and increase in $\delta^{13}C$, because sedimentary inorganic carbon from the Tertiary does not contain any ^{14}C and $\delta^{13}C$-values are around 0 ‰.

Microbial degradation of sedimentary organic carbon (SOC). $\delta^{13}C$ of DOC is expected to be around -25 to -27 ‰. ^{14}C is 0 pmc in the tertiary organic material from the clay/lignite layers and expected to be around 50 to 60 ‰ in infiltration areas under forest prior to nuclear atmospheric testing (s. below).

Input of endogenic CO_2 from exhalations leads also to a decrease in ^{14}C and increase in $\delta^{13}C$ of infiltration waters. Typical $\delta^{13}C$-values determined in the Ohre rift area are -2.7 ‰ (Weise et al. 2001). ^{14}C values are as a matter of course 0 pmc.

Another important observation is the low DOC concentration in groundwater from Ruprechtov site with values in the range of approx. 1 - 10 mg C/l with only slightly elevated values in water from the clay/lignite layers compared to granite. The concentrations are much lower than those observed in the overburden from Gorleben site where concentrations up to 200 mg C/l occur, although Ruprechtov clay/lignite layers contain up to 50 % SOC. In Gorleben aquifers conversion of sedimentary organic matter occurs by microbial reduction with release of DOC (Buckau et al. 2000a). This process can also be expected at Ruprechtov site, since the prerequisites for sulphate reduction in the clay/lignite layer are fulfilled: (1) SO_4 is available in distinct amounts in all boreholes. Concentrations vary between 0.1 and 2 mmol/l (cf. Tab. 1). (2) Existence of sulphate reducing bacteria in the clay/lignite layer has exemplary been shown in sediments from borehole NA4 (Noseck et al. 2006). Carbon and sulphate concentrations and isotope data are evaluated to understand the processes at Ruprechtov site. In the following only selected results are shown. A detailed description can be found in (Noseck et al. 2007).

The isotopic analysis of DIC at Ruprechtov site shows general trends. The $\delta^{13}C$ values decrease with increasing content of DIC. Additionally, ^{14}C-values decrease with increasing $\delta^{13}C$ (Noseck et al. 2006).

Fig. 4 shows the correlation of DIC vs DOC. On the left only the biogenic DIC is plotted, assuming that the ^{13}C content of the source water is of inorganic origin with -27 ‰ and additional DIC is of organic origin. It is obvious that data for NA8 are different from the other infiltration waters with an extremely low DIC/DOC ratio. It is an additional indication that this water acts only to a low extent as source for water in the clay/lignite layers. Despite a spread of data they follow a line, with increase of biogenic DIC from infiltration waters NA10 and RP1 to waters

from the clay/lignite layer. These data sugggest that formation of DOC takes place in the clay/lignite horizon.

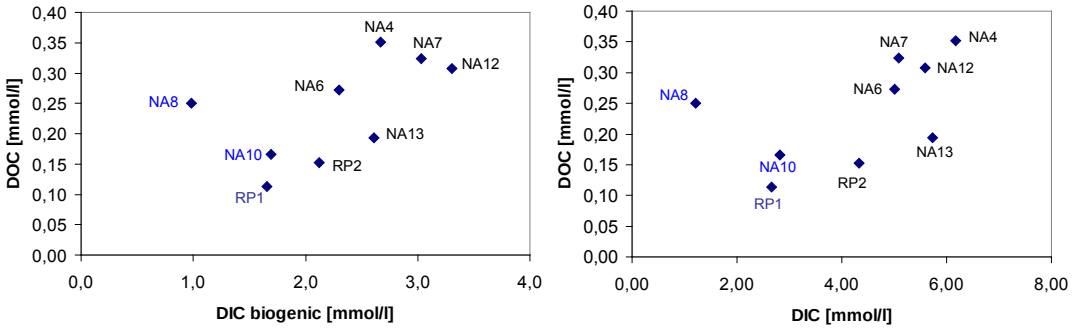

Fig. 4: DIC and biogenic DIC vs DOC in selected boreholes

If microbial activities are involved, these should be detectable, since microbial sulphate reduction is accompanied by isotope fractionation. The lighter isotope ^{32}S is preferentially metabolized by the microbes and therefore residual sulphate molecules in solution become enriched in the isotope ^{34}S. Therefore, DOC generation by sulphate reduction in the clay/lignite layers should be detectable by increased $\delta^{34}S$ values water from these layers.

The results of $\delta^{34}S$ analyses in water samples from the infiltration area as well as from clay/lignite layer are shown in Fig. 5. For the wells with infiltration water in the south and west of the area NA10 and RP1, the $\delta^{34}S$-values are low and vary between 0.2 and 3.48 ‰. Once more the water from infiltration area around NA8 is different with an even lower value of -8.45 ‰.

In contrast waters from the clay-lignite layer show increased $\delta^{34}S$-values in the range of 16.43 to 24.63 ‰. The significant enrichment of $\delta^{34}S$ in these boreholes is a clear indication that sulphate reduction occurs in the clay/lignite layers.

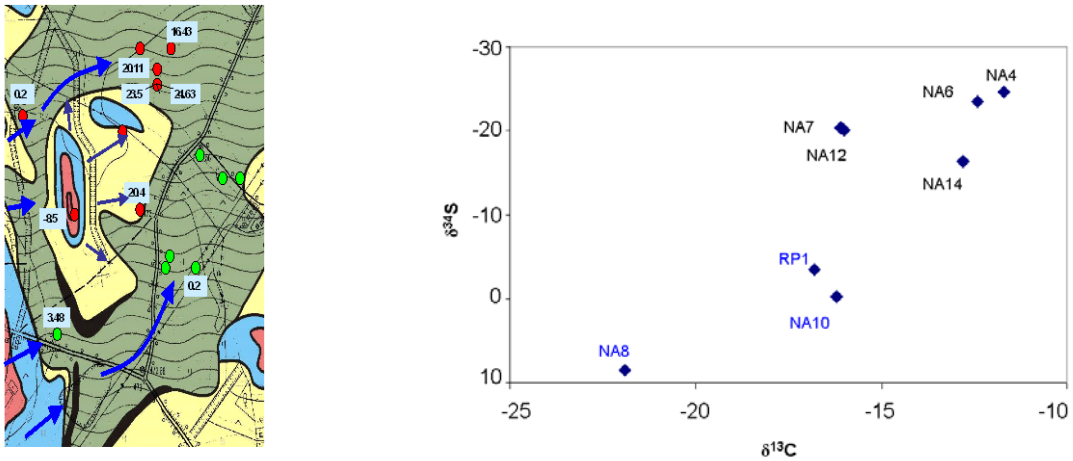

Fig. 5: Distribution of $\delta^{34}S$ in different boreholes at Ruprechtov site (left) and $\delta^{34}S$ vs $\delta^{13}C$ (right)

Conclusions

Isotope data from Ruprechtov site are evaluated with respect to the hydrogeological flow regime and behaviour of carbon in the system. The results so

far show a rather complex hydrogeological situation with infiltration areas in the outcropping granites in the western and southern part, water flow in zones of only few metres thickness, which do not represent a continuous aquifer, but distinct areas with increased water flow. There is strong indication for very local connections of the flow systems in the underlying granite and in the tertiary sediments in the northern part, where kaolin thickness is low and fault zones are expected.

The complex hydrogeological situation hampers the interpretation of the carbon isotope data. Nevertheless, a general picture can be drawn. NA10 and RP1 are considered as water from infiltration areas in the western and southern part, respectively. There is strong indication that microbial reduction of sulphate contributes to the formation of DOC and biogenic DIC in the clay/lignite layers given by differences between water from infiltration area and water from clay/lignite layers especially by increase of $\delta^{34}S$ in dissolved sulphate and increase of biogenic DIC with increasing DOC.

Acknowledgements

This work has been / is financed by the European Commission, the German Federal Minstry of Economics and Technology (BMWi) under contract no. 02 E 9551 and no. 02 E 9995 and by the Czech Radioactive Waste Repository Authority (RAWRA) under contract no. 1999/31/NACH.

References

Buckau, G.; Artinger, R.; Geyer, S.; Wolf, M.; Fritz, P.; Kim, J.I. (2000a) Groundwater in-situ generation of aquatic humic and fulvic acids and the mineralization of sedimentary organic carbon, Appl. Geochem., **15**, 819-832.

Buckau, G.; Artinger, R.; Geyer, S.; Wolf, M.; Fritz, P.; Kim, J.I. (2000b) ^{14}C dating of Gorleben groundwater, Appl. Geochem., **15**, 583-597.

Noseck, U.; Brasser, Th. (2006) Radionuclide transport and retention in natural rock formations - Ruprechtov site, Gesellschaft für Anlagen- und Reaktorsicherheit (GRS) mbH, GRS-218, Braunschweig, May 2006.

Noseck, U.; Rozanski, K.; Dulinski, M.; Laciok , A.; Brasser. Th.; Hercik, M.; Buckau, G.; Hauser, W. (2007) Characterisation of hydrogeology and carbon chemistry by use of natural isotopes – Ruprechtov site, Czech Republic, Appl. Geochem. (under preparation).

Weise, S.M.; Bräuer, K.; Kämpf, H.; Strauch, G.; Koch, U. (2001) Transport of mantle volatiles through the crust traced by seismically released fluids: A natural experiment in the earthquake swarm area Vogtland/NW Bohemia, Central Europe, Tectonophysics, **336**, 137-150.

A.5 Colloid detection in natural ground water from Ruprechtov by laser-induced breakdown detection

W. Hauser [a,*], H. Geckeis [a], R. Götz [a], U. Noseck [b], A. Laciok [c]

[a] Institut für Nukleare Entsorgung (INE), Forschungszentrum Karlsruhe GmbH D-76021 Karlsruhe, Germany
[b] Gesellschaft für Anlagen- und Reaktorsicherheit (GRS) mbH, Abt. Geochemie, Theodor-Heuss-Str. 4, D-38122 Braunschweig, Germany
[c] Nuclear Research Institute Res, Czech Republic
* Corresponding author: hauser@ine.fzk.de

Abstract

A borehole ground water sampling system and a mobile laser-induced breakdown detection (LIBD) equipment for colloid detection combined with a geo-monitoring unit have been applied to characterize the natural background colloid concentration in ground waters of the Ruprechtov natural analogue site (Czech Republic). Ground water has been sampled using steel cylinders. To minimize artifacts during ground water sampling the contact to atmospheric oxygen has been excluded. The ground water samples collected in this way are transported to the laboratory where they have been connected to a series of flow-through detection cells. Argon gas is used to press the ground water through these detection cells for colloid analysis (LIBD), pH, Eh, electrical conductivity and oxygen content. After the above mentioned analysis additional samples are taken for chemical analysis by ICP-AES, ICP-MS, IC- and DOC-detection.

Our data obtained by in-situ- and laboratory- measurements point out that the natural colloid concentration found at the Ruprechtov site is a strong function of the ground water ionic strength.

The LIBD determined natural background colloid concentrations found at Ruprechtov are compared with data of studies performed in Äspö (Sweden) and Grimsel (Switzerland).

Introduction

Colloid analysis has been performed in ground water samples collected at a site near Ruprechtov, Czech Republic. During a drilling programme clayey sediment layers with lignite intercalations and local uranium enrichment have been found. The geological situation at the Ruprechtov site is at a first glance very similar to the overburden of the Gorleben salt dome system and can serve as a natural analogue to study processes relevant for radionuclide and notably uranium accumulation in such a far-field environment. The uranium is assumed to be released from weathered granite in the neighbourhood of the investigated area and subsequently enriched within the clay/lignite sediment layers.

The migration and enrichment processes are up to now not fully understood. Aquatic colloids are known to be one parameter controlling the radionuclide mobility in ground water systems. Therefore, sampling campaigns were accomplished to gain information on the current background colloid concentration in these ground waters. Samples are taken with a modified sampling system avoiding artifial oxidation of samples through atmospheric contact. Colloid analysis was subsequently performed by laser-induced breakdown detection (LIBD) in the laboratory using a closed flow-through detection cell under oxygen exclusion. Furthermore, a complete chemical analysis of the water samples was performed.

Experimental

The principle of LIBD as well as the instrumentation for the colloid detection are described in detail elsewhere [1]. A new flow-through detection cell has been developed for water pressures up to ~35 bar. This set-up is suitable to measure on-site in-line colloids under the natural water pressure found e.g. in the Äspö Hard Rock Laboratory (Sweden) [2] or at the Grimsel Test Site (Switzerland) [3]. This detection cell has also been applied in combination with a borehole sampling system for the detection of ground water colloids at the Ruprechtov site.

For the borehole sampling five steel cylinders with 3 litres internal volume were used. These cylinders have been intensively cleaned and checked in the laboratory. The tests included leak tests as well as the examination of the compatibility of the sampling cylinder coupling to the LIBD laboratory setup, e.g. with regard to a possible release of particles from the inner container surface (e.g. corrosion products). Prior to the sampling campaign the cylinders were flushed with Argon gas and successively evacuated (pressure ~10^{-2} bar) to avoid any oxygen introduction and artificial colloid generation in the borehole during the sampling procedure.

At the Ruprechtov site a complete sampling system with cable winch, three-leg crane and sampling cylinder was installed on top of each borehole. The system allows a remote ground water sampling in deep boreholes. The locations of the boreholes are displayed in Fig. 1. Besides the investigated boreholes with sampling horizons in granite (RP1, NA8), in kaolin (NA7) and in clay / lignite sediments (NA6, NA12, NA13, NA10, RP2), a private well was sampled at a depth of about 7 m to obtain reference colloid input data upstream of the investigation area. The sampling depths in the investigated boreholes varied from –15 m to –37 m below ground level with about 1 m water column between sampling container and borehole bottom.

Several days after field sampling, each cylinder was connected in the laboratory with the LIBD setup containing the high-pressure flow-through detection cell of the LIBD system and a geo-monitoring unit consisting of pH, Eh, electrical conductivity, oxygen probes. A scheme of the corresponding laboratory setup is plotted in Fig. 2.

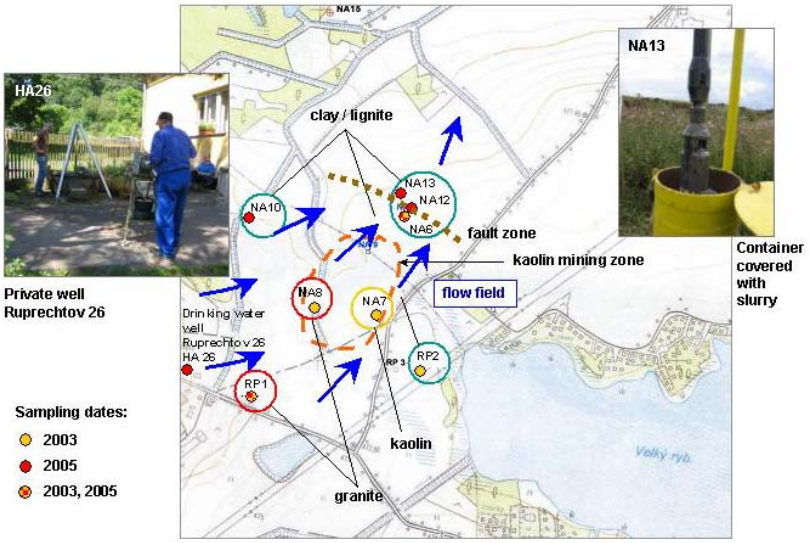

Fig. 1: Ruprechtov sampling positions

Ground water samples were collected at the outlet of the pressure holder (PH) for subsequent chemical analysis with ICP-AES, ICP-MS and for the detection of inorganic carbon (IC) and dissolved organic carbon (DOC).

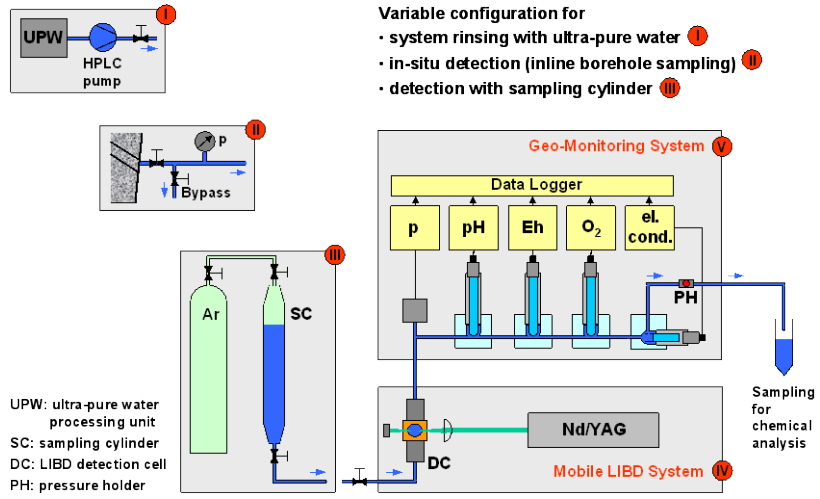

Fig. 2: Laboratory setup for in-line LIBD colloid analysis and ground water monitoring

Results

In Table 1, the measured geochemical parameters Ruprechtov ground water characteristics and colloid concentrations are summarized. The data have been measured between May, 2003 and March, 2006.

One of the aims of the study was to verify that geochemical conditions (especially weakly reducing conditions) are maintained within the sampling container during transport and storage. A comparison of Eh and pH values (RP1, NA8, NA7,

NA6) measured 14 days and 161 days after sampling show that with the exception of sample RP 2 no clear shift could be observed. We take that as an indication that the sample cylinders are gas tight and original geochemical conditions are maintained.

Eh and pH values detected in the laboratory were additionally measured with an in-situ borehole probe at Ruprechtov site (Table 1; GRS data given in brackets). In some cases, the data correspond closely with the laboratory determined data (RP1, NA8, NA7). In the case of significant deviations (NA6, NA12, NA13) it is not clear, whether hydrochemical conditions in the flow field have changed (contact with oxygen) or sampling cylinders were leaking. The fact that all Eh values measured in-situ in March 2006 were positive even though they have been negative in some boreholes (e.g. NA7 and NA6) during an earlier measuring campaign (Mai 2003), suggests a change in geochemistry with time.

Table 1: Ruprechtov ground water properties and colloid concentrations

Ground water characterisation (geological horizon)	Borehole ID	Sampling depth m	Sampling date	Electrical conductivity mS/cm	Redox (AgCl) mV	Eh (SHE) mV	pH	Colloid diameter nm	Colloid conc. µg/l
Private well	**HA26**	- 7.4	27.7.05	**0.500**	**73**	**287**	**7.02**	**347**	**361**
Ground water from (altered?) granite	**RP 1**	- 15	21.5.03	0.320	101 (49)	315 (246)	6.35 (6.81)	2170	2306
				0.303 [a]	**20** [a]	**234** [a]	**6.50** [a]	**830** [a]	**193** [a]
			27.7.05	**0.350**	**39**	**253**	**6.78**	**910**	**281**
			30.3.06		(- 25)	(172)	(6.45)		
	NA 8	- 18	21.5.03	0.216	19 (48)	233 (245)	6.16 (6.2)	726	1676
				0.206 [a]	**20** [a]	**234** [a]	**6.30** [a]	**422** [a]	**170** [a]
Ground water from kaolin	**NA 7**	- 17.5	21.5.03	0.673	- 178 (- 232)	34 (- 35)	7.77 (8.0)	169; 918	3; 239
				0.640 [a]	**- 190** [a]	**24** [a]	**7.85** [a]	**228** [a]	**239** [a]
			30.3.06		(- 180)	(17)	(7.47)		
Mixed ground water from clay/lignite	**NA 6**	- 35	21.5.03	0.530	- 257 (- 360)	- 43 (- 163)	7.28 (8.0)	overflow	overflow
				0.520 [a]	**- 280** [a]	**- 66** [a]	**7.39** [a]	**165; 1463**	**18; 271**
			26.7.05	**0.590**	**- 111**	**103**	**7.53**	**232; 1167**	**10; 97**
			27.7.05	0.590	0	214	7.65	170; 1367	4; 463
	NA12		25.5.04		(- 275)	(- 78)	(6.5)		
		- 37	26.7.05	**0.480**	**87**	**301**	**6.86**	**1177**	**744**
			30.3.06		(36)	(233)	(6.44)		
	NA13		28.5.04		(- 275)	(- 78)	(7.28)		
		- 36 [b]	26.7.05	**0.620** [b]	**39** [b]	**253** [b]	**7.57** [b]	**772** [b]	**688** [b]
	NA10		26.5.04		(43)	(240)	(7.43)		
		- 26	26.7.05	**0.430**	**47**	**261**	**7.19**	**329; 1642**	**15; 359**
			30.3.06		(- 109)	(88)	(6.89)		
	RP 2	- 26	21.5.03	**1.050**	**- 54**	**160**	**7.30**	**84; 1589**	**1; 396**
				0.970 [a]	105 [a]	319 [a]	7.40 [a]	1519 [a]	448 [a]

[a] : Detection 161 days after borehole sampling
( ): GRS data, in situ detected in borehole

[b] : After lifting, container was completely covered with slurry

The measured pH/Eh-data of different ground waters measured at the Ruprechtov site suggests that the system is anoxic and buffered by the Fe(II)/Fe(III) or Mn(II)/Mn(IV) redox pairs [4]. Similar data were determined in ground water samples taken along the access tunnel in the underground laboratory Äspö / Sweden, and in Forsmark / Sweden (Site investigation program).

Colloid concentrations vary between 170 and 740 µg/l with a number weighted mean diameter mostly larger 450 nm (Table 1). As such large colloids are expected to settle in the absence of hydrodynamic forces as e.g. fast ground water flow velocities, it is presently not clear, whether those colloids are stable for long time periods. The concentrations may, however be considered as upper limit values. A clear correlation of colloid concentration with element concentrations could not be observed. Therefore, we cannot draw any conclusions towards the chemical nature of the colloids. Furthermore,

a dependency of the detected colloid concentrations on the sampling site, i.e. the borehole geology, could not be drawn.

DOC (dissolved organic carbon) concentrations were rather low (1 – 4 mg/l) and did not show any correlation with LIBD determined colloid concentrations. This is a clear difference to the Gorleben system, where an increase of ground water DOC concentrations up to ~ 100 mg/l and the production of humic/fulvic acids due to the microbiological turn-over of lignite intercalations has been observed [5]. Such significant differences call for a closer inspection of the geochemical conditions and most notably the type of organic material and the microbiology in this system.

Earlier colloid studies claimed the existence of a significant correlation of colloid concentrations in ground water with the salinity (ionic strength) of the ground water [6, 7]. New LIBD results from in situ investigations at Äspö corroborate earlier studies and show colloid concentrations < 0.1 µg/l for ground waters with chloride concentrations ≥ 4 g/l. In two high saline ground waters with chloride concentrations > 10 g/l, the colloid concentrations were even close to the LIBD detection limit (~ 8 ng/l).

A comprehensive representation of colloid concentrations in different water samples as determined by LIBD as a function of the respective ionic strength is given in Fig. 3. Increasing ionic strength usually forces colloid aggregation which is reflected in lower colloid concentration in the respective groundwater.

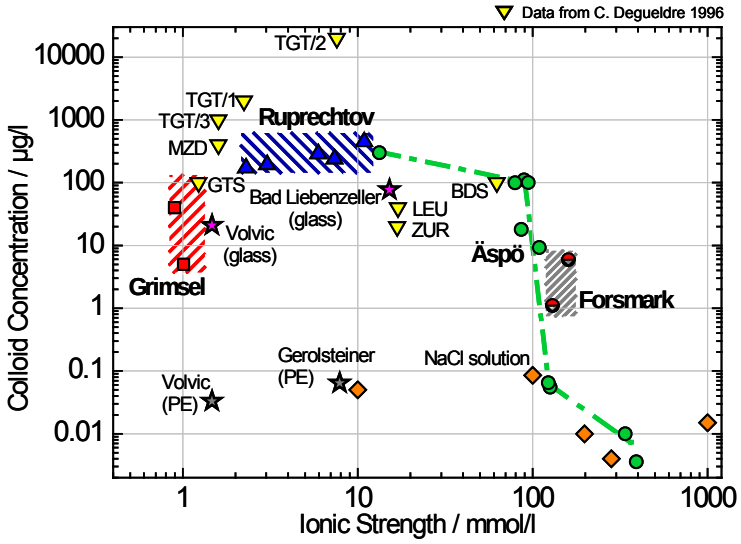

Fig. 3: Comparison of colloid concentration in different types of natural ground water, mineral water and synthetic NaCl-solution versus ionic strength (8 Ruprechtov; □ Grimsel CRR tunnel; O Äspö tunnel; ψ mineral water; M NaCl solution ; X Data from [8]: TGT: transit gas tunnel, MZD: Menzenschwand, GTS: Grimsel test site, BDS: Bad Säckingen, LEU: Leuggern, ZUR: Zurzach)

In the Ruprechtov ground water samples the ionic strength varies in the range of 2 x 10^{-3} to 1.1 x 10^{-2} mol/l without any significant influence on the measured colloid concentration. The broad bandwidth of detected colloid concentrations in ground water of ionic strength < 100 mmol/l (Grimsel, Ruprechtov) suggests that different parameters besides ionic strength as e.g. pH and/or ground water velocity may control the actual colloid concentrations.

However, our studies suggest that an ionic strength of 100 mmol/l represents some kind of upper limit: colloids may persist in ground water with ionic strengths below this value for considerable time scales and variable colloid concentrations. At ionic strengths above 100 mmol/l natural aquatic colloid stability is effectively decreased. As a consequence, for ground water samples from Äspö and simulated NaCl

solutions a clear dependency of the maximum colloid concentrations with the salinity of the solution is found.

Conclusions

The investigations demonstrate that the mobile LIBD with a geo-monitoring unit and a borehole sampling system allows the characterization of natural ground water and colloids under in-situ conditions. In cases where on-site analysis is not possible, a remote borehole sampling technique with steel cylinders and the subsequent sample characterization with in-line LIBD detection of colloids and measurement of electrical conductivity, pH, Eh is found to provide reasonable data. For this strategy it is shown that the genuine redox conditions of samples can be maintained in most cases with minimal access of atmosphere oxygen.

Our in-situ- and laboratory- obtained data point out that the relevant natural colloid concentration can be strongly limited by the ionic strength of the natural ground water. A critical value of 100 mmol/l for the ionic strength is suggested. Above this limit natural groundwater colloids appear to be rather unstable. The quantitative role of dissolved natural organic matter as a colloid stabilizing component is still unclear and requires further studies in this context. The measured ionic strengths of the sampled Ruprechtov ground waters are fairly below this limit (I < 100 mmol/l) so that the relatively high colloid concentrations found are coherent.

References

[1] W. Hauser, H. Geckeis, J.I. Kim, Th. Fierz, A mobile laser-induced breakdown detection system and its application for the in situ-monitoring of collod migration, Coll. Surf. 203, 2002, 37-45

[2] W. Hauser, H. Geckeis, R. Götz, In situ determination of natural ground water colloids in granite shear zones along the Äspö HRL Tunnel by LIBD, 27th Int. conf.on Scientific Basis for Nuclear Waste Management, Kalmar, S, June 15- 18, 2003

[3] Geckeis, H., Schäfer, T., Rabung, T., Hauser, W., Möri, A., Missana, T., Eikenberg, J., Degueldre, C., Fierz, T., Alexander, W.R., Inorganic colloid borne actinide migration studied under in-situ conditions at the Grimsel test site, 9th Int. conf. on Chemistry and Migration Behavior of Actinides and Fission Products in the Geosphere, Migration ’03, Gyeongju, Korea, Sept. 21- 26, 2003

[4] L. Sigg, W. Stumm, Aquatische Chemie, VDF, Zürich, Teubner, Stuttgart, 1989

[5] G. Buckau, R. Artinger, P. Fritz, S. Geyer, J.I. Kim, M. Wolf, Origin and mobility of humic colloids in the Gorleben aquifer system, Appl. Geochem., 15 (2000) 183-191

[6] Degueldre, C., Triay, I., Kim, J.I., Vilks, P., Laaksoharju, M., Miekeley, N., Ground water colloid properties: a global approach, Appl. Geochem. 15 (2000) 1043-1051

[7] Hauser, W., Geckeis, H., Götz, R., In situ determination of natural ground water colloids in granite shear zones along the Äspö HRL Tunnel by LIBD, 27th Int. Conf. on Scientific Basis for Nuclear Waste Management, Kalmar, S, June 15- 18, 2003

[8] C. Degueldre, R. Grauer, A. Laube, A. Oess, H. Silby, Colloid properties in granitite ground water systems. II. Stability and transport study, Appl. Geochem. 11 (1996) 697-710

A.6 Uranium enrichment at Ruprechtov Site - characterisation of key processes

Vaclava Havlova[1*], Ulrich Noseck[2], Radek Cervinka[1], Thomas Brasser [2,]
Melissa Denecke[3], Mirek Hercik [1]

[1]Nuclear Research Institute Rez plc, Waste Disposal Dpt., Husinec- Rez, 250 68 Rez (CZ)
[2]Gesellschaft für Anlagen- und Reaktorsicherheit, Theodor-Heuss-Str. 4, 38122 Braunschweig (DE)
[3]Forschungszentrum Karlsruhe, Institut für Nukleare Entsorgung, P.O. Box 3640, 76021 Karlsruhe, (DE)
* Corresponding author: hvl@ujv.cz

Abstract
Ruprechtov natural analogue site is a unique example for association of U-rich and organic layers within clay sediments, being underlain by granite. It can be used as a good example to demonstrate that clayey sediments can exert a strong barrier function for uranium migration, when specific prerequisites are fulfilled. Sedimentary organic matter degradation is biologically mediated and influences dissolution of sedimentary carbonate and U immobilisation. Uranium is immobilised due to complex processes, sorption of U onto arsenopyrite, U(VI) reduction to U(IV), interaction with microbially produced phosphate and forming tetravalent U mineral phases. U remains stable and immobilised for time periods relevant for PA.

Introduction
Ruprechtov natural analogue site is a unique example for association of U-rich and organic layers within clay sediments, being underlain by granite. This site has been extensively studied in order to understand the processes of U-enrichment as a natural analogue for radionuclide transport and retention in organic rich clay formations, which often represent constituent parts of the overburden of potential host rocks for radioactive waste disposal. In particular, investigations of immobile uranium forms and organic matter performed within the FUNMIG project contributed to the understanding of key processes, which occurred at the site.

Uranium forms in the sediment
The geological situation of the site is described in detail elsewhere (Noseck et al., 2006; Havlova et al., 2007). The most important feature, relevant to this study is the occurrence of lignitic-like layers, heterogeneously distributed within the sedimentary sequence. Moreover, U-enriched seams were identified on the site. They occur in the direct vicinity of these lignite-rich argillaceous sedimentary layers with concentrations up to 400 ppm. (Noseck et al., 2004). Even though organic matter is usually presumed

to be an efficient U sorbent, uranium was not directly accumulated within the organic layers, but only in their vicinity. The further striking inconsistency found on the site was the discrepancy between the high content of sedimentary organic matter (up to 40 % SOC) and its low content in the groundwater (max. 5 mg/l), accompanied also with low content of colloids (cf. e.g. .Noseck and Brasser, 2006).
Modern material surface analyses (micro x-ray fluorescence µ-XRF and micro x-ray absorption fine structure µ-XAFS) methods were employed to assess mechanisms leading to immobilization of uranium. µ-EXAFS and µ-XRF results showed uranium to be present as a tetravalent phosphate/oxide in the regions studied and that U(IV) was associated with As(V) (Fig. 1). Arsenic is present in the sediment as either As(V) or As(0); no evidence for As(III) is found. (Denecke et al., 2007a). Sequential extraction as a broadly used tool confirmed the association of U with As and moreover with P (Denecke and Havlova, 2007b).

Fig. 1: *Left: U L3 µ-EXAFS recorded at the position in the bore core indicated on the right. And corresponding Fourier transformed data. Right: µ-XRF-elemental distribution of Fe, As and U in a 2D-depth profile from near the surface to app. 225 µm below the surface. Dark pixels represent areas with relatively high and light areas with relatively low element content (Denecke et al. 2005)*

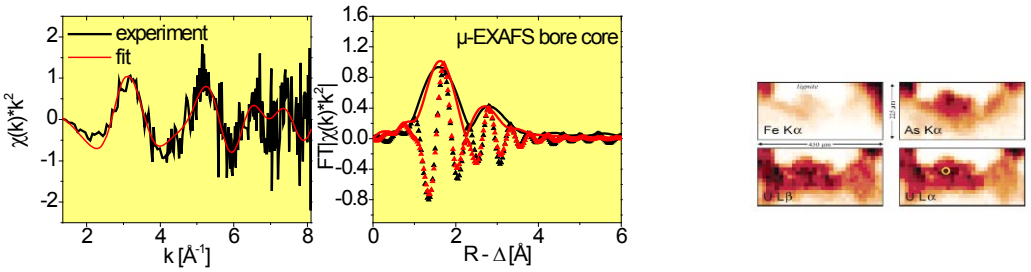

Mineralogical investigation performed by ASEM in combination with microprobe identified in the forms of either primary U-bearing detritic minerals (xenotime, zircon, monazite) or secondary minerals (ningyoite, uraninite) (Noseck et al. 2007a). Moreover, very rare grains of non-identified uranium phases were observed (probably U(VI) sulphate). Ningyoite, also detected by micro structural analyses, occur in the form of small crystals, with dimensions below 5 µm. µ-XRF showed it accumulated on As-rich layers on the surface of iron sulphide minerals (Denecke et al., 2007).

Furthermore, a detailed complementary method for analysing uranium (IV) and uranium (VI) proved that both U(IV) and U(VI) forms existed in the Tertiary clay horizon. The dominant fraction was U(IV) and its content varied from app. 50 to 90 % in the investigated samples. The generally low $^{234}U/^{238}U$-activity ratios (< 1) in the uranium(IV) fraction gave evidence that this phase was rather stable and immobile over geological time scales (Noseck et al. 2007a, Suksi et al. 2007).
All of that evidence suggest reducing conditions being established within the Tertiary sediment over very long time frames but did not explain the correlation of the U immobilisation process with organic matter occurrence in the Tertiary sediments. Therefore, the behaviour of organic matter and its impact on U immobilisation is another focus of the study within FUNMIG.

Sedimentary organic matter on the site

Sedimentary organic matter (SOM) composition
Sedimentary organic matter (SOM) from the clay/lignite layers was studied using methods from coal micropetrography aiming to characterize plant remnants according to their origin, morphology and optical qualities dependent on the degree of coalification. The study showed that SOM at Ruprechtov site was generally formed by partly dispersed matter with a low stage of coalification. The stage of coalification goes up to lignite or brown coal. The main components of detritic and xylodetritic coal samples and clay-lignite samples are mineral admixtures and huminite maceral groups. Huminite is represented by fragments of plant tissues and formations of lignite-cellulose character. Organic matter probably originated from peat bogs with clastic sedimentation under changing redox conditions (for details see Cervinka et al., 2007). Total organic carbon (TOC) content varies between 0.1 to app. 40 wt.%. $\delta^{13}C$ values of about –27 ‰ in sedimentary organic matter correspond to carbon from terrestrial environment, for example peat bog (Noseck et al. 2007b).
From a chemical-analytical point of view SOM is composed of humic substances, non-humic substances, bitumens and kerogen. Three different fractions can be distinguished in humic substances: humic acids (HA), fulvic acids (FA) and humins. Investigations by the alkali separation method showed that sedimentary organic matter within Tertiary sediments contain only a very small amount of humic acids (0.15%). Besides, those are released only to very low extent into the groundwater where dissolved organic carbon (DOC) was predominantly formed by fulvic acids (DOC up to 5 mg/l, MALDI TOF analyses). DOC released from sedimentary organic matter shows as expected similar $\delta^{13}C$ values of about –27 ‰ as SOM.

Sedimentary organic matter (SOM) degradation
Several indices signalled microbial degradation of SOM in the clay/lignite layers. Furthermore, laboratory data (Abdelous et al. 2007) suggested that indigenous sulphur reducing bacteria, extracted from samples taken at the site, helped maintaining the redox potential low enough for reduction of U(VI) to U(IV). They also very likely played an important role during formation of sulphide minerals, as pyrite, which are frequently found in the clay/lignite layers at the site. Their potential impact is shown in Fig. 2. In this experiment the microbial reaction was stimulated by addition of sulphate, lactate and phosphate at 22°C. During sulphate reduction by-products such as thiosulphate (S_2O_3) formed and ultimately were reduced into sulphide. The sudden drop of sulphide concentration is due to precipitation of sparingly soluble iron sulphide.

Fig. 2: *Evolution of sulphate, thiosulphate and sulphide concentrations in sediment/GW-system NA4-33. Growth of SRB was stimulated by addition of sulphate, lactate and phosphate at 22°C (Abdelous et al. 2007)*

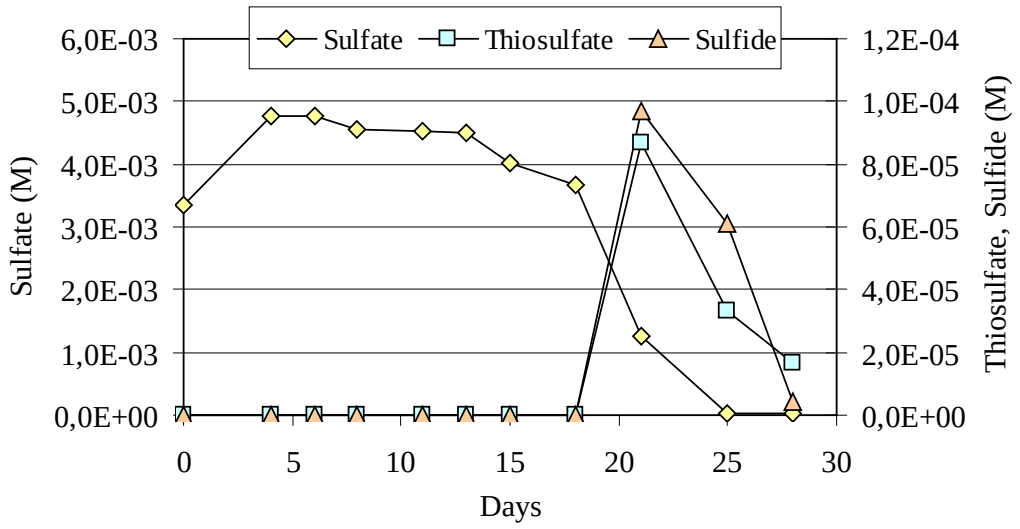

Generally, degradation of organic matter can follow the scheme published in (Buckau et al. 2000). Microbial processes lead to oxidation of SOC and reduction of oxidising agents, like SO_4^{2-} or NO_3^-. SOC is then partly oxidised to dissolved inorganic carbon (DIC with $\delta\ ^{13}C$ values of about –27 ‰) and partly released as DOC, i.e. humic, fulvic and hydrophilic acids (with $\delta\ ^{13}C$ value also about –27‰).

The first indication of the microbial mediated process at Ruprechtov site is presented in Fig.3. Dissolved inorganic carbon concentration increase, particularly in the clay/lignite horizon, is generally followed by increase of DOC release. We assume that water from borehole NA8, which falls slightly out of the trend, only to very low extent acts as infiltration water for the clay/lignite area.

Figure 3*: DIC production due to DOC oxidation (Ruprechtov groundwater samples. The right upper part – Tertiary lignite)*

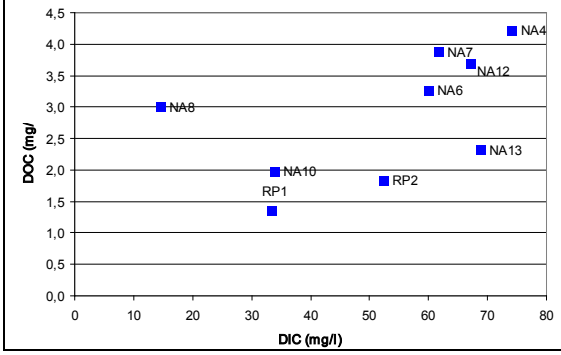

Figure 4*: 1/DIC vs. $\delta^{13}C$ in different wells from Ruprechtov site*

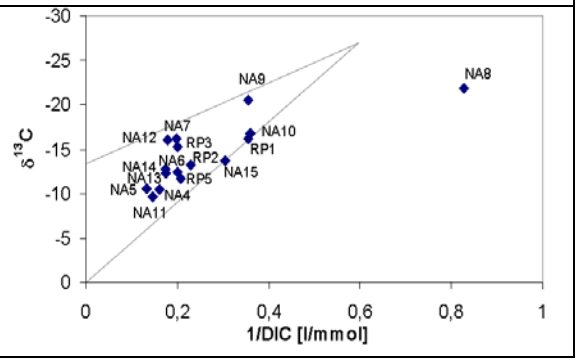

The more DIC is released the more DOC is oxidised. The formation of carbonic acid releases one proton and dissolves as HCO_3. In contact with carbonate containing sediments (sedimentary inorganic carbon - SIC) this process results in its dissolution and additional release of DIC of sedimentary origin with $\delta^{13}C$-values of app. 0 ‰. Isotopic signature of DOC in different boreholes leads to value of $\delta^{13}C$ approx. -13.5 ‰ (equimolar mixing line, s. Buckau et al., 2000). This fact could be considered as an indication of mixing of both processes: organic matter oxidation and sedimentary inorganic carbon dissolution (cf. Fig. 4).
Furthermore, as described above, mineralisation (oxidation) of SOC is accompanied by reduction of oxidising agents as SO_4^{2-} and NO_3^- if present, i.e. a decrease of these species concentrations with increasing DOC is expected. This general trend is traceable within species concentration analyses in the Ruprechtov groundwater as shown in Fig. 5. On the other hand, general reverse increasing trend with increasing DOC could be spotted for phosphates (PO_4^{3-}). Those are produced by microbial mediated SOC metabolism, causing reduction of sulphates and nitrates and release of originally SOC-bound phosphates into the solution (cf. Fig. 5).

Fig. 5: *Concentration of sulphates, nitrates and phosphates in Ruprechtov wells vs. DOC (mg/l).*

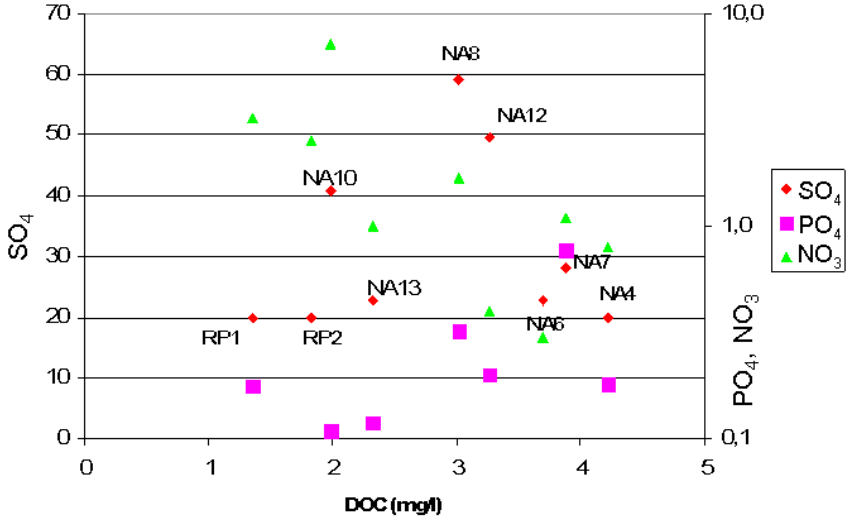

The last (but not least) indication for microbial degradation of SOM is found in isotopic signatures of groundwater sulphate in the clay/lignite layers, being enriched in ^{34}S-isotopes ($\delta^{34}S$ in the range of 16.43 to 24.63 ‰) compared to those observed in the infiltration water ($\delta^{34}S$ ranging from -8.5 to 3 ‰). The enrichment is a result of microbially driven reduction of sulphate and concurrent enrichment of sulphide with lighter ^{32}S. Fig. 6 gives a very clear explanation of the processes. Firstly the origin of the samples can be distinguished: the samples in the upper right are from Tertiary clay boreholes, the others are from infiltrating water from granite. With input of inorganic carbon from two sources in the clay lignite layers (SOM and SIC) $\delta^{13}C$ approaches values in the range of -13.5 ‰ in the clay/lignite samples. The correlated increase of $\delta^{34}S$ in groundwater sulphate, in the these samples clearly shows that this process is microbially driven.

***Figure 6**: Isotopic composition of Ruprechtov groundwater samples ($\delta^{13}C$ vers. $\delta^{34}S$) in samples from infiltration boreholes (granite) and from clay/lignite layers*

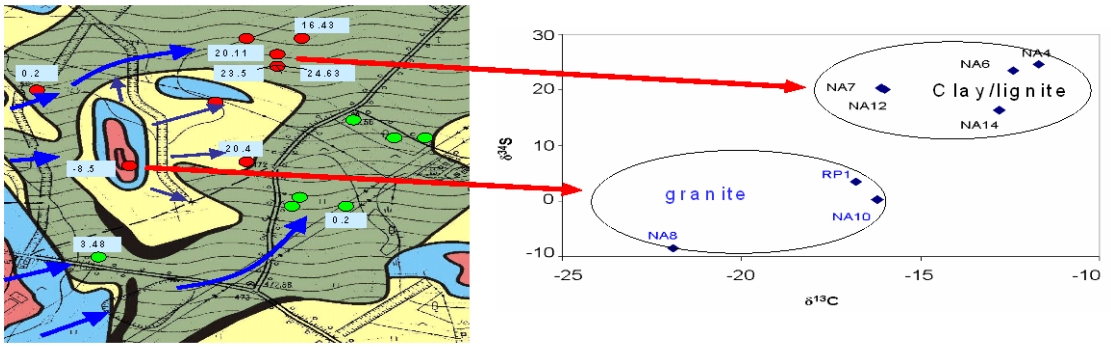

The reduction of sulphates to sulphides resulted in the formation of pyrites. Fig.7 shows an image of framboidal pyrite, whose shape is a strong indication for the mineral growth by activity of microbes. Even if microbes are not directly involved in the reduction of uranium, the formation of sulphide minerals seem to be very important for uranium immobilization at Ruprechtov site. One of the major uranium enrichment processes is assumed to be by reaction with arsenopyrite layers on pyrite nodules (s above).

***Fig. 7:** Microbially formed framboidal pyrite from clay/lignite layer*

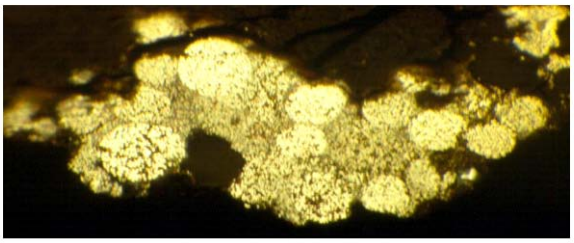

DOC content in the groundwater

Still there remains a question why the content of DOC and colloid are so low in the groundwater on the Ruprechtov site. The two possible reasons are as follows:

1. Sedimentary organic matter is not easily degradable. Simple supplement leaching experiments, using solution with different pH (6; 6.5; 7; 8 pH buffered

with 0.1 M phosphate puffer) in contact with organic rich sedimentary Ruprechtov samples (0.97 %; 2.33 %; 4.04 %; 4.07 %; 7.85 % TOC in sample) showed that the max. 4 % of TOC was released into the solution. The rest remains within the sediment.

2. Strong sorptive properties of clay on the site. Sorption experiment with natural humic acid Leonardite 1S104H (IHSS), Ruprechtov clay (TOC 0.14%) and standard SWy-2 clay showed that sorption of humic acid is sorbing more intensively on Ruprechtov clay samples than on smectite clay standard SWy-2

Uranium immobilisation on the Ruprechtov site

On the basis of the presented results a conceptual model of Uranium immobilisation is proposed:
Sedimentary organic matter did not play a so important role as a direct sorbent but as a reducing conditions mediator and the source of substance necessary for uranium mineral formation. It can be concluded that SOC within the sedimentary layers was (and to some extent still is) microbially oxidised. DOC was released by this process, providing protons to dissolve SIC. Oxidation agents, in particular SO_4^{2-} were reduced leading to the formation of iron sulphides like pyrite (FeS_2). Reducing conditions, being maintained amongst others by sulphate reducing bacterias, lead to reduction of As. Arsenic sorbed onto FeS_2 surfaces, formed thin layers of arsenopyrite (FeAsS) precipitate. Uranium U(VI), originally being released from the underlying granite, was reduced to U(IV) on the FeAsS surfaces and reacted with phosphates PO_4^{3-}, produced by microbial SOC oxidation. Uranium phosphates (ningyoite) were thus formed. These uranium(IV) minerals have been stable and immobile over geological time frames.

Summary and Conclusions

Ruprechtov site can be used as a good example to demonstrate that clayey sediments can exert a strong barrier function for uranium migration, when specific prerequisites are fulfilled. Key processes for the behaviour of organic matter and for immobilisation of uranium in the clay/lignite layers have been identified. Sedimentary organic matter contains only a small fraction of humic acid (0.15%). The low content of DOC in the groundwater could be caused either by the low SOC availability for degradation or by the high sorptive affinity of the clay for organic degradation products. The SOM degradation is microbially mediated, influencing also dissolution of sedimentary carbonate and uranium immobilisation by formation of pyrite as consequence of sulphate reduction, by maintaining reducing conditions in the clay/lignite layers, and by production of phosphates.

Abbreviations:
SOC – sedimentary organic carbon; SIC – sedimentary inorganic carbon, DOC – dissolved organic carbon (in groundwater), TOC – total organic carbon (in the sediment), SOM – sedimentary organic matter

Acknowledgement

The research was supported by the German Federal Ministry of Economics and Technology (02E9551, 02E9995), RAWRA (CZ), EC FUNMIG project - 6th European Framework Programme and the Czech Ministry of Trade and Industry (POKROK 1H-PK25).

References

Abdelous A, Grambow B, Andres Y, Noseck U (2007). Uranium in argillaceous sediments: sorption/desorption processes and microbial effects. Submitted to Environ. Sci. Technol.

Buckau G. et al. (2000): Groundwater in-situ generation of aquatic humic and fulvic acids and the mineralization of sedimentary organic carbon. Appl. Geochemistry, 15, pp. 819-832.

Cervinka R., Havlova V., Noseck U., Stamberk K. (2007): Characterisation of organic matter and natural humic substances extracted from real clay clay environment (Ruprechtov, CZ). S+T presentation 3rd annual meeting of IP FUNMIG, Edinborough, GB, Nov. 25 – 29, 2007.

Denecke M. and Havlova V. (2007a): Elemental correlations observed in Ruprechtov Tertiary sediment: micro-focus fluorescence mapping and sequential extraction. In Buckau G. and Kienzler B., Duro L., Montoya V. (eds.): 2nd Annual Workshop Proceedings of the IP Project FUNMIG", 315 ppt. SKB Technical Report, TR-07-05.

Denecke, M.A., Somogyi, A., Janssens, K., Simon, R., Dardenne, K., Noseck, U., (2007b). Microanalysis (micro-XRF, micro-XANES and micro-XRD) of a Tertiary sediment using synchrotron radiation. Microscopy Microanal. 13(3), 165-172.

Denecke, M.A., Janssens, K., Proost, K., Rothe, J. & Noseck, U. (2005): Confocal Micrometer-Scale X-ray Fluorescence and X-ray Absorption Fine Structure Studies of Uranium Speciation in a Tertiary Sediment from a Waste Disposal Natural Analogue Site.- Environ. Sci. Technol. 39 (7), pp. 2049-2058,.

Havlová V., Brasser Th., Cervinka R., Noseck U., Laciok A., Hercik M., Denecke M., Suksi J., Dulinsku M., Rozanski K. (2007): Ruprechtov Site (CZ): Geological Evolution, Uranium Forms, Role of Organic Matter and Suitability as a Natural Analogue for RN Transport and Retention in Lignitic Clay. Proc. Of Reposafe Conference, Braunschweig Nov. 5 – 9- 2007, submitted.

Noseck, U., Brasser, Th., Raijlich, P., Laciok, A., Hercik, M., 2004: Mobility of uranium in Tertiary argillaceous sediments - a natural analogue study. Radiochim. Acta 92, 797-803.

Noseck U. and Brasser Th. (2006): Radionuclide transport and retention in natural rock formations. Ruprechtov site. GRS.218.

Noseck U, Brasser Th, Suksi J, Havlova V, Hercik M, Denecke MA, Förster HJ (2007a): Identification of Uranium enrichment Scenarios by Multi-Method Characterization of Immobile U phases. Submitted to Physics and Chemistry of Earth.

Noseck U. et al.(2007b): Characterisation of Hydrogeology and carbon chemistry by use of environmental isotopes – Natural Analogue site Ruprechtov, Czech Republic. To be submitted to Applied Geochemistry.

Suksi J, Noseck U, Salminen S (2007): Uranium redox state and $^{234}U/^{238}U$ ratio analyses in uranium rich samples from Ruprechtov site. In Buckau G. and Kienzler B., Duro L., Montoya V. (eds.): 2nd Annual Workshop Proceedings of the IP Project FUNMIG", 315 ppt. SKB Technical Report, TR-07-05.

A.7 Uranium enrichment at Ruprechtov Site - uranium disequilibrium series and geological development

Ulrich Noseck[1*], Juhani Suksi [2], Vaclava Havlova [3], Thomas Brasser[1]

[1] Gesellschaft für Anlagen- und Reaktorsicherheit (GRS) mbH (D)
[2] University of Helsinki (FIN)
[3] Nuclear Research Institute (NRI) (CZ)

* Corresponding author: Ulrich.Noseck@grs.de

Abstract

As part of the characterisation of immobile uranium forms at Ruprechtov site uranium disequilibrium series, as well as separation of U(IV) / U(VI) and sequential extraction with subsequent analysis of the $^{234}U/^{238}U$ activity ratio in the distinctive phases are performed on samples from the uranium-enriched clay/lignite layers. The observations of $^{234}U/^{238}U$ and $^{230}Th/^{238}U$ activity ratios below unity and very low $^{234}U/^{238}U$ ratios between 0.14 and 0.8 in the U(IV)-bearing fractions in the majority of samples clearly show that the predominant part of uranium was fixed over very long time scales in the form of U(IV) minerals. This finding is in agreement with results from other analyses and supports the scenario outcome of the geological development of the site assuming that uranium input occurred preferentially during the Upper Tertiary. The occurrence of immobile U(VI) with activity ratios above one indicates some recent uranium input.

Introduction

Major focus on the investigations at Ruprechtov site is put on the uranium accumulation in clay/lignite layers at the interface of kaolin and pyroclastic sediments (e.g. Noseck et al. 2007). By application of different microscopic and macroscopic methods immobile uranium phases are characterised in order to understand the whole uranium enrichment scenario. In particular, analyses of uranium disequilibrium series and $^{234}U/^{238}U$ activity ratios (ARs) in different phases separated by wet chemical U(IV)/U(VI) separation and sequential extraction methods give insight into time frames of enrichment and stability of distinct uranium forms. First results of U(IV)/U(VI) separation have been discussed at the 2nd annual workshop. In this presentation new results are presented and it is shown how these results correlate to the assumed geological development of the site.

Experimental Method

U series disequilibrium measurements have been performed over several years to date bulk U accumulations. The sample material was extracted in boiling concentrated HNO_3

to dissolve U. ^{238}U, ^{234}U and ^{230}Th were analysed applying both liquid-liquid extraction and ion exchange methods. Radionuclide concentrations were measured by α-spectrometry.
Oxidation states U(IV) and U(VI) were determined using a wet chemical method as decscribed in (Noseck et al. 2007). Dissolution of U(IV) and U(VI) phases was performed by extracting the sample material under anoxic conditions in an ultrasonic bath with a mixture of 4 M HCl and 0.03 M HF under Ar-atmosphere for 10 min. The solid to solution ratio was adjusted to about ~0.1. The solution obtained was fed into an anion-exchange column. U(IV) passes the column, whereas U(VI) is retained. U(IV) was collected in the first 20 ml and U(VI) then eluted with 20 ml of 0.1 M HCl. Separation is quantitative and no overlap of U(IV) and U(VI) fractions has been observed in tracer experiments. Concentration of ^{234}U and ^{238}U in the U(IV) and U(VI) fractions were determined using the procedure described above.

A sequential extraction (SE) scheme consisting of five steps was applied to samples from the clay/lignite horizon. The samples were leached using the following different extractants to identify and quantify uranium association in the sediment:

1. U bound onto exchangeable sites (leaching with magnesium chloride)
2. U bound to carbonates (leaching with ammonium acetate with acetic acid)
3. U associated with Fe/Mn oxides (leaching with hydroxylamine hydrochloride in acetic acid)
4. U bound in reduced form/onto organic matter (leaching with H_2O_2 and HNO_3)
5. U in residuum (boiling in HNO_3)

Uranium concentrations and isotope activities in different steps were determined as described above.

Results and Discussion

U series data obtained from analyses of clay/lignite samples from several boreholes are presented in Fig. 1 in the form of Thiel's diagram. By considering a closed system, the diagram can be divided into four segments, which are determined on the one hand by the $^{234}U/^{238}U$ equilibrium line (i.e. AR =1) and on the other hand by a line obtained when a tangent is drawn on the closed system chain decay curves evolving towards radioactive equilibrium ($^{230}Th/^{238}U$=1 and $^{234}U/^{238}U$=1) after sudden accumulation and removal of U. The segments denoted S1 and S2, between the U addition and removal areas, cannot be reached by closed system chain decay. Data plots in segment S1 represent samples in an open system from which ^{234}U has been selectively removed. Segment S2 can be reached if samples with recently accumulated U (within the last million years) have subsequently experienced U removal.
Most of the data points appear in segment S1, indicating that the system in the clay/lignite layers has been open but stable conditions with respect to bulk U occurred. AR<1 is caused by ^{234}U removal from the system as a consequence of α–recoil and related processes. Thus at least a significant fraction of uranium in the clay/lignite horizon is more than 1 Million years old, i.e. beyond the time range of the U series method. A number of data points in the bulk U addition area give rise that some uranium accumulation is still in progress.

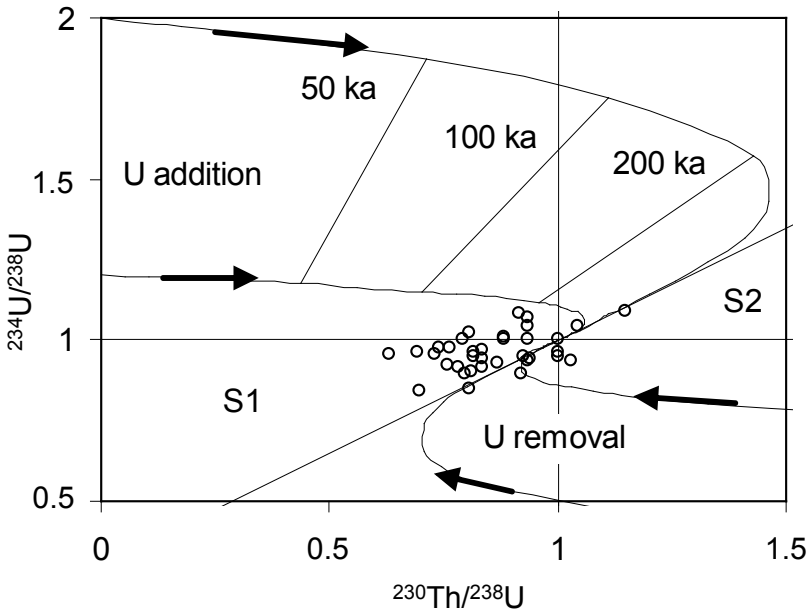

Fig. 1: *$^{230}Th/^{238}U$ and $^{234}U/^{238}U$ activity ratios of samples from the clay/lignite horizon plotted in Thiel's diagram with isochrones. Curves started from $^{230}Th/^{238}U=0$ and $^{234}U/^{238}U=1.2$ and 2 in the U addition area have been taken as examples to show how activity ratios change as a function of time in the closed system after sudden U accumulation. Curves in the U removal sector describe changes in isotope ratios back to secular equilibrium after sudden U removal.*

In order to better understand the uranium enrichment and distinguish between different immobile phases, a separation method for U(IV) and U(VI) (Ervanne et al. 1996) has been modified and applied to samples from the clay/lignite layers from different boreholes NA6, NA11, NA12, NA13 and NA14. The results are listed in Table 1. The analytical error of the measured activity ratios is usually in the range of 1 to 5 %, and only in exceptional cases up to 10 %.
Total uranium content in the samples ranges from 27 to 468 ppm, with lowest uranium content in sample NA12. High uranium content is observed in samples NA13, NA14 and NA6 from app. 35 m depth, with the highest value of 468 ppm in NA6. We observe that uranium in the borecore samples consists of both U(IV) and U(VI). The extraction does not dissolve all uranium. The content of uranium in this insoluble phase is denoted as U(res).
The AR differs significantly in the U(IV) and U(VI) phases, with ratios <1 in the U(IV) phase and ratios >1 in the U(VI) phase in nearly all samples. The AR of the U(res) phase is with exception of NA12 similar to that observed in the U(IV) phase. Different (higher) AR in the NA12 residue may indicate involvement of different U compounds in the sample material, i.e. U(IV) and insoluble U(res) represent different compounds. Taking into account the higher stability of U(IV) phases we assume that insoluble uranium exists as a stable mineral phase in oxidation state IV. Most uranium in all samples is U(IV), with contents between 50 and 90 wt.%. The highest U(IV) fraction is found in sample NA6-37.

That U(res) and U(IV) exhibit in nearly all samples an AR below one is a strong indicator for their long-term stability. AR values significantly below unity are caused by

the preferential release of ^{234}U, which is facilitated by α-recoil process and subsequent ^{234}U oxidation (see, e.g., Suksi et al. 2006). In order to attain low AR values of approx. 0.2 in the U(IV) phase, it must have been stable for a sufficiently long time, i.e. no significant release of bulk uranium has occurred during the last million years. This is in agreement with the hypothesis that the major uranium input into the clay/lignite horizon occurred during Tertiary, more than 10 My ago as described in the next chapter and in (Noseck et al. 2006). The prevailing groundwater conditions, with low Eh values especially in the clay-lignite horizon of borehole NA6, is another indication that stable, insoluble U(IV) phases such as uraninite can be expected under the present conditions. The AR in groundwater generally reflects the nature of water-rock interaction and is therefore sensitive to groundwater conditions (see Suksi et al. 2006). Under oxidising conditions both isotopes are released into the groundwater with the ratio they occur in the uranium source. Under anoxic conditions, where bulk uranium release is strongly suppressed, the release of the more mobile ^{234}U(VI) is favoured. The low ARs in the U(IV) phase observed in this study are correlated with AR values >1 in pore and groundwater from the clay/lignite horizon (Noseck et al. 2007). This is expected because of the anoxic sediment conditions and preferred mobilisation of ^{234}U.

Tab. 1: *Amount of uranium and $^{234}U/^{238}U$-activity ratios (ARs) in the different phases from uranium separation*

sample	U [ppm]	U(IV)		U(VI)		U(res, IV)		U(IV) total
		[%]	$^{234}U/^{238}U$	[%]	$^{234}U/^{238}U$	[%]	$^{234}U/^{238}U$	[%]
NA6 35a	356±7	28.7	0.54 ± 0.01	41.9	1.42 ± 0.02	29.5	0.65± 0.01	58.1
NA6 35b	468±9	45.9	0.56± 0.01	33.3	1.69 ± 0.03	20.7	0.64± 0.02	66.7
NA6 35c	369±8	23.3	0.47± 0.01	47.4	1.16± 0.02	29.3	0.67± 0.01	52.6
NA6 37a	37.3±2	73.7	0.79 ± 0.03	15.7	2.66± 0.07	10.6	0.73± 0.01	84.3
NA6 37b	47.5±1,5	66.2	0.52± 0.01	9.0	3.37± 0.15	24.8	0.86± 0.02	91.0
NA6 37c	35.7±2	51.3	0.58± 0.01	19.8	2.56 ±0.08	28.9	0.71± 0.04	80.2
NA11 a	52.5±2,2	4.2	0.44± 0.02	34.1	0.94± 0.01	61.7	0.55± 0.02	65.9
NA11 b	53.6±2,5	6.1	0.39± 0.02	49.6	0.94± 0.025	44.3	0.67± 0.02	50.4
NA12 a	27.2±1,4	3.9	0.26± 0.02	47.5	1.31± 0.04	48.6	1.22± 0.03	52.5
NA12 b	31.4±2,1	4.2	0.13± 0.02	57.4	1.25± 0.04	38.4	1.04± 0.03	42.6
NA13 a	216±7	5.4	0.53± 0.02	46.8	1.15 ± 0.02	47.8	0.55± 0.01	53.2
NA13 b	230±9	1.6	0.58± 0.03	46.2	1.15± 0.02	52.2	0.53± 0.01	53.8
NA14 b	317±10	13.3	0.87± 0.02	68.8	1.28± 0.02	18.0	0.44± 0.01	31.2
NA14 c	354±11	25.4	0.88± 0.02	39.6	1.11± 0.01	41.5	0.54± 0.01	58.5

Results from SE are described elsewhere (Denecke et al. 2007, Noseck et al. 2007). In general those results correlate well with the U(IV)/U(VI)-separation results, since both methods observed the major part of uranium to be associated with the U(IV) phase, which are expected in step 4 and 5 from sequential extraction (U bound in reduced form/onto organic matter and U in residuum).
In order to confirm that uranium in steps 4 and 5 is really in the tetravalent state, analyses of AR in the different SE leachates from sample NA13 were performed. The analyses were limited to the leachates from step 1, 2, 4 and 5, since the uranium content in the third step is always very low, < 3 % of total uranium. The results are shown for sample NA13 in Fig. 2. AR values in steps 1 and 2 are quite similar, with values above

1.75. Upon comparing this value with results from U(IV)/U(VI)-separation we conclude that uranium extracted in these first two steps was U(VI). In contrast, ARs in leachates from steps 4 and 5 are around 0.5 to 0.6, which matches well the values observed in the U(IV) and U(res) fractions from U(IV)/U(VI)-separation. This confirms that uranium extracted in steps 4 and 5 was U(IV).
The amount of U(VI) determined by the two methods differs. From the U(IV)/U(VI)-separation, 44 % U(VI) was found, whereas uranium extracted by steps 1 and 2 consists of only 22.5 % U(VI). One possible explanation for this discrepancy is that part of the U(IV) in the sample was oxidised during the U(IV)/U(VI)-separation. We expect such an oxidation to affect a AR decrease in the U(VI) phase by dilution with originally U(IV) having a lower AR. The lower value of 1.2 observed in the separation, compared to values of 1.75 and 1.76 from steps 1 and 2, might be an indication that partial oxidation of U(IV) to U(VI) actually occurred. In order to reliably use the U(IV)/U(VI)-separation method for quantification of uranium redox state, a more systematic work on determining redox states during uranium dissolution is necessary.

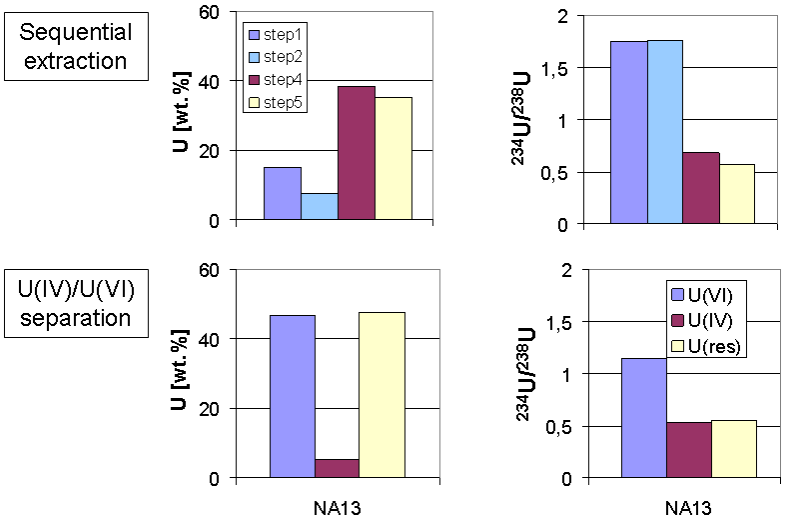

Figure 2: *Uranium content and $^{234}U/^{238}U$ activity ratios in SE leachates from steps 1, 2, 4 and 5 (top) compared to U(IV), U(VI) and U(res) fractions (bottom) in sample NA13*

Geological development and uranium enrichment scenario

In order to evaluate how the results support the ideas about uranium enrichment at Ruprechtov site, firstly the geological development is described. Recent studies about the geological evolution of the Ruprechtov area have shown that the bedding conditions are governed by a strong morphology of the Pre-Oligocene surface (now transition between kaolin and pyroclastics, e.g. Noseck et al. 2006). This morphology is a key feature for the analysis of the geological development. The assumptions about the major steps, based on current knowledge, comprise 5 main phases a–e as illustrated in Fig. 3. A major contribution to the uranium accumulation occurred in phase "c" which is shown in Fig. 4. Preceding the sedimentation of the pyroclastics, weathering of the underlying granite in particular took place as a result of the reaction of feldspars with CO_2-rich groundwater and the formation of kaolin. CO_2-rich groundwater furthermore

initiated the mobilisation of uranium from accessory minerals by formation of soluble UO_2-carbonate complexes. Within the kaolin, uranium was mainly transported by diffusion. At the boundary layer between kaolin and overlying pyroclastic sediments, advective transport was also possible over short distances in a local horizon with increased hydraulic conductivity. The main immobilisation processes occurred in/close to lignite-rich sediments. The key processes contributing to the uranium immobilisation are described in the contribution of Havlova et al. 2007 to the 3rd annual FUNMIG workshop. Hexavalent uranium was reduced and U(IV) was immobilised in secondary uranium phases ningyoite and uraninite due to processes connected with microbial reduction of organic matter and arsenopyrite formation.

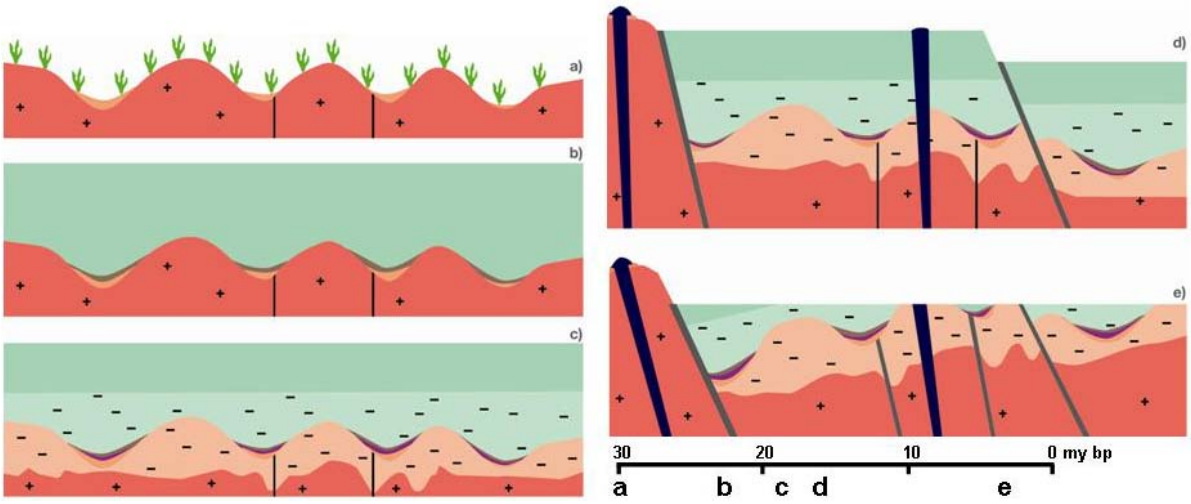

Figure 3: *Schematic representation of relevant phases of the geological evolution of the Sokolov basin: a) Pre-Oligocene,> 30 My: influx of detritic material (orange) by physical weathering of the granite present at the surface (red); b) Lower Oligocene – Miocene, 30-16 My: deposition of organic material (brown) in trough areas; after that, main phase of volcanic activity with wide-area sedimentation of pyroclastics / tuff (green); c) Lower Oligocene – Miocene, 30-16 My: alteration of granite (kaolinisation - light red, dashed) and tuff (bentonisation - light green, dashed); d) Miocene (16-15 My): rift formation, combined with fault zones (grey) and basalt intrusions (dark blue) e); Pliocene - Quaternary (< 5 My): further evolution of the Ohre rift and partial erosion of the pyroclastic sediments (after Noseck et al. 2006)*

Uranium series disequilibria results and results from U(IV)/U(VI) separation support the hypothesis that a major part of uranium has formed more than a million years ago. The results also show that to some extent a transport and immobilization of uranium in the clay/lignite layers continued following the major influx during Tertiary. This more recently enriched uranium seems to occur at least partially in the U(VI) state. However, we have not yet been able to identify the form of this uranium. We assume that it occurs adsorbed on clay or organic material or in an amorphous mineral phase.
The impact of the major uranium input processes on AR in sediment and groundwater is illustrated in Fig. 5. We assume that at the time of major uranium influx during Upper Tertiary the AR in infiltrating groundwater was unity as it is observed today. Inflowing U(VI) was reduced in the clay/lignite horizon and immobilised in secondary minerals (Havlova et al. 2007). Thus, the immobile U(IV) phase formed had the same ratio of 1.

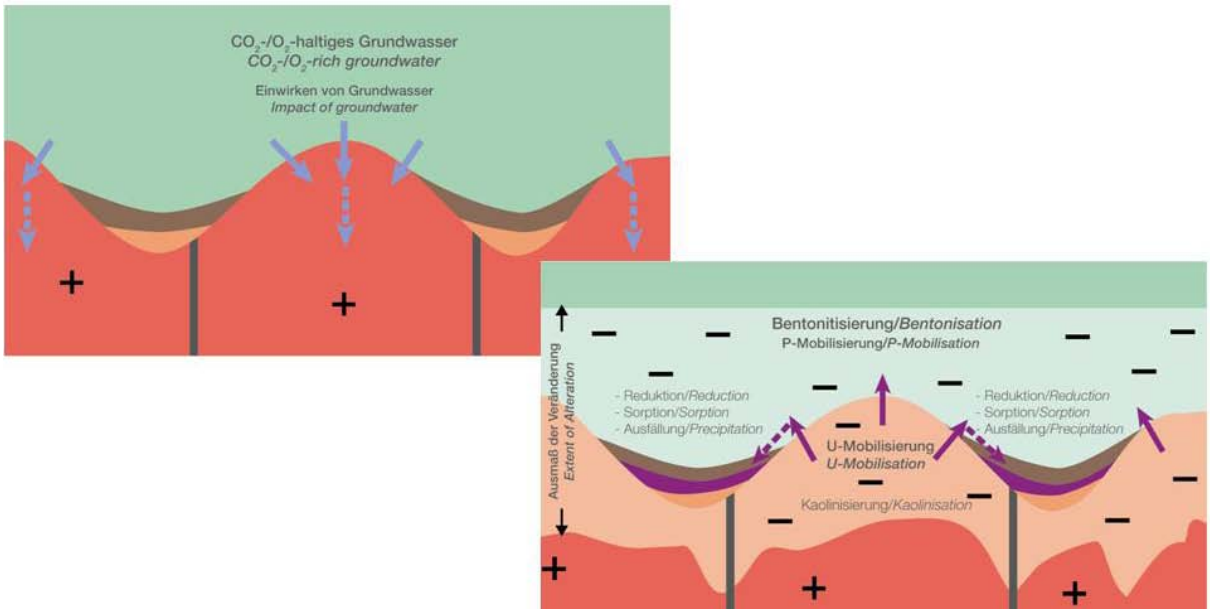

Figure 4: *Schematic illustration of the alteration processes in granite (kaolinisation) and tuff (bentonisation) by impact of CO_2- and O_2-rich groundwaters in phase "c" of the geological evolution. Kaolin is largest at previously morphological elevations of the granite due to Previous sedimentation of pyroclastic sediments. Uranium (magenta) is accumulated in those former valleys in which lignite or lignitic clay also accumulated*

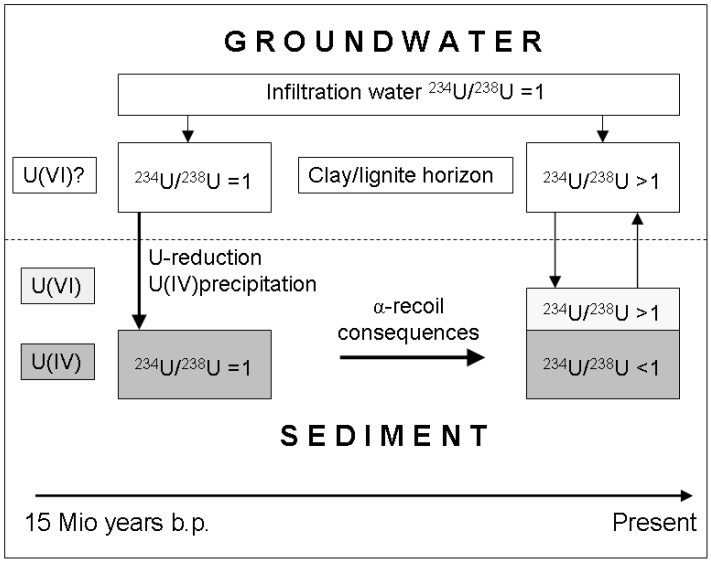

Figure 5: *Schematic illustration of the $^{234}U/^{238}U$ activity ratios evolution in the immobile secondary uranium phases and groundwater*

Due to α-recoil related processes, selective leaching of ^{234}U decreases AR in the stable secondary U(IV) phase. The preferred mobilisation of ^{234}U over ^{238}U also leads to an AR increase in the porewater and the groundwater-bearing layers with low flow velocity in the clay/lignite horizon. The AR in the porewater and groundwater-bearing layers is also affected by slow inflow of water from the infiltration area, containing uranium with AR around 1. Typical AR values in the clay/lignite layer water lie in the range between

2 and 4. Similar values are found in more accessible uranium fractions in the immobile phase, which have been more recently accumulated in the clay/lignite horizon.

Summary and Conclusions

Uranium series disequilibria and analyses of ARs in immobile uranium phases with different redox state contribute to the understanding of uranium enrichment at Ruprechtov site in the geological past. Using U(IV)/U(VI)-separation and SE coupled with analysis of AR in each phase, both U(IV) and U(VI) forms were identified in the clay/lignite horizon. We also found that the U(IV) phase has been stable over geological time frames, whereas the U(VI) phase was formed more recently. This is in accordance with the current understanding of the geological development of the site.
The wet chemical method to separate U(IV) and U(VI) was applied for the first time to the samples from Ruprechtov site. The results are very promising but the quantification of U(IV) and U(VI) phases using the separation method needs to be assessed, to ascertain if possible redox disturbances are caused by the uranium dissolution. Systematic investigations to compare U(IV)/U(VI)-separation and SE methods with homogenised samples are planned. In addition, the effect of iron present in the samples on the redox state of uranium during the sample dissolution will be investigated.

Acknowledgement

This work has been financed by the German Federal Ministry of Economics (BMWi) under contract no 02E 9995, by RAWRA and Czech Ministry of Trade and Industry (Pokrok 1H-PK25) and by the European Commission within the IP FUNMIG.

References

Denecke M, Havlova V (2007): Elemental correlations observed in Ruprechtov tertiary sediment: micro-focus fluorescence mapping and sequential extraction. In Buckau G., Kienzler B., Duro L., Montoya V. (eds.): 2nd Annual Workshop Proceedings of the IP Project FUNMIG", 315 ppt. SKB Technical Report, TR-07-05.

Havlová V., Brasser Th., Cervinka R., Noseck U., Denecke M., Suksi J (2007). Uranium enrichment at Ruprechtov site – Characterisation of key processes. S&T contribution to the 3rd annual workshop of the IP FUNMIG, 26.-29. November 2007.

Noseck U, Brasser Th, Suksi J, Havlova V, Hercik M, Denecke MA, Förster HJ (2007): Identification of Uranium enrichment Scenarios by Multi-Method Characterization of Immobile Uranium phases. Submitted to Physics and Chemistry of the Earth.

Noseck U, Brasser Th (2006): Application of transport models on radionuclide migration in natural rock formations - Ruprechtov site. Gesellschaft für Anlagen- und Reaktorsicherheit (GRS) mbH, GRS-218, Braunschweig.

Suksi J, Rasilainen K, Pitkänen P (2006): Variations in the $^{234}U/^{238}U$ activity ratio in groundwater – A key to characterise flow system? Physics and Chemistry of the earth, 31 (10-14), 556-571.

A.8 Uranium geochemistry at Ruprechtov Site

Ulrich Noseck [1*], Juhani Suksi [2], Vaclava Havlova [3], Radek Cervinka [3]

[1] Gesellschaft für Anlagen- und Reaktorsicherheit (GRS) mbH (D)
[2] University of Helsinki (FI)
[3] Nuclear Research Institute Řež plc (CZ)

* Corresponding author: Ulrich.noseck@grs.de

Abstract
Groundwater data from Ruprechtov site have been evaluated with special emphasis on uranium behaviour in the uranium-rich clay/lignite horizon. In this horizon in-situ Eh-values in the range of -160 to -280 mV seem to be determined by the SO_4^{2-}/HS^- couple. Under these conditions U(IV) is expected to be the preferential redox state in solution. However, first measurements in borehole NA6 showed only an U(IV) fraction of about 20 %. Thermodynamic calculations revealed that the high CO_2 partial pressure in the clay/lignite horizon can stabilise hexavalent uranium, which can explain the occurrence of U(VI). The calculations indicated that the low uranium concentrations in the range between 0.2 and 2.1µg/l are controlled by amorphous UO_2. This also confirms the findings from previous work that the U(IV) phases are long-term stable under the reducing conditions in the clay/lignite horizon.

Introduction
During the investigations at Ruprechtov site key processes leading to immobilisation of uranium in the so-called clay/lignite horizon were identified (e.g. Noseck et al. 2008a). It could be shown that the major amount of uranium was deposited in form of U(IV) minerals and that these immobile U(IV) phases have been stable for more than 1 Million years. Uranium series disequilibria showed no evidence for uranium removal from the system. In order to understand the long-term stability of uranium in the clay/lignite horizon the geochemical conditions at Ruprechtov site are evaluated and discussed with major emphasis on the mobility of uranium.

Methods
The methods applied for sampling and the analytical methods for detection of major and trace elements are described in (Noseck et al. 2008b). Eh and pH-values have been measured in-situ by a multi parameter probe with a Pt-electrode for Eh measurement. Analyses of U(IV)/U(VI) fractions in groundwater have been performed by co-precipitation with NdF_3 using the method from (Anderson 1984) following the scheme of (Suksi et al. 2007).

Thermodynamic calculations have been performed with Geochemists Workbench (GWB; Bethke, 2006) and with the updated NEA TDB database (Guillaumont et al. 2003, Yoshida 2004). All input data for the calculations are taken from (Noseck et al. 2008b, table 1) and from additional data listed in this paper.

Results and discussion

A detailed compilation and description of the Ruprechtov groundwater data can be found in (Noseck et al. 2008b). The geochemical conditions at the site are characterised by low mineralised waters with ionic strengths in the range of 0.003 mol/l to 0.02 mol/l. Nearly all waters in the clay/lignite horizon are of Ca-HCO_3-type with total DIC concentrations up to 450 mg/l. The pH-values vary in a range of 6.2 to 8, the Eh-values from 435 mV to -280 mV. More oxidising conditions with lower pH-values are found in the near-surface granite waters of the infiltration area.

In the clay/lignite horizon the conditions are reducing supported by the mineral phases pyrite and siderite occurring with content up to 2 % in sediment samples from this horizon. Eh-values have been measured on-site and in-situ. The first method is more susceptible to disturbances by the contact with atmosphere, which is probably responsible for higher Eh values observed in on-site measurements. In-situ probe measurements of Eh-values in the clay/lignite horizon always showed an Eh decrease during the analyses. In order to find the stable values long-term measurements for three boreholes (NA6, NA12 and NA13) have been performed. This measurement showed a stabilisation of the Eh-value after few days. We decided to trust these values most and used them for the following interpretation. Selected data for boreholes considered here are compiled in Tab. 1.

Tab. 1: *Specific groundwater data for selected boreholes*

Well No.	Area	Horizon [m]	Eh [mV]	U [µg/l]	Fe^{2+} [mg/l]	S^{2-} [mg/l]	$\delta^{34}S$ [‰]	SO_4^{2-} [mg/l]
NA4	Clay / lignite	34.5 – 36.5	n.a.	0.15	1.8	0.1	24.63	19.8
NA6		33.4 - 37.4	-280	0.8	0.7	0.11	23.5	49.5
NA12		36.5 - 39.3	-160	0.2	2	n.a.	20.11	22.9
NA13		42.2 - 48	-252	2.1	0.7	0.065	n.a.	22.9
NA8	granite	8.5 - 24	48	1.58	n.a.	n.a.	-8.5	59.1
NA10		19.5 - 27.5	240	8.6	n.a.	n.a.	0.2	40.8
RP1		5 - 18	149	11.1	n.a.	n.a	3.48	19.8

n.a. = not analysed

Figure 1 shows uranium concentrations of all groundwater wells at Ruprechtov. The boreholes from the infiltration area in granite, NA8, NA10 and RP1 are depicted on the right of the diagram. These values are in a range of 1.8 to 12 µg/l. The uranium concentrations in the clay/lignite horizon are below 2.1 µg/l and with two exceptions below 1µg/l. As expected the values in the more reducing clay/lignite horizon are lower than those in the more oxidising granitic waters.

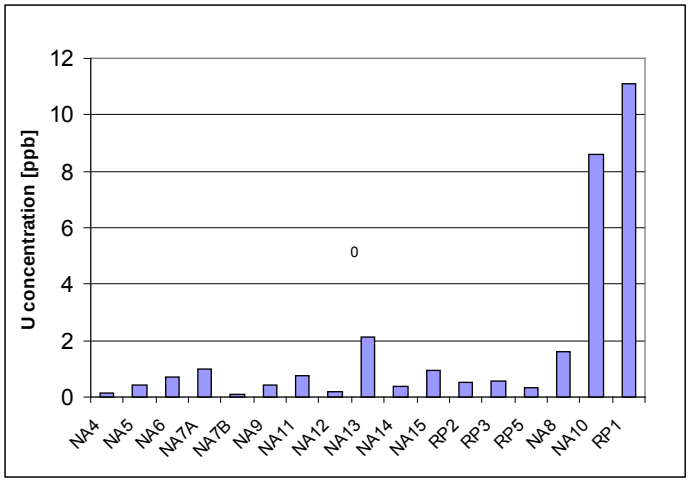

Figure 1: *Uranium concentrations in Ruprechtov wells*

The uranium mobility is strongly impacted by its speciation, in particular by the local redox conditions and the availability of complexing agents like carbonates (e.g. Langmuir 1978). Therefore, firstly, the redox conditions in the clay/lignite horizon are discussed. Redox conditions in natural systems could be controlled by different and heterogeneous redox couples. The clay/lignite layers are quite heterogenous typically containing quartz and clay minerals (smectite, illite, kaolinite) as major components, organic matter and to lower extent minerals as anatase, pyrite and siderite (Noseck and Brasser 2006). Due to the occurrence of significant amounts of dissolved sulphide and sulphide minerals the redox pairs SO_4^{2-}/HS^-, and the heterogeneous redox pairs SO_4^{2-} /pyrite have been included. Many natural systems are dominated by redox pairs of iron. Therefore we also calculated the couple $Fe^{2+}/Fe(OH)_3$ considering a relatively fresh amorphous precipitate according to data from (Langmuir 1997). There is no indication of goethite or haematite occurring in the clay/lignite horizon. The results are shown in Figure 2. The measured Eh- values from the three boreholes are compared with values calculated from these redox pairs.

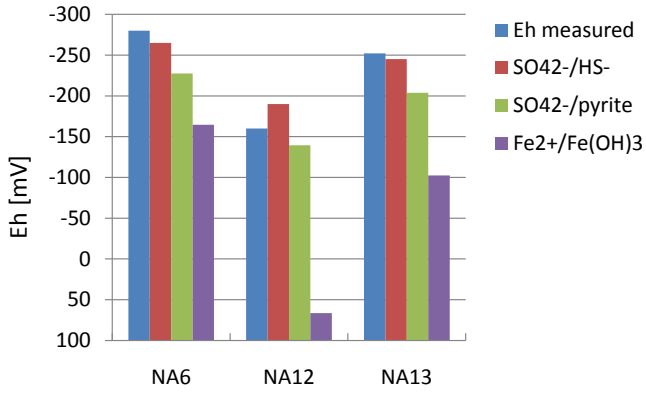

Figure 2: *Measured Eh-values compared to potential redox pairs*

A reasonably well agreement is found between the redox potential measured by the Pt-electrode and the SO_4^{2-}/HS^- couple, whereas the redox pair $Fe^{2+}/Fe(OH)_3$ shows low

agreement in particular for borehole NA12. As discussed in (Noseck et al. 2008b) there is strong evidence that microbial sulphate reduction and oxidation of organic matter occurs in the clay lignite horizon. In particular the $\delta^{34}S$ values in the boreholes from the clay/lignite horizon are strongly increased with respect to the values in the infiltration waters (see table 1). The observed sulphide values in the clay/lignite waters are significant but not too high, lying in a range of 0.05 and 0.12 mg/l. Microbial catalysis efficiently accelerates the sulphate reduction and operational redox potentials resulting from this kinetic process may closely approximate equilibrium values (e.g. Stumm et al. 1996). This might explain the agreement of measured and calculated values for the SO_4^{2-}/HS^- couple.

The uranium speciation calculations have been performed with GWB and the updated NEA TDB database. A major difference to the NEA TDB version from 1992 is the value for the uranium(IV)-hydroxo complex in solution:

$$U(OH)_4 + 4H^+ = U^{4+} + 4H_2O \quad (1)$$

The lower stability of this complex (log K = 10.05 for reaction (1)) compared to the value from 1992 database (log K = 4.54) is leading to lower redox potentials calculated for the U(IV)/U(VI) transition in the neutral pH range. The Eh/pH diagram for typical conditions at Ruprechtov site is shown in Figure 3. The data for granite groundwater from the infiltration area are dominated by uranyl-carbonato complexes, whereas the groundwaters from the clay/lignite horizon are at the boundary of the stability fields for the tetravalent aqueous $U(OH)_4$ complex and the hexavalent complexes $UO_2(CO_3)_3^{4-}$ and $UO_2(CO_3)_2^{2-}$.

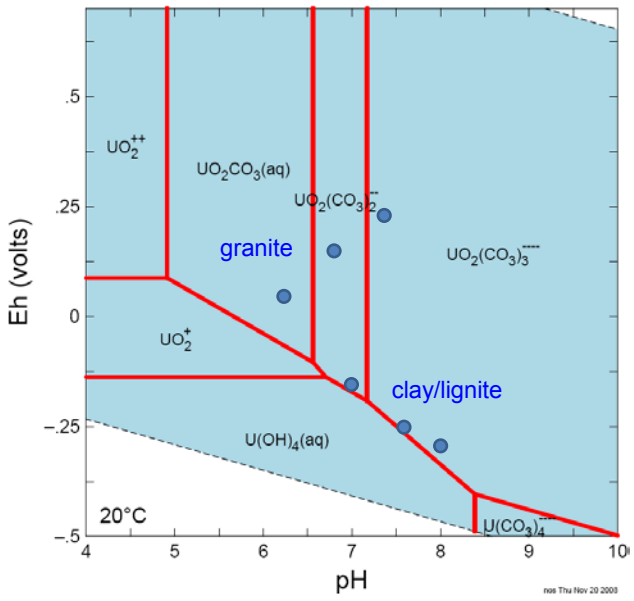

Figure 3: *pH/Eh-diagram for Ruprechtov groundwaters. U concentration 10^{-3} mg/l, CO_2 activity = 10^{-3}.*

Results from speciation calculations for the conditions found in NA6 and a pH range between 6 and 8 are shown in Figure 4. The increasing role of carbonate complexes with increasing alkalinity is clearly illustrated. Due to the high CO_2 partial pressure (from microbial SOC degradation and probably CO_2 exhalation; cf. Noseck et al.

2008b) in this system even for quite reducing conditions part of the dissolved uranium can be stabilised as U(VI) by carbonato complexes. The calculated fraction of U(IV) in groundwater NA6 at pH8 assuming equilibrium is shown on the right in Figure 4.

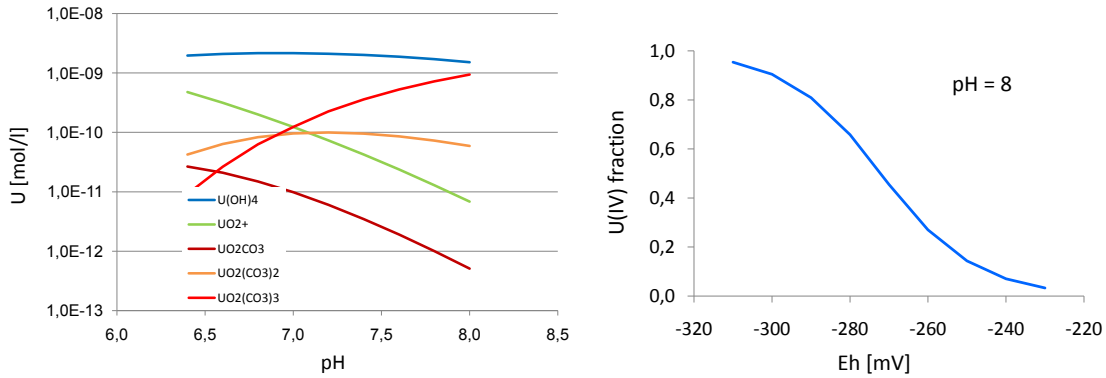

Figure 4: *Left: Uranium speciation in solution for NA6 groundwater in dependence of pH (Total U concentration $6 \cdot 10^{-4}$ mg/l, total DIC concentration as HCO_3 =290 mg/l)) Right: fraction of U(IV) in dependence of Eh-value at pH 8, for conditions of NA6 groundwater.*

For all three clay/lignite groundwaters the expected U(IV) fractions in solution have been calculated. To verify the oxidation state of uranium in groundwater a method for separation of U(IV) and U(VI) in solution was applied (see section methods). So far, only data for NA6 are available. In the first campaign total U concentration of 5.5 µg/l with U-fractions of 15.2 % and 22.2 % and from the second campaign a total U concentration of 0.91 and a U(IV) fraction of 16.6 % was found. According to the thermodynamic calculations a uranium(IV) fraction of about >60 % is expected. The results from the calculations for the different groundwaters and the measured values are listed in Tab. 2.

Tab. 2: *Calculated and measured U(IV) fractions in groundwaters from clay/lignite horizon*

Borehole	U(IV) fraction in groundwater [%]	
	calculation	analysis
NA6	66	15 - 22
NA12	35	n.a.
NA13	55	n.a.

n.a = not analysed

U(IV)/U(VI) analyses have also been performed in groundwaters from Forsmark site. These waters are slightly less reducing with Eh-values between -140 and -200 mV and pH-values between 7 and 8.5 (Laaksoharju et al. 2006). Here groundwater is dominated by U(VI) with U(IV) fractions of <5 %.

An appropriate method to understand which uranium phases control the uranium solubility in the natural system is the calculation of saturation indices. In many reducing groundwater systems uraninites or pitchblendes of stoichiometry UO_{2+x} are found to be the phases controlling the dissolved uranium concentration. In the uranium enriched

sediments at Ruprechtov site two secondary uranium(IV) phases have been observed, UO_2 and ningyoite ($CaU(PO_4)_2 \cdot 1\text{-}2H_2O$). Since no stoichiometric determination of the UO_2 phase was performed, saturation indices of different U(IV) mineral phases are taken into account. Thermodynamic data for ningyoite are not available in the NEA TDB and have been taken from recommendations in (Langmuir 1997).

The calculation results are shown in Figure 5. The groundwaters from the clay/lignite horizon are strongly oversaturated with respect to the crystalline uraninite and coffinite indicated by saturation indices (SI) in the range between 5 and 7. The mixed valence uranium oxides $UO_{2.25}$ and $UO_{2.33}$ are also oversaturated (SI between 2.5 and 4). The mixed valence oxide $UO_{2,66}$ is always undersaturated with SI values below -0.8. No saturation of U(VI) minerals was found. Assuming an uncertainty range of ±0.6 (shadowed area in Figure 4) for the saturation index resulting from uncertainties in the thermodynamic data, the results indicate that the uranium concentration is controlled by amorphous UO_2. SI values for ningyoite are also near saturation in groundwater NA6 and NA13 but not for NA12. So, there is generally good agreement with observed mineralisations in the clay/lignite horizon. Metastable amorphous UO_2 has been shown also in other studies to be likely the uranium controlling mineral phase, e.g. (Iwatsuki et al. 2004). These results also indicate that no U-release is expected under the geochemical conditions in the clay/lignite horizon, in agreement with very low $^{234}U/^{238}U$ activity ratios observed in the uranium(IV) mineral phases as indicators for their long-term stability (Noseck et al. 2008a).

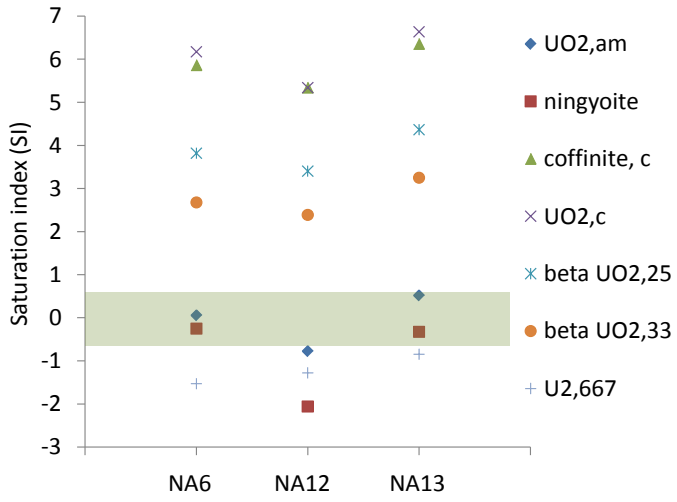

Figure 5: *Saturation indices of various U(IV) minerals calculated for groundwaters NA6, NA12 and NA13.*

Conclusions

The thermodynamic evaluation of the aqueous speciation and solubility behaviour of uranium in the reducing clay/lignite horizon indicate that the uranium concentrations are controlled by amorphous UO_2 or ningyoite. Saturation indices of crystalline uraninite and coffinite as well as mixed oxides are greatly exceeded. The results clearly explain the high stability of immobile uranium phases in the clay/lignite horizon, which was shown by uranium decay series disequilibria and described in previous papers.

All results from thermodynamic calculations indicate that U(IV) is the predominant redox state in the clay/lignite layers at Ruprechtov site. However, due to the high CO_2 partial pressure in the system carbonato complexes can stabilise hexavalent uranium in solution, which might explain that redox state analyses performed in borehole NA6 showed only 20 % U(IV). Nevertheless, there is also a need to optimise the U(IV)/U(VI) determination method in order to completely avoid contamination by atmosphere. This optimisation as well as improvement of Eh determination by use of additional electrodes is planned to be performed within a future national project eventually in association with the new European project RECOSY.

Acknowledgement

This work has been financed by the German Federal Ministry of Economics (BMWi) under contract no's 02 E 9551 and 02 E 9995, by RAWRA (CZ) and Czech Ministry of Trade and Industry (Pokrok 1H-PK25) and by the European Commission within the integrated project FUNMIG (EURATOM, FP6, Contract No. 516514).

References

Anderson RF, (1984): A method for determining the oxidation state of uranium in natural waters. Nucl. Inst. Meth. Phys Res. 223, 213-217.

Bethke CM (2006): The Geochemist's Workbench Release 6.0, Hydrogeology Program, University of Illinois.

Guillaumont R, Fanghänel Th, Fuger J, Grenthe I, Neck V, Palmer DA, Rand MH, OECD (2003): NEA-TDB, Chemical Thermodynamics, Vol. 5. Update on the chemical thermodynamics of uranium, neptunium, plutonium, americium and technetium. Elsevier.

Iwatsuki T, Arthur R, Ota K, Metcalfe R (2004): Solubility constraints on uranium concentrations in groundwaters of the Tono uranium deposit, Japan. Radiochim. Acta 92, 789 – 796.

Langmuir D (1978): Uranium solution-mineral equilibria at low temperatures with application to sedimentary ore deposits. Geochim. Cosmochim. Acta 42, 547-569.

Langmuir, D (1997): Aqueous environmental geochemistry. Prentice Hall, Upper Saddle River, New York, p. 600.

Laaksoharju M, Smellie J, Tullborg E-L, Gimeno M, Gómez J, Gurban I, Hallbeck L, Auqué L, Buckau G, Gascoyne M., Raposo J (2006): Hydrogeochemical evaluation of the Forsmark site, modelling stage 2.1. SKB-R06-96, Stockholm.

Noseck U, Brasser Th, Suksi J, Havlova V, Hercik M, Denecke MA, Förster HJ (2008): Identification of Uranium enrichment Scenarios by Multi-Method Characterization of Immobile Uranium phases. Phys. Chem. Earth, 33, 969-977.

Noseck U, Rozanski K, Dulinski M, Havlova V, Sracek O, Brasser Th, Hercik M, Buckau G (2008b): Characterisation of hydrogeology and carbon chemistry by use of natural isotopes – Ruprechtov site, Czech Republic. Accepted by Appl. Geochem.

Stumm W, Morgan JJ (1995): Aquatic Chemistry. 3rd ed. John Wiley & Sons, New York.

Suksi J, Salminen S (2007): Forsmark Site investigation. Study of U oxidation in groundwater with high U concentrations. SKB P-07-54, Stockholm.

Yoshida Y, Shibata M (2004): Establishment of Data Base Files of Thermodynamic Data developed by OECD/NEA Part II - Thermodynamic data of Tc, U, Np, Pu and Am with auxiliary species, JNC Technical Report, JNC TN8400 2004-025.

A.9 Interrelation of mobile organic matter and sedimentary organic matter at the Ruprechtov Site

Václava Havlová[1], Radek Červinka[1*], Josef Havel [2]

[1] Nuclear Research Institute Rez plc, Waste Disposal Department, Husinec- Rez, 250 68, Czech Republic
[2] Department of Analytical Chemistry, Faculty of Science, Masaryk University, Kotlářská 2, 611 37 Brno, Czech Republic

* Corresponding author: crv@ujv.cz

Abstract
The study was focused on mobile organic matter quantification from the Ruprechtov natural analogue site (CZ) and its characterisation. Only a small fraction of sedimentary organic matter can be released into the solution: 2.8 % of C_{org}. The release rate is dependent on the organic matter composition and the degree of coalification. The mobile organic matter is represented by extracted natural humic acid. This was identified by MALDI-TOF MS spectra which show a high degree of similarity with those from natural mobile organic matter in Ruprechtov groundwater and those from organic substances leached from the sediment in contact with solution. MALDI-TOF spectra also proved that the mobile organic matter consists of small independent molecules with molecular weight around 500 Da.

Introduction
The study was focused on mobile organic substances and their characterisation from the Ruprechtov natural analogue site (CZ). Mobile organic matter (MOM), as defined in Maes et al., 2004, is the fraction of total natural organic matter (NOM) that can be released into the system (groundwater) from sedimentary organic matter and is available for complexation/sorption interactions with other ions (radionuclidesradionuclides are of particular interest in this context). However, the determination of MOM availability is complicated. The problems can be formulated into several questions:

1. How can we define the MOM fraction of sedimentary organic matter (SOM) in the Ruprechtov sedimentary samples?
2. Is the fraction, which is released during simple leaching experiments from SOM into the leaching solution, representative for the MOM fraction?
3. Moreover, can the extracted humic acid (HA), being widely recognised as a strong complexing agent and used for complexation experiments with radionuclides, also be considered as MOM representative?
4. How do these artificially released organic substances correspond with mobile natural organic substances in Ruprechtov groundwater?

The attempt to answer the questions is presented in the following.

The site characterisation

The geology of the Ruprechtov site was described in detail in several contributions (e.g. Havlova et al., 2007; Noseck et al., 2008 a, b). The main accumulation of SOM is situated within Tertiary argillitized tuffs and tuffits in the so-called clay/lignite horizon. The SOM forms partly massive coal seams, partly is being dispersed in the clayey sediments. The highest SOM content was determined up to 40 wt. %. However, the groundwater content of dissolved organic matter (DOM) was found to be low (below 5 mg/l C_{org}.).

Methods

An outline of the SOM investigation and characterization from Ruprechtov site can be found in Cervinka et al., 2007. The key approach taken in this study was to extract natural organic substances from SOM, using two different methods (batch leaching experiment, and alkaline extraction), to characterize them using the modern analytical method MALDI-TOF MS, and to compare the results with natural dissolved organic matter from Ruprechtov groundwater.

Batch leaching experiment

The batch leaching experiments were aimed to demonstrate SOM degradability in contact with groundwater and the rate of MOM release. Four sediment samples (NA-13, NA-12/4, NA-12 and NA-14) with different SOM content were selected for the experiment (see Tab. 1).

Table 1: *Sample from the Ruprechtov site, selection for batch leaching experiment*

Sample	Depth (m)	SOM content (wt. % of C_{org})
NA-12	36.44 – 36.90	4.07
NA-12/4	38.9	2.33
NA-13	46.4	0.97
NA-14A	51.73	7.85

The experiments were performed in the pH range from 6 to 8 using a simple batch technique. 1 g of each sediment sample (ground and homogenized) was contacted with 40 ml of solution at different pH (6, 6.5, 7, 8). Due to the high content of pyrite in the sediment samples (namely NA-14) the original Ruprechtov groundwater could not be used because it is not possible to keep the pH constant during the experiments. Instead, a 0.1M phosphate buffer (Na_2HPO_4 + NaH_2PO_4) was used as solvent. The vials were agitated for 12 days, then centrifuged and decanted. Organic carbon content (C_{org}) in the leachate was analysed using an automatic analyser Schimadzu TOC-5000A (Czech Institute of Chemical Technology, Prague). All the experiments were performed under oxidising conditions.

The released MOM fraction was determined as a ratio of released C_{org} per 1 g of sample (mg/g) vers. content of C_{org}. in sediment (mg/g).

Natural humic acid extraction

By this method the natural humic substance HA-12/3 from Ruprechtov sample (borehole NA-12, 36.44 – 36.90 m, C_{org} = 4.07 wt. %) was extracted using the alkaline extraction procedure referred by IHSS after Swift, 1996, (see Fig. 1, Cervinka et al., 2007).

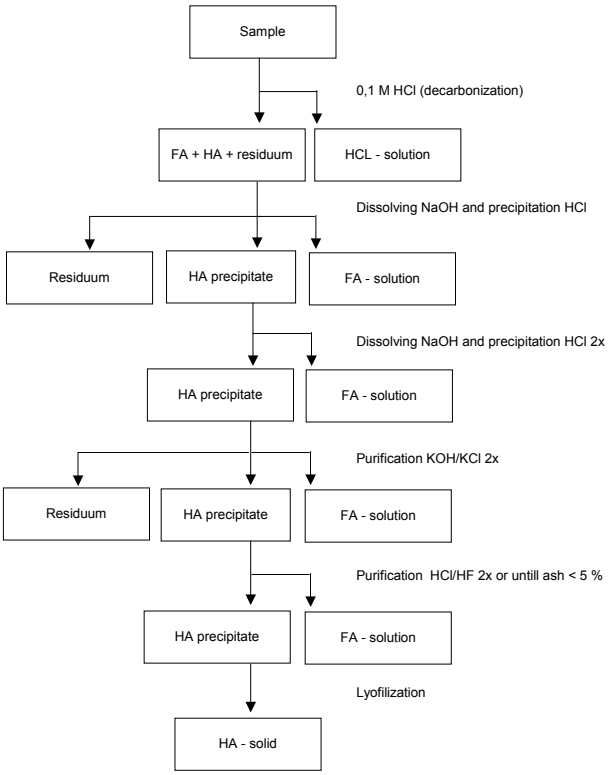

Figure 1: *Alkaline separation scheme according to IHSS (after Swift, 1996)*

The extracted natural humic acid (HA-12/3; 3 g) was characterized using element analysis, ash and moisture content, UV-Vis spectroscopy, FTIR spectroscopy, acidobasic titrations and MALDI-TOF MS (Cervinka et al., 2007).

MALDI-TOF MS

The modern analytical method MALDI-TOF MS (Matrix Assisted Laser Desorption/Ionisation Time of Flight Mass Spectrometry; Masaryk University, Brno; e.g. Remmler et al., 1995) was used for characterization of the organic substances.

Mass spectra were measured using the AXIMA-CFR mass spectrometer from Shimadzu (Kratos Analytical, Manchester, UK). The spectra were measured in the laser desorption ionization (LDI) mode without using any matrix. All samples used were dissolved in NaOH solution. 1 µl of solution was dropped to a sample plate, dried in an air stream at room temperature and inserted into the vacuum chamber of the instrument. After reaching a vacuum of $1 \cdot 10^{-5}$ Pa the mass spectra were measured. The resulting spectra were always accumulated from at least 1000 shots.

Following that, the following three organic substances were used for intercomparison:

- leachate from the degradation experiment (sample NA-12/4 leachate; 38.9 m)

- extracted natural humic acid HA-12/3 (extracted from borehole NA-12; 36.44-36.90 m, Cervinka et al., 2007)
- groundwater sample from borehole NA-12 (sampled in 36.5-39.3 m filter horizon)

Results

The average of the released fraction from sedimentary samples using the batch leaching technique was 2.8 % of SOM as C_{org}. The released fraction was inversely proportional to the total content of SOM in the sample: the more SOM present in the sample, the less the fraction of OM released. The trend is illustrated in Fig. 2. A decrease of the releasable fraction can be obviously connected with a higher humification stage of OM-rich samples, reported elsewhere e.g. Pettersson et al. (1994), Gonzales et al. (1994). The content of organic matter increased in the sequences NA-13 (carbonaceous clay) < NA-12/4 < NA-12 < NA-14A (coal).

The maximum released C_{org}. concentration for Ruprechtov samples did not exceed 40 mg/l, which is quite low. MOM fractions of Boom clay leached out by synthetic groundwater reached C_{org} concentrations up to 650 mg/l (Maes et al., 2004).

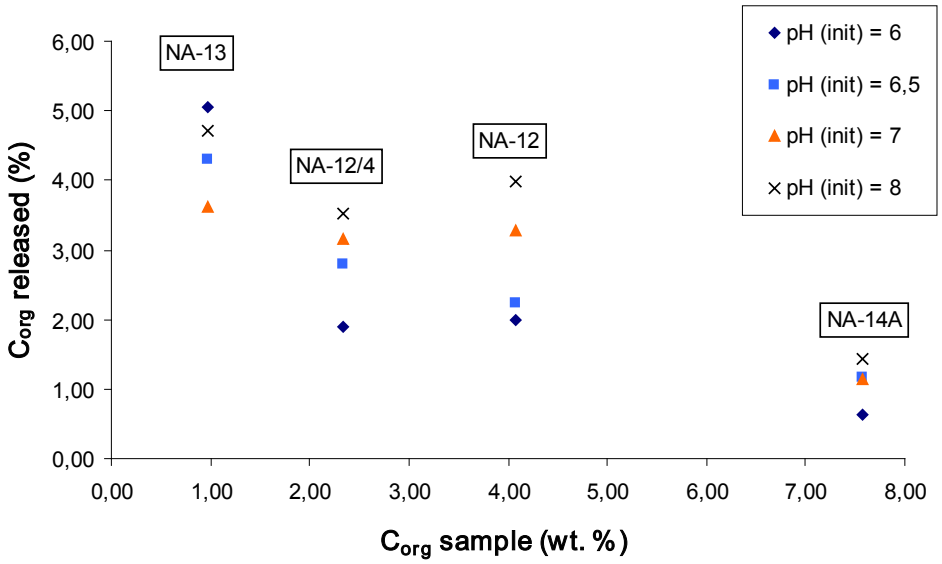

Figure 2: *OM fraction released into the solution (C_{org} released (%) = TOC solution / TOC sample) in relation to C_{org} sample (wt. %) as TOC content in the sample and pH-value.*

The MALDI-TOF MS measurement showed that the spectra was dominated by lower molecular weight peaks, confirming the presence of low molecular compounds with a number of peaks about 400 – 600 Da (mass/charge in chart) and about 800 Da. High molecular weight compounds were presented in less extent. The spectra is presented in Fig. 3, green colour)

The results support a recent change in natural humic acid consideration: humic acids are presumed to consist of small independent molecules with low molecular weight below 1000 Da (Simpson et al., 2002). The shift was made mainly due to new analytical

methods involved in HA characterization, e.g. MALDI-TOF MS, ESI-MS, TOF-SIMS and Overhauser-NMR.

Finally, MALDI-TOF MS spectra were measured for the NA-12/4 leachate and groundwater MOM (NA-12 borehole). The results are also presented in Fig. 3.
A noticeable fingerprint can be found: The peaks in the range about 25 – 145, 250, 353 – 381, 413, 492 – 500 and 590 – 600 Da (mass/charge in the chart) can be identified for all three samples. Those are composed of molecules with similar, predominantly low molecular weight . Analytical uncertainties caused by the content of other dissolved substances in solution and different laser intensities caused slight differences and shifts in the spectra. However the congruence of the main peaks is evident.
Therefore, the compounds released by either artificial dissolution of SOM (batch leaching and alkaline extraction) or natural groundwater at the Ruprechtov site are characterised by similar molecular weight composition. Moreover, due to the good agreement with natural groundwater DOM, the extracted and characterised humic acid HA-12/3 can be considered as representative of MOM at the Ruprechtov site and be used for further experiments simulating MOM interaction with radionuclides (Cervinka et al., 2008).

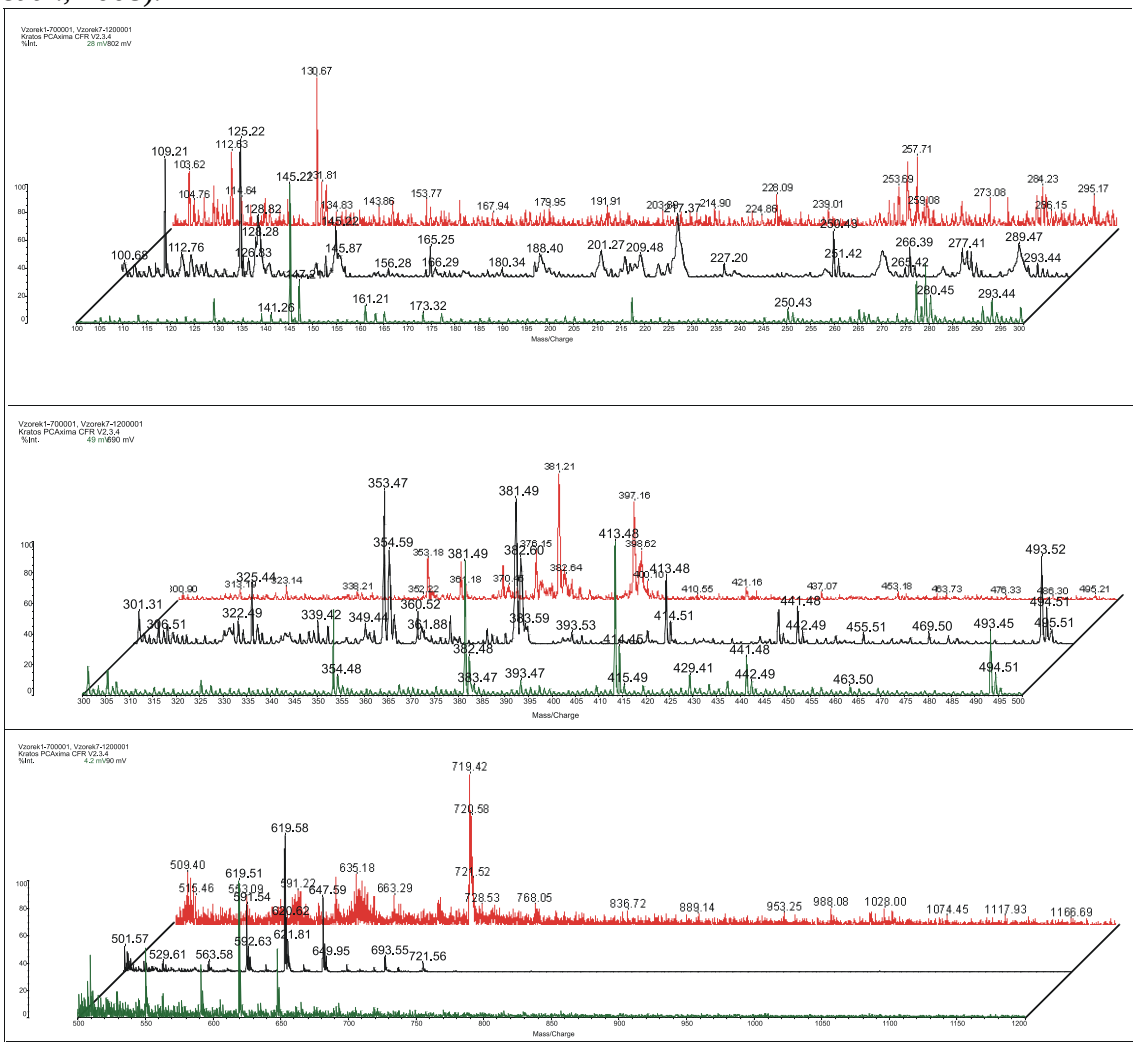

Figure 3: *Comparison of MALDI-TOF spectra: green – extracted HA-12/3 (NA-12 [36.44-36.9 m]), black – NA-12/4 leachate [38.9 m], red – NA-12 groundwater [36.5-39.3 m filter horizon], (mass/charge here = Da).*

Conclusions

The availability of mobile organic matter at the Ruprechtov site is mainly dependent on the sedimentary organic matter composition and degree of coalification. Only a small fraction of mobile organic matter from Ruprechtov sediment samples, i.e an avg. 2.8 wt. % of SOM, can be released into the solution. This probably explains the low DOM concentration (< 5mg/l) in Ruprechtov groundwater.

The extracted natural humic acid HA-12/3 from SOM is characterised by low molecular weight molecules (below 1000 Da). This compound can be considered as a mobile organic matter representative for Ruprechtov site. MALDI-TOF MS spectra showed a high similarity with those from organic matter released using batch leaching experiments and those from natural groundwater MOM from NA-12 borehole. The MALDI-TOF MS spectra identified a fingerprint, i.e. spectra segments, that are to some extent identical for all organic compounds studied here.

Acknowledgement

This work has been financed by the German Federal Ministry of Economics (BMWi) under contract no's 02 E 9551 and 02 E 9995, by RAWRA (CZ) and Czech Ministry of Trade and Industry (Pokrok 1H-PK25) and by the European Commission within the integrated project FUNMIG (EURATOM, FP6, Contract No. 516514).

References

Hauser W., Geckeis H., Götz R., Noseck U., Laciok A. (2006): Colloid Detection in Natural Ground Water from Ruprechtov by Laser-Induced Breakdown Detection. 2nd Annual Meeting of EC Integrated Project FUNMIG, SKB Report TR 07-05.

Cervinka R. (2008): Report on Uranium complexation by isolated humic substances from the Ruprechtov site. PID 2.2.20, EC Integrated Project FUNMIG.

Cervinka, R., Havlova, V.; Noseck, U.; Brasser, Th., Stamberg, K. (2007): Characterisation of organic matter and natural humic substances extracted from real clay environment. 3rd annual meeting of IP FUNMIG, 25-29.11.2007, Edinborough, Great Britain, submitted.

Gonzalez-Vila F. J, del Rio F. C, Almendros G. Martin G. (1994): Structural relationship between humic fractions from peat and lignites from the Miocene Granada basin. Fuel, Vol.73, No. 2.

Havlova V., Brasser Th., Cervinka R., Noseck U., Laciok A., Hercik M., Denecke M., Suksi J., Dulinski M., Rozanski K. (2007): Ruprechtov Site (CZ): Geological Evolution, Uranium Forms, Role of Organic Matter and Suitability as a Natural Analogue for RN Transport and Retention in Lignitic Clay. Proc. of REPOSAFE Conference, Braunschweig, Nov. 5-9, 2007, submitted.

IHSS, International Humic Substances Society, http://www.ihss.gatech.edu/.

Lenhart, J. J. Cabaniss, S. E. MacCarthy, P. Honeyman, B. D. (2000): Uranium(VI) complexation with citric, humic and fulvic acids. Radiochim. Acta, 88, 345-354.

Maes N. (2004): Migration Case Study: Transport of radionuclides in a reducing clay environment. Final Report. Nuclear Science and Technology. EUR 21025 EN. European Commission.

Noseck U., Brasser Th., Suksi J., Havlova V., Hercik M., Denecke M.A., Förster H.J., (2008a): Identification of uranium enrichment scenarios by multi-method characterisation of immobile uranium phases. J.Phys.Chem.Earth, doi:10.1016/j.pce.2008.05.018.

Noseck U., Rozanski K., Dulinski M., Havlova V., Sracek O., Brassera Th., Hercik M., Buckau G., (2008b): Characterisation of hydrogeology and carbon chemistry by use of natural isotopes – Ruprechtov site, Czech Republic. Submitted to Applied Geochem.

Pettersson et al., 1994 chybějící citace

Remmler, M., A. Georgi and F.-D. Kopinke (1995): Evaluation of matrix assisted laser desorption time of flight (TOF) mass spectrometry as a method to determine the molecular mass distribution of humic acids. Eur. Mass. Spectrom., 1, 403–407.

Simpson A. J., Kingery W. L., Hayes M. H., Spraul M., Humpfer E., Dvortsak P., Kerssebaum R., Godejohann M., Hofmann M. (2002): Molecular structures and associations of humic substances in the terrestrial environment. Naturwissenschaften 89, 2, 84-88.

Swift, R.S. (1996): Organic matter characterization. , in Sparks D.L., Methods of Soil Analysis, část 3. Chemical Methods. Soil Science Society of America Book Series Number 5. American Society of Agronomy, Madison, WI., pp.1018.

A.10 Geochemical study of uranium mobility in tertiary argillaceous system at Ruprechtov Site, Czech Republic

V. Havlová[**)], A. Laciok

Nuclear Research Institute Řež plc., CZ-250 68 Řež near Prague, Czech Republic

D. Vopálka, M. Andrlík

Faculty of Nuclear Sciences and Physical Engineering, Czech Technical University, Břehová 7, CZ-115 19 Prague 1, Czech Republic

The natural analogue study at the Ruprechtov site is aimed to investigate and understand the behaviour of natural radioelements in plastic clay formation. Uranium is present predominantly in U(+IV) form, either in secondary uranium minerals (uraninite, ningyoite) or in detrital immobile phases (monazite, rhabdophane, xenotime, zircon) and in hardly characterisable non-crystalline forms as well. Process of uranium accumulation probably proceeded via reduction of U(VI) and U(IV) precipitation with involvement of As. Sorption also played important role in U accumulation formation. The sequential extraction experiments were performed in order to specify phases causing uranium retention and accumulation. The isotopic exchange tests with ^{233}U were used to determine the amount of exchangeable uranium. The contradictions in the extraction schema used for the Ruprechtov sediment samples were found. The results prompt careful approach and potential sequential schema modification.

1 Introduction

Underground repositories of radioactive waste are based on a multibarrier concept. In this concept clay plays important role as either engineered (near field) or natural barrier (clay formations as host rocks, overburden of host rock formations). Detailed study of appropriate natural analogue systems (NAS) may help to better understanding of retardations processes in the vicinity of the deep nuclear waste repository under natural conditions in a long time scale, relevant for performance assessment (PA)

The natural analogue study at the Ruprechtov site was aimed to investigate and understand behaviour of natural radioelements in plastic clay formation. Ruprechtov system was chosen as an analogue for sedimentary overlayers of radioactive waste repository host rocks (salt, granite, clay). Gorleben (Germany) and Mol (Belgium) are the most similar systems studied abroad. The site was investigated within the project of NRI Řez (CZ) and GRS Braunschweig (D) with several other institutions involved in order to identify the main mobilisation/immobilisation processes for PA-relevant elements, namely uranium, thorium and radium [1, 2, 3]. Currently, some specific aspects of Ruprechtov NAS are

[*] The project was supported by RAWRA (CZ), BMWA (D), EC (FUNMIG project – 6th European Framework Programme) and the Czech Ministry of Trade and Industry (in the frame of the POKROK Programme)

[**] hvl@ujv.cz

studied as part of EC PAMINA project. Comprehensive investigation of U-argillized clay-organic matter-granite system-groundwater has been performed so far, including drilling, field tests, groundwater monitoring, sediment and groundwater sampling and characterisation, laboratory experiments and geochemical and hydrogeological modelling.

2 Site Description

The Ruprechtov site is situated in the NW part of the Czech Republic (Fig. 1) in Hroznetin part of Sokolov Basin. The basin is filled with Oligocene and Miocene sediments, represented mainly by argillitized pyroclastical complex (Nové Sedlo Formation) with thickness of 0 – 100 m. Low-grade U accumulation is unevenly distributed within some volcanodetritic layers in the depth of 10 – 40 m. The simplified geological profile is presented on Fig. 2. [2, 3]

Fig. 1. Geographical position of the Ruprechtov site. Czech Republic

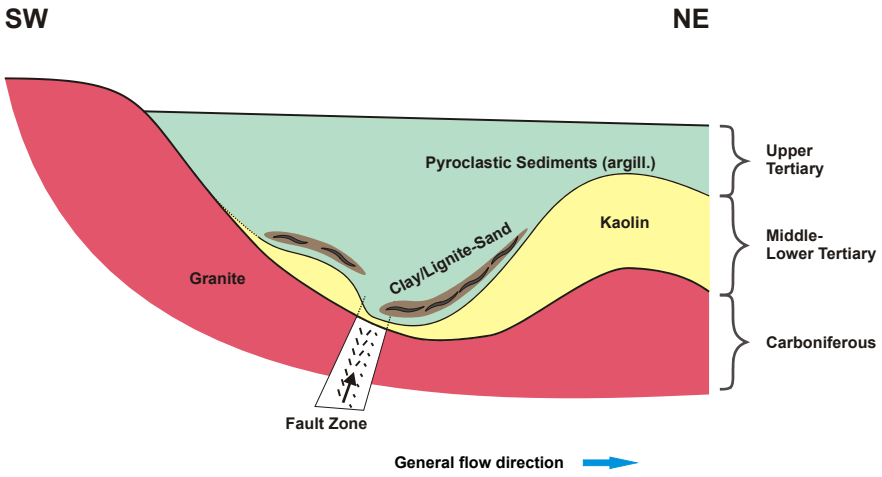

Fig. 2. Schematic geological profile through the rock sequence on the Ruprechtov site (simplified)

Carboniferous age granitic rocks, forming the Karlovy Vary Massif, occur under the sequence of sediments. Granites underwent intensive weathering in Mesozoic ages, causing kaolinization. These granitic bodies are elongated roughly in the NW–SE direction. Two rock types can be distinguished: older Horský granite (325–310 Ma) and younger Krušnohorský granite (< 305 Ma). The Horský granite type is medium grained monzogranite–granodiorite [4]. This shows high average content of Th (23 ppm, up to 42 ppm) at low U (total range 3.4–13.4 ppm) and Th/U > 1 (1.2–8.7, on average 4.0). Krušnohorský granite is extremely structurally variable [4] with higher concentrations of transition metals (Cr, Ni), HREEs and U (maximum 28 ppm) in contradiction with relatively low Th content (median 17 ppm) and significantly lower Th/U (0.5–4.8).

Volcanic material (pyroclastics), deposited in Hroznetin part of Sokolov Basin, originated in Doupovské hory Mts., situated eastward of the Ruprechtov site (basic neovolcanites – alkaline basalts, basanites and olivine nephelinites, with acid volcanites). The age of all volcanic rocks is roughly similar (22–28 Ma). The neovolcanites have low Th concentrations accompanied also by relatively low U contents.

The underlying Krušnohorský granite is the most presumable U source. This is also indicated by relatively high mean primary content of uranium. U concentrations can raise with sharp peaks in the sediment layers and can vary from some tens up to hundreds of ppm.

The current results indicate that U-mineralization is mainly located on the top of kaolin layer usually associated with organic-rich parts, which is – due to strong heterogeneity – usually described as "clay/lignite-sand-layer". The concentration profile of uranium shows a gradient from the top of granite up to the upper part of kaolin, suggesting leaching of uranium from weathered granite followed by diffusive transport through kaolin to the aquiferous horizon. Other processes could have been involved in origin of uranium accumulation, e.g., U transport in solution via fracture/fault zones, transport of U from surrounding granitic bodies by permeable layers, influence of hydrothermal volcanic activity in Tertiary ages.

3 Uranium Mineral Forms

Uranium could be found in the system mainly in U(IV) form. According to the separation experiments, using exchange chromatography, U(IV) forms 80 – 90 % of total uranium content in the enriched parts in the depth (experimental samples from approx. 40 m depth) [5]. That proves reducing conditions under which the U accomulation had been formed.

Mineral phases were studied either using classical methods (XRF, microprobe) and modern microscale surface methods, i.e., micrometer scale X-ray fluorescence and X-ray absorption (μ-XRF and μ-XAFS) [6]. Firstly, detrital immobile uranium phases were found, originated probably from granite source (monazite, rhabdophane, xenotime, zircon). U content in the detrital minerals is usually low and the phases forms minor part of U enrichment. Further, secondary uranium mineral phases of U(IV) predominantly, were identified: uraninite (UO_2), ningyoite (U, Ca, Ce)$_2$(PO_4)$_2$.1-2H_2O, tristamite (Ca, U, Fe)(PO_4, SO_4).2H_2O. According to μ-XRF maps of element distribution, U seems to be accumulated close to Fe nodules where it is associated with As [6]. Content of U in these

phases is high, forming major part of U-mineralisation. There is no spectral evidence for U(VI). Uranium accumulation was probably formed due to reduction of U(VI), that had been remobilized from granitic source and had precipitated with involvement of As.

Important part of accumulation is formed by U phases in non-crystalline form, not being able to be identified with XRF or any other spectral method. They could represent amorphous phases, sorbed U complexes, non-crystalline gel-like substances, etc. Their composition and U content are variable as well as their the occurrence [7]. The non-crystalline phases are not strictly bound neither on organic rich layers nor on pyrite enriched layers.

4 Sequential Extraction and ^{233}U Experiments

The sequential extraction method (SE) is classical approach used in order to found trace metal "forms" in sedimentary rocks. It consists of consecutive extraction steps, leaching the sediment with different extractants in order to define trace metal bonds on/onto sediment. The widely used method was published in [8] and consequently the number of modifications according to purpose of use was made so far, e.g., investigation of Cigar Lake natural analogue (Canada) [9].

To find the U forms on Ruprechtov site following schema was used (simplified):

1. U bound on exchangeable positions (leaching with $MgCl_2$)
2. U bound on carbonates (leaching with ammonium acetate with acetic acid)
3. U on Fe/Mn oxides (leaching with hydroxylamine hydrochloride in acetic acid)
4. U bound onto organic matter (using H_2O_2 and HNO_3)
5. U in residuum (using boiling with HNO_3)

Four samples were selected: NA 10 (kaolinized granite), NA11 and NA12 (argillaceous clay) and NA14 (high content of organic matter and uranium). Boreholes sampled were characterised in [2, 3]. 1 g of grained sample was used in the sequential extraction procedure. After each step the leachate was obtained in which U content was analysed. The fraction of U in each step was recalculated according to the total U content. Results are presented in Table 1 and in Fig. 3.

Simultaneously, easily mobilisable fraction of U was quantified by ^{233}U exchange method, using simulated groundwater from the Ruprechtov site. Methodology was published elsewhere, i.e., in [10].

Table 1. Fractions of U forms bound on the sediment. Samples: NA10 – kaolinized granite, NA 11 and NA 12 argil.clay, NA 14 argil.clay with high content of org. matter and U

Fractions (%)	NA10 A	NA10 B	NA11 A	NA11 B	NA12A	NA12 B	NA 14 A	NA 14 B
U in exch. positions	1.52	0.88	1.50	1.30	1.08	0.47	84.39	83.23
U on carbonates	73.93	72.97	64.42	67.96	12.34	12.62	4.84	5.25
U on Fe/Mn oxides	17.11	19.03	9.74	8.91	7.17	6.66	1.13	1.12
U on organics	4.87	3.99	14.39	11.76	34.97	34.87	7.15	8.03
Residuum	2.57	3.14	9.94	10.08	44.45	45.38	2.49	2.37
q_{ex} ($\mu g.g^{-1}$)	16.95		34.03		<0.238		380.08	

Considering increased content of organic matter, Fe and S (pyrite) in some samples (NA14), it seemed obvious that U should be sorbed on some of those element constituents. Surprisingly, high contents of U bound on carbonates were identified (see Fig. 3). However, XRF or any other method did not prove existence of important amount of carbonates in the sediments. Rarely some siderite concretions were found. This contradiction could be caused by either sorption of U(IV) carbonate complexes on the rock surface or by leaching of other mineral phases present in the sediment but not considered by sequential extraction schema.

Furthermore, the most of U is bound on exchangeable sites for NA14 samples with high content of U, TOC and S. This transfer onto easily removable fraction could be connected with high sulphur content and oxidising conditions under which samples were analysed. The rock samples from the depth (NA 14 60.69 m) were analysed under oxidation conditions. Reduced sulphide compounds (pyrite, etc.) could be therefore oxidised onto sulphates, releasing uranium from the sediment that could re-sorbed on different, easily accessible sites.

Exchangeable U amount, found with ^{233}U experiment, reached almost the same values (comparing concentration in $\mu g.g^{-1}$) as the sum of step 1 and step 2 in SE (U bound on exchangeable sites and on carbonates).

As mentioned above, phosphate U minerals form important portion of mineralisation. However, neither classical nor modified sequential extraction gave hint in which step phosphates were leached and consequently U bound is released. The only possible resolution of the question is to analyse U and P in the leachates from every SE step to identify selectivity of chemical agents.

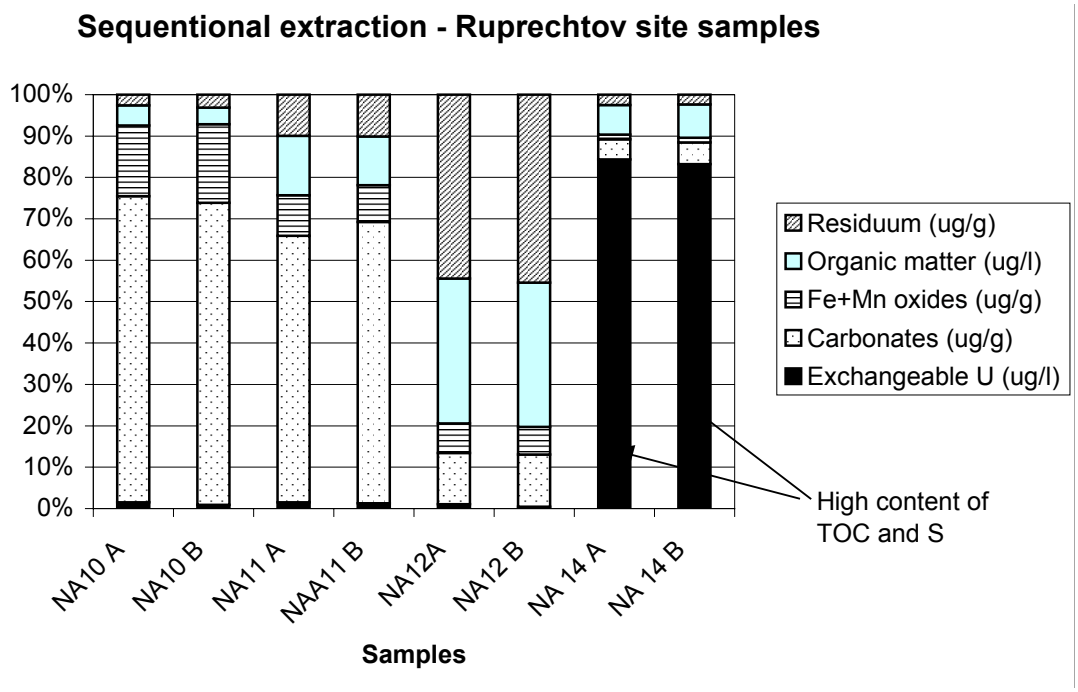

Fig. 3. Fraction of U forms (%) in the sediments from the Ruprechtov site (SE method)

5 Conclusions

The sequential extraction method has been and is still widely used in migration/remobilisation studies. The contradictions in widely used schema were found, analysing the Ruprechtov sediment samples. The discrepancy again drew out necessity that any result should not be taken into account without detailed analyses of phases, really leached out in every SE step. In Ruprechtov case further analyses of U, Th, P, Al, As, Fe, S, K, Ca, Na, K and alkalinity will be performed for each SE step in order to define and model solution/solid system and U forms. Furthermore, this problem proved necessity to use the SE method not as a solitaire and all-to-prove method, but in integration with modern surface and phase analyses methods (XRF, μ-XRF, XAFS…)

References

[1] Noseck U. et al.: *In:* Uranium in Aquatic Environment (Merkel B. el al. ed.) Springer, Berlin, Heidelberg (2002).
[2] Hercík M.: Technická a geologická dokumentace vrtných prací. Přírodní analog. Report ÚJV Řež a.s., 2005.
[3] Hercík M.: Závěrečné shrnutí výsledků projektu Přírodní analog. Report ÚJV Řež a.s., 2005.
[4] Breiter K., Knotek M. and Pokorny L: Folia Musei Rerum Naturalum Bohemia Occidentalis *33* (1991) 1.
[5] Suksi: *In:* Noseck U. et al.: Geochemical behaviour of uranium in a natural argillaceous system at Ruprechtov site. MIGRATION, Avignon, 2005.
[6] Denecke M. et al.: Env. Sci. Technol. *39* (2005) 2049.
[7] Sulovský P.: Mineralogy of Ruprechtov site samples. Expert report. NRI Řež, 2004.
[8] Tessier A., Campbell P. G. C. and Bosson M.: Anal. Chemistry 51 (1979) 844.
[9] Percival J. B. (1990): Clay mineralogy, geochemistry and partitioning of uranium within the alternative halo of Cigar Lake uranium deposit, Saskatchewan, Canada. Carleton University, Ottawa, PhD Thesis.
[10] Sachs S. et al.: FZKA 6969, Wissenschaft Berichte (Buckau G., ed.) Research Centre Karslruhe, Karlsruhe 2004, 79.

A.11 Identification of uranium enrichment scenarios by multi-method chracterisation of immobile uranium phases

Ulrich Noseck[*a], Thomas Brasser[a], Juhani Suksi[b], Vaclavá Havlová[c], Mirek Hercik[c] Melissa A. Denecke[d], Hans-Jürgen Förster[e]

[a]Gesellschaft für Anlagen- und Reaktorsicherheit (GRS) mbH, Germany
[b]University of Helsinki, Department of Chemistry, Finland
[c]Nuclear Research Institute (NRI), Czech Republic
[d]Forschungszentrum Karlsruhe, Institut für Nukleare Entsorgung, Germany
[e]University of Potsdam, Institute of Earth Sciences, Germany

Abstract

We investigate natural uranium occurrences as analogues for uranium migration and immobilisation in the post-operational phase of a radioactive waste repository. These investigations are aimed at gaining insight into the behaviour of uranium in a complex natural system. We characterise the immobile uranium phase and trace elements distributions in argillaceous uranium-rich samples from the Ruprechtov site, Czech Republic, applying a combination of different analytical methods. We use wet chemistry to determine the distribution of U(IV) and U(VI), sequential extraction to characterise different uranium phases, and $^{234}U/^{238}U$-activity ratios to correlate results between U(IV) and U(VI) distributions and the various uranium phases. Most of the uranium was determined to occur in a very long-term stable, tetravalent phase. Results from chemical methods are in good agreement with the results from spectroscopic methods. U(IV) mineral phases are identified by SEM-EDX spectroscopy and synchrotron-based µ-EXAFS. Electron-microprobe analysis confirmed that uraninite is newly formed and not a relictic phase from the altered granite. Correlation of uranium with As(V) located on thin As-rich layers on pyrite surfaces determined by confocal µ-XRF supports element correlations obtained by the sequential extraction. The key processes involved in uranium immobilisation in the argillaceous layers have been identified and can be used to reconstruct the geological history at the site.

[*] Author, to whom correspondence should be addressed

1 Introduction

The Ruprechtov site, located in the north-western part of the Czech Republic, is geologically situated in a Tertiary basin, which forms part of the Ohře rift (Noseck et al., 2004 and 2006). The study area itself is characterised by a granite, which partly crops out in the west and in the south, but is covered by kaolin layers of varying thickness (up to several tens of metres) in the central part. Large parts of the basin are overlain by pyroclastic Tertiary sediments. A multi-method study of these, now argillised sediments – in combination with lignitic intercalations and uranium enrichments close to such intercalations – permitted to gain a better understanding of the complex interrelations between transport and retention of radionuclides in argillaceous media with considerable amounts of organic matter under natural conditions, especially on very long-term scales relevant for performance assessment.

The interface between the kaolinised granite and the overlain pyroclastic sediments mimics the surface of the region in Tertiary time. Its strong morphology, i.e. former humps and hollows, is still preserved underground, with variations in altitude of more than 60 m. The horizon of major scientific interest is a clay/lignite layer at this interface at hollow positions, with a high content of sedimentary organic carbon (SOC), zones of uranium enrichment, and local zones of higher hydraulic conductivity (Noseck and Brasser, 2006). The occurrence of pyrite and siderite reflects the reducing conditions in this horizon containing up to 400 ppm U.

Previous investigations identified the sources of uranium and its transport pathways (Noseck et al., 2004). Adopting the strategy of combining analytical methods, as described subsequently in this paper, enables understanding of, and differentiating between individual uranium enrichment mechanisms at the site and provides information about their age and duration and the long-term stability of the respective uranium-bearing phases.

2 Experimental

Figure 1 shows a sketch of the area and the location of the boreholes, from which drill-core samples have been collected for analyses. RP1, NA8, and NA10 are boreholes located in the outcropping granite, in the south-western part of the study area. The clay/lignite samples originate from the northern and north-eastern part of the area. Due

to the morphology of the kaolin and underlying granite the depth of the uranium enriched clay/lignite layers varies between approx. 10 m and 60 m, as indicated by the gamma spectra for the drill cores in Figure 2.

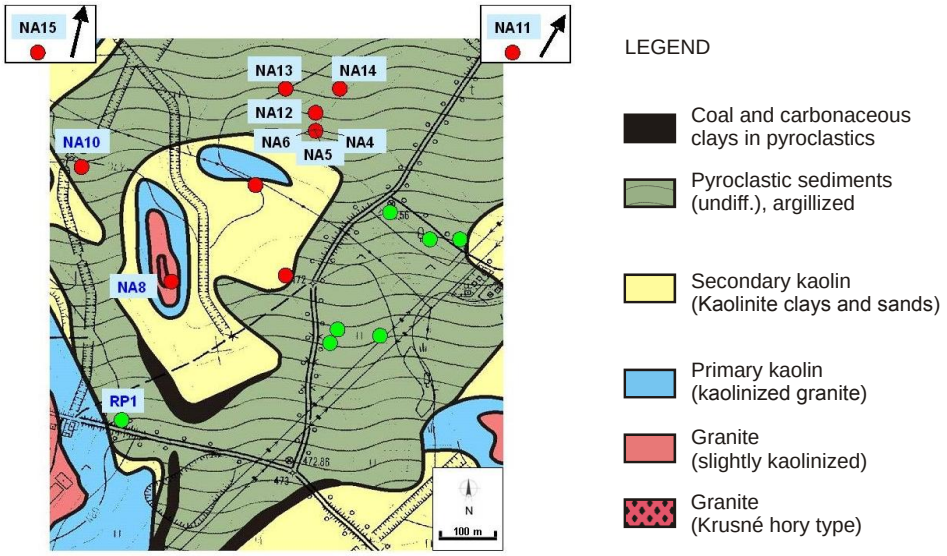

Fig. 1: Location of the boreholes, from which the core samples used in this paper were collected. NA11 and NA15 are app. 1 km outside of the depicted area, in the north and north-east, respectively.

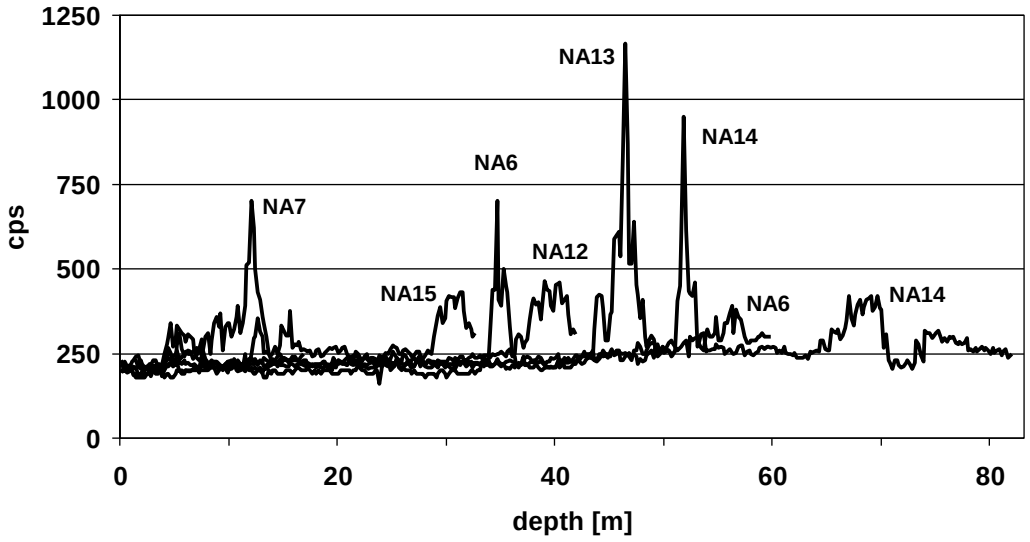

Fig. 2: Uranium concentrations in different drillcores detected by the on-site gamma log with a differential gamma ray spectrometer.

Different macroscopic and microscopic methods, summarised in Table 1, have been applied to samples from the boreholes and are briefly described here.

Table. 1: Different methods applied to clay/lignite samples from different boreholes

Method applied	NA4	NA5	NA6	NA11	NA12	NA13	NA14	NA15
U series measurement	x	x	x	x	x	x	x	x
$^{234}U/^{238}U$-activity ratios			x	x	x	x	x	x
U(IV)/U(VI)-separation			x	x	x	x	x	x
Sequential extraction				x	x	x	x	x
ASEM	x	x	x					
Electron microprobe	x		x					
µ-XRF, µ-XAFS	x		x					

U series measurements: U series disequilibrium measurements were performed to date bulk U accumulations. The sample material was dissolved in boiling concentrated HNO_3. ^{238}U, ^{234}U and ^{230}Th were analysed applying both liquid-liquid extraction and ion exchange methods. Radionuclide concentrations were measured by α-spectrometry.

U(IV)/U(VI) separation and $^{234}U/^{238}U$ activity ratios: The oxidation states U(IV) and U(VI) were determined using a method slightly modified from that presented in Ervanne and Suksi (1996). U(IV) and U(VI) phases were dissolved simultaneously by extracting the sample material in anoxic conditions with a mixture of 4 M HCl and 0.03 M HF under Ar atmosphere for 10 min. The solid to solution ratio was adjusted to about ~0.1. Uranium dissolution was intensified by performing extractions in an ultrasonic bath, while mixing the solution with Ar bubbling. Uranium was not totally dissolved during the extraction; the dissolution yield varied between 50% and 90%, indicating the presence of U-bearing minerals resistant to the used acid mixture. The extraction solution containing dissolved U(IV) and U(VI) was fed into a Dowex 1x4 (in Cl-form) anion-exchange column, which was regenerated with the same solution used for extraction. U(IV) passes the column, whereas U(VI) is retained. U(IV) was collected in the first 20 ml and U(VI) then eluted with 20 ml of 0.1 M HCl. Separation is quantitative and no overlap of U(IV) and U(VI) fractions has been observed in the tracer experiments. Uranium concentrations in the U(IV) and U(VI) fractions were determined using the procedure described in the context of U series measurements.

Sequential extraction: Sequential extraction (SE) is a widely used tool for studying the geochemical distribution of elements (e.g., Tessier et al., 1979, Percival, 1990, Havlová et al., 2006). In practice, operationally defined phases and their elemental content are dissolved and separated with specific reagents. The following SE scheme was applied to the Ruprechtov samples from the clay/lignite horizon:

1. U bound onto exchangeable sites (leaching with with 1M $MgCl_2$ for one hour, pH4 - 5)
2. U bound to carbonates (leaching with 1 M ammonium acetate in 25 % acetic acid for five hours, pH 4.8)
3. U associated with Fe/Mn oxides (leaching with 1 M hydroxylamine hydrochloride in 25 % acetic acid for 12 hours, pH 2)
4. U as U(IV) and/or onto organic matter (leaching with 30 % H_2O_2 and 0.02 M HNO_3 for 5 hours, continuously heating, pH 2)
5. U in residuum (boiling with 8 M HNO_3) at least for two hours)

In each step the solid residuum and the leachate were separated by 4000 rpm centrifugation for 10 minutes. The uranium content in the leachate solutions was determined by ICP-MS. Multi-element analyses (Na, K, S, Fe, As, P) of SE leachates were performed for two samples (NA14 and NA15), in order to better define the phases dissolved in each extraction step. A statistical procedure, i.e. cluster analysis, was used to identify possible correlations between elements and the dissolving/leaching phases of the sediment (Denecke and Havlová, 2006).

ASEM and Electron Microprobe: Analytical Scanning Electron Microscope (ASEM) observations were made using a ESEM-XL30TMP (Philips/Fei) instrument scanning electron microscope equipped with an EDAX detector. Quantitative analyses of accessory minerals were performed using CAMEBAX SX-50 and SX-100 electron microprobes operating in the wavelength-dispersive mode. The operating conditions during analysis of accessory minerals were as follows: accelerating voltage 20 kV, beam current 40–60 nA, and beam diameter 1–2 µm. Counting times, data reduction, analyzing crystals, standards, analytical precision and detection limits are described in detail in Förster (1998a, 1998b).

µ-XRF/µ-XAFS: The main feature of the set up used is two polycapillary half-lenses in a confocal geometry. This confocal set up allows probing defined volumes below the surface of the sample with a µm-scale resolution. By scanning arbitrary sample areas (x,y scans) at different depths (z), stacks of tomographic cross sections can be recorded. A detailed description of the method is given by Denecke et al. (2005).

Micro-X-ray fluorescence (µ-XRF) measurements, using a band pass of wavelengths, are made at the Fluo-Topo Beamline (ANKA) and at Beamline L (HASYLAB). Monochromatic X-rays are used for collecting some µ-XRF data and all micro-X-ray absorption fine structure (µ-XAFS, consisting of XANES and EXAFS) spectra at

Beamline L. The measurements focused on uranium hot spots identified previously by autoradiography. All results reported in this paper originate from core samples of the U-enriched horizon in borehole NA4 and NA6.

3 Results and discussion

U series activity ratios and U(IV)/U(VI) separation

Uranium series data are presented in the form of a Thiel's diagram (Thiel et al., 1983), which is generally used to interpret U series disequilibria (Figure 3). The diagram is divided into segments determined by (i) the $^{234}U/^{238}U$ equilibrium line (i.e., AR = 1) and (ii) the line obtained when a tangent is drawn on the closed system chain decay curves evolving towards radioactive equilibrium ($^{230}Th/^{238}U$ = 1 and $^{234}U/^{238}U$ = 1) after sudden accumulation and removal of U. The segments S1 and S2 between the U addition and removal areas represent U series disequilibria, which cannot be created by closed system chain decay. Data plots in segment S1 are interpreted to represent an open system, where selective ^{234}U removal is favoured. U series disequilibria determined by the segment S2 are interpreted to represent an open system affecting bulk U. Data plots in this segment represent samples with recently accumulated U (within the last million years) and subsequent U removal.

Most of the data points plot in segment S1, indicating stable conditions with respect to bulk U. The ages of U phases in the respective samples are beyond the U series method. Thus, at least a significant fraction of U in the clay/lignite horizon is more than one million years old. The number of data points in the bulk U addition area indicates that some U accumulation is still in progress. In order to better characterise the different U forms and to distinguish between U valencies, different separation methods were applied.

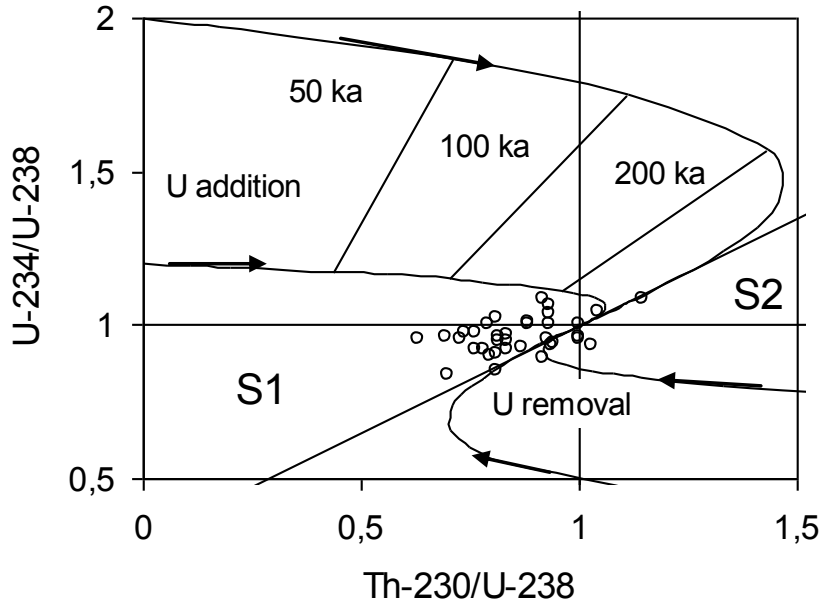

Fig. 3: $^{230}Th/^{238}U$ and $^{234}U/^{238}U$ activity ratios of bulk samples from the clay/lignite horizon plotted in Thiel's diagram, with isochrones. Curves started from $^{230}Th/^{238}U=0$ and $^{234}U/^{238}U=1.2$ and 2 in the U addition area have been taken as examples to show how activity ratios change as a function of time in the closed system after sudden U accumulation with the $^{234}U/^{238}U$ activity ratios 1.2 and 2. Curves in the U removal sector describe changes in isotope ratios back to secular equilibrium after sudden U removal. Segments S1 and S2 between U removal and addition areas represent open system (see text).

U(IV)/U(VI) separation was performed on four samples from three different boreholes (NA6, NA13, NA14). Two samples were taken from borehole NA6, one from the major U-peak at 35 m depth and one from a second, smaller peak at 37 m depth. The other two samples were taken from depths with the highest U concentration in boreholes NA13 and NA14. The distance between each borehole is approx. 50 m.

The U(IV)/U(VI)-separation results are listed in Table 2. The analytical error of the measured activity ratios (denoted AR) is usually in the range of 1 to 5 %, and only in exceptional cases up to 10 %.

The total U concentration in the samples ranges from 35 to 468 ppm, with the lowest concentration in sample NA6, from a depth of 37 m (35 to 48 ppm). In all other samples, U concentrations are significantly higher, with the largest value of 468 ppm in NA6 from 36 m depth. We observe that U in the core samples consists of both U(IV) and U(VI). Note that the extraction does not dissolve all U. The U content in this insoluble phase is denoted as U(res).

Table 2: Amount of uranium and $^{234}U/^{238}U$-activity ratios in the different phases from U(IV)/U(VI)-separation. U(res) is assumed to be U(IV) (see text for explanation)

sample	U [ppm]	U(IV)		U(VI)		U(res)	
		[%]	$^{234}U/^{238}U$	[%]	$^{234}U/^{238}U$	[%]	$^{234}U/^{238}U$
NA6-35a	356±7	28.7	0.54±0.01	41.9	1.42 ± 0.02	29.5	0.65± 0.01
NA6-35b	468±9	45.9	0.56± 0.01	33.3	1.69 ± 0.03	20.7	0.64± 0.02
NA6-35c	369±8	23.3	0.47± 0.01	47.4	1.16± 0.02	29.3	0.67± 0.01
NA6-37a	37.3±2	73.7	0.79± 0.03	15.7	2.66± 0.07	10.6	0.73± 0.01
NA6 37b	47.5±2	66.2	0.52± 0.01	9.0	3.37± 0.15	24.8	0.86± 0.02
NA6 37c	35.7±2	51.3	0.58± 0.01	19.8	2.56 ±0.08	28.9	0.71± 0.04
NA13 46	216±5	5.8	0.53± 0.02	43.9	1.15± 0.02	40.3	0,55± 0.01
NA14 51	354±9	25.5	0.88± 0.02	39.5	1.28± 0.02	35.0	0.54± 0.01

The $^{234}U/^{238}U$ AR differs significantly in the U(IV) and U(VI) phases, with ratios <1 in the U(IV) phase and ratios >1 in the U(VI) phase. The AR of the U(res) phase is similar to that observed in the U(IV) phase. Taking into account the higher stability of U(IV) phases, we suppose that U(res) exists as a stable mineral phase in oxidation state IV. Most U in all samples is U(IV), with fractions between 52 and 90 wt.%. The largest U(IV) fraction is found in sample NA6-37, which also displays the lowest total U concentration.

That U(res) and U(IV) exhibit an AR below one is a strong indicator for their stability. AR values significantly below unity are caused by the preferential release of ^{234}U, which is facilitated by α-recoil process and subsequent ^{234}U oxidation (e.g., Suksi et al., 2006). In order to attain low AR values of approx. 0.5 in the U(IV) phase, the phase must have been stable for a sufficiently long time, i.e. no significant release of bulk U has occurred during the last million years. This is in agreement with the hypothesis that the major U input into the clay/lignite horizon occurred during the Tertiary, more than 10 million years ago (Noseck and Brasser, 2006). The prevailing groundwater conditions, with low Eh values especially in the clay/lignite horizon of borehole NA6, is another indication that stable, insoluble U(IV) phases such as uraninite can be expected under the present physicochemical conditions (cf. section 4).

The AR in groundwater generally reflects the nature of water-rock interaction and is, therefore, sensitive to groundwater conditions (see Suksi et al., 2006). At oxidising conditions, both isotopes are released into the groundwater in the ratio they have in the U source. At anoxic conditions, where the bulk U release is strongly suppressed, the release of the more mobile ^{234}U(VI) is favoured. The low AR in the U(IV) phase observed in this study is correlated with AR values >1 in pore and groundwater from the

clay/lignite horizon (Figure 4). This is expected because of the anoxic sediment conditions and preferred mobilisation of ^{234}U.

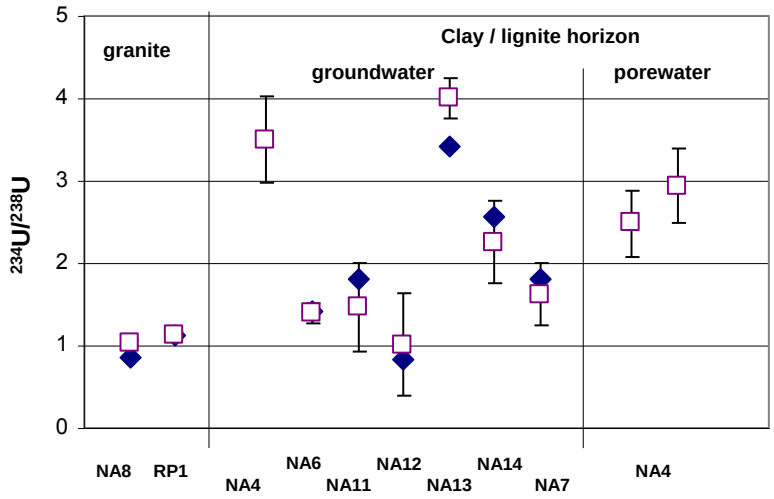

Fig. 4: $^{234}U/^{238}U$ activity ratios in groundwater from outcropping granite boreholes with high water flow and from groundwater/porewater from the clay/lignite horizon measured by α-spectrometry (open symbols) and ICP-MS (filled symbols).

Sequential extraction

The distribution patterns of U obtained from the five SE steps are illustrated in Figure 5. All samples stem from the clay/lignite horizon at the interface kaolin/pyroclastic rock and show remarkable similarities in that all released only a small amount of U in step 1 and step 3 leachates. The leachates from the first three steps always contain less than 25 % of the total U. The major portion of U in these samples is associated with the U(IV)/organic matter and/or the residual phase. In samples NA12, NA14A and NA14B, U leached in step 4 makes up nearly 70 % of total U. NA11 is exceptional in that more than 70 % of its U content is associated with the residual phase.

Results of Na, K, S, Fe, As, and P analyses in the leachates from each extraction step are evaluated by cluster analysis with the programme PAST (Hammer et al., 2001), in order to more accurately characterise phases and U forms dissolved in each extraction step. The results, shown in Figure 6, reveal that in both samples, P, As and U are assigned into one group. This is in close agreement with the results from µ-XRF and µ-XAFS measurements shown below. Fe and S are not correlated with U, i.e. there is no evidence for U dependence on Fe and S, although high contents of those two elements are observed in the sediment. As a large amount of K is leached in step 2, alumosilicates

or carbonate complexes are likely more responsible for U distribution than are carbonate minerals.

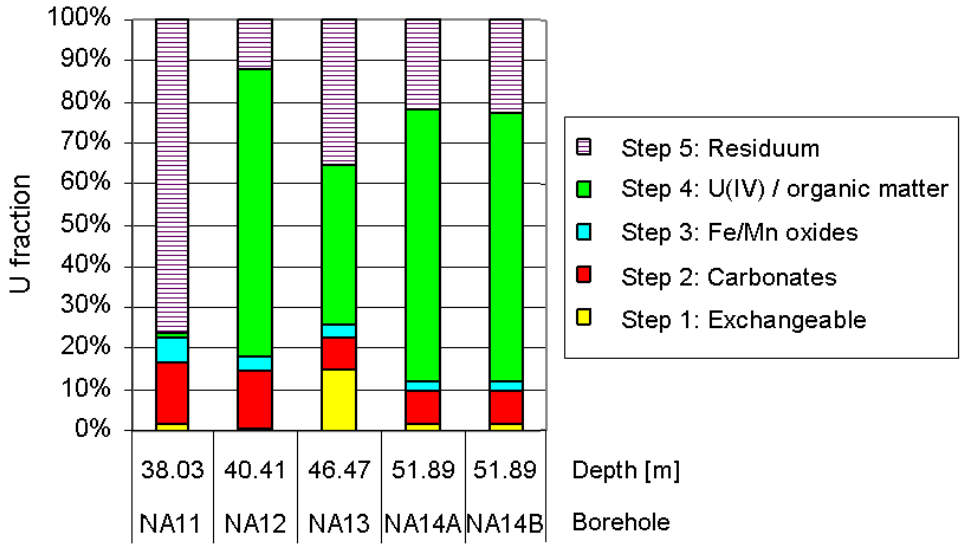

Fig. 5: Uranium content in the five fractions of the different samples from the clay/lignite horizon (borehole depth of each sample is indicated).

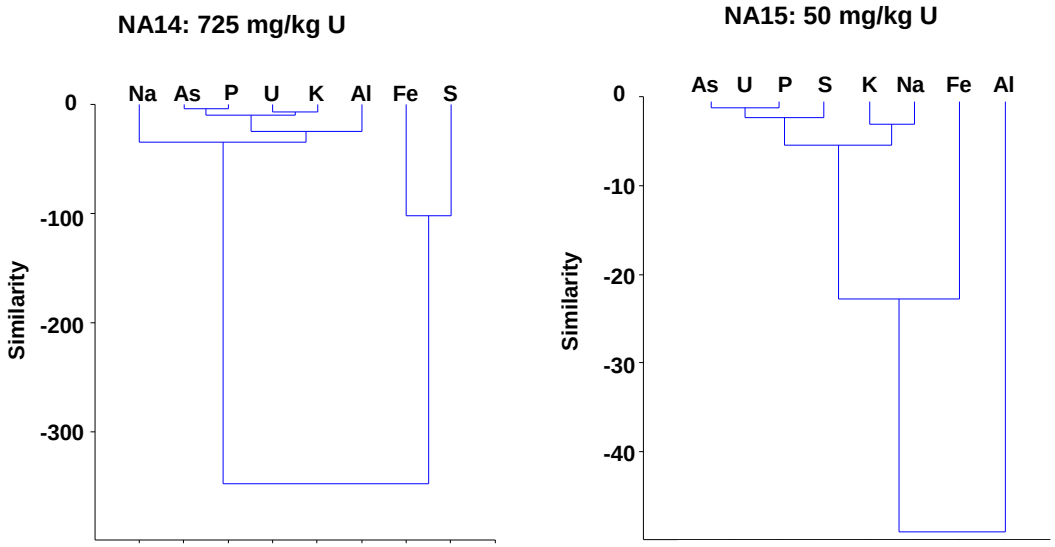

Fig. 6: Cluster analyses for extended SE results of samples from the boreholes NA14 and NA15.

The results from the SE study correlate with U(IV)/U(VI)-separation results, where the major part of U was identified to be associated with the U(IV) phase. In order to confirm that U in steps 4 and 5 is really in the tetravalent state, analyses of AR in the different SE leachates from sample NA13 were performed. The analyses were limited to

the leachates from step 1, 2, 4 and 5, since the U content in the third step is too low, <3 % of total U. The results are shown in Figure 7. The AR in steps 1 and 2 are quite similar, with values of app. 1.75. Upon comparing this value with results from U(IV)/U(VI)-separation we conclude that U extracted in these first two steps is U(VI). In contrast, the $^{234}U/^{238}U$-AR in leachates from steps 4 and 5 are around 0.5 to 0.6, which matches well the AR values observed in the U(IV) and U(res) fractions from U(IV)/U(VI)-separation. This correspondence confirms that U extracted in steps 4 and 5 is U(IV).

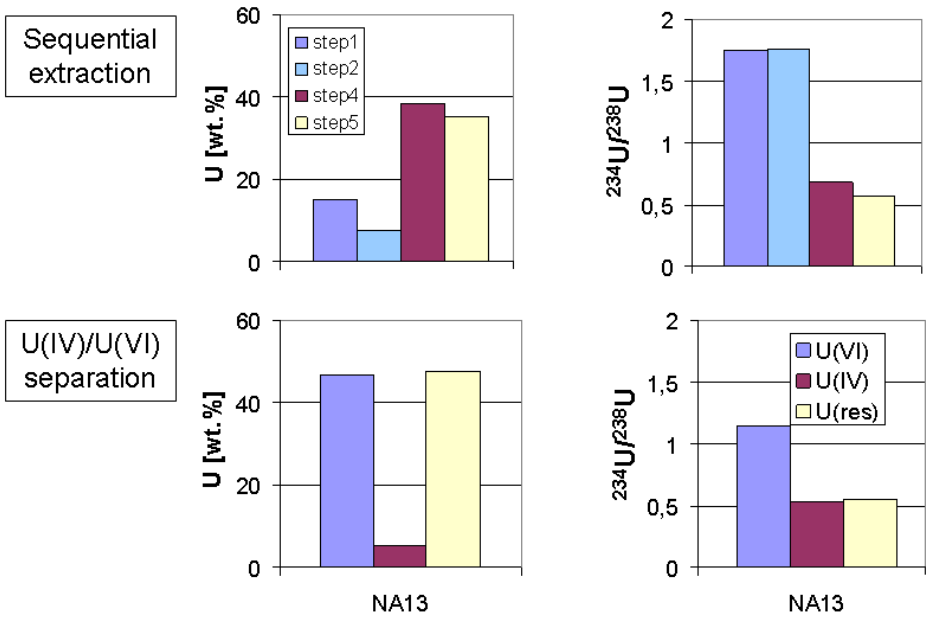

Fig. 7: Uranium content and $^{234}U/^{238}U$ activity ratios in SE leachates from steps 1, 2, 4 and 5 (top), compared to U(IV), U(VI) and U(res) fractions (bottom) in sample NA13.

The amount of U(VI) determined by the two methods differs. From U(IV)/U(VI)-separation, 44 % of U(VI) was obtained, whereas U extracted by steps 1 and 2 consists of only 22.5 % U(VI). One possible explanation for this discrepancy is that part of the U(IV) was oxidised during the U(IV)/U(VI) separation. We expect such an oxidation to affect a AR decrease in the U(VI) phase by dilution with U(IV) originally having a lower AR. The lower 1.2 AR value observed in the separation, compared to values of 1.75 and 1.76 from SE steps 1 and 2, might be an indication that partial oxidation of U(IV) to U(VI) actually occurred. In order to confirm this supposition, a systematic study on the U redox states during U dissolution is under way.

Microscopic methods

No U(VI)-bearing mineral phase was observed in the sediment by means of any of the applied microscopic methods. The U-bearing minerals identified by ASEM, in combination with electron microprobe, are monazite, zircon, xenotime, uraninite and ningyoite. Monazite-(Ce) (nominally $CePO_4$) is the most frequent actinide-bearing mineral in all samples. Most monazite occurs as angular grains up to 25 µm in diameter. The grains are often fractured and regions along fractures appear darker in BSE images than the unfractured portions of grains (Figure 8). The angular shape of the monazite grains, including shards, suggests that the grains are broken fragments of larger crystals.

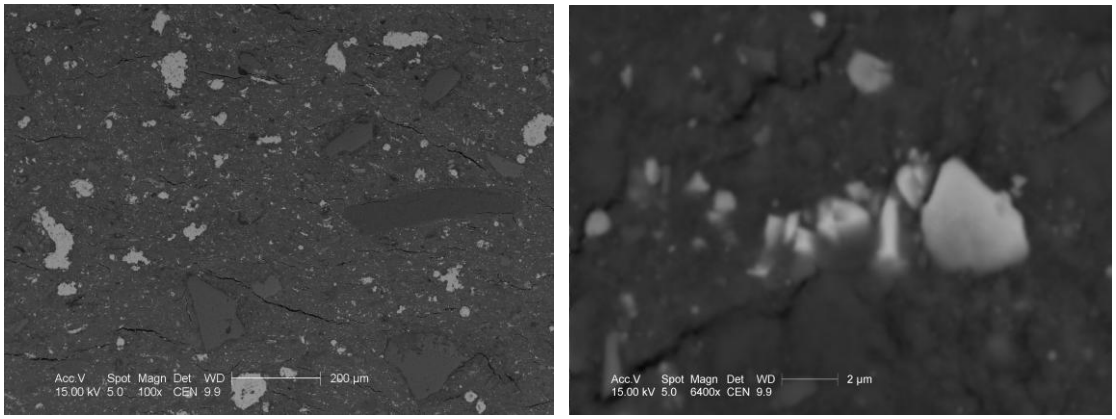

Fig. 8: Image of monazite grains in the sample from 36 m of borehole NA6.

Xenotime-(Y), containing Th and U in concentrations (in wt.%) $0.06<ThO_2<1.18$ and $0.89<UO_2<3.93$, occurs in all sediment sections in minor amounts. It forms overgrowths on zircon or independent grains usually less than 20 µm in size. The REE contents and patterns of xenotime from the sediment are indistinguishable from that in the underlying granite of the same borehole.

The similar composition of xenotime, monazite and zircon in the clay/lignite horizon and in the granite, as well as the angular shape of a large number of mineral grains, indicate that they are primary minerals of detritic origin. The determined U/Th-ratios indicate that less than 10% of the U in the enriched clay/lignite horizon is associated with primary minerals monazite, xenotime and zircon. The bulk of the uranium must, therefore, be associated with secondary U-minerals.

Ningyoite and uraninite have been identified as secondary minerals in samples NA4, NA5 and NA6 characterised by a high U content. To ascertain whether uraninite is really of secondary nature, two single, idiomorphic grains (8 x 8 µm in size) from the

clay/lignite horizon in NA6 were probed by electron microprobe. These grains exhibit a near-endmember composition and containing only traces of Si, Ti, and Al. Whether these three elements form part of the mineral structure or represent analytical artefacts from adjacent phases is impossible to resolve. The most important chemical feature of the uraninite in sample NA6 is that Th, Pb and (Y+REE) are present in amounts below their detection limits. This is distinctly different from the composition of the uraninite in the deeper, non-kaolinised granite, which contains several oxide weight percentages of Th and Pb, Y-contents (0.1 - 0.3 wt%) and yields a Th–U–total Pb age of 315.1 +/– 2.8 Ma (2σ STDW), in accordance with the age of other Erzgebirge granites of similar composition. These compositional differences are an unequivocal indication that the clay/lignite horizon uraninite is of secondary nature.

µ-XRF and µ-XAFS

Confocal µ-XANES results show uranium to be present in the tetravalent state and µ-EXAFS indicates the existence of a tetravalent uranium phosphate/sulphate phase (Denecke et al., 2005). The analyses of a number of tomographic cross-sections of elemental distributions recorded over different sample areas show a strong positive correlation between U and As. From µ-XANES measurements at the As K-edge at numerous sample positions, the presence of As(0) and As(V) was established. Furthermore, analysis of tomographic cross-sections of Fe, As(0), As(V), and U distributions reveal a correlation between As(V) and U and a linear correlation between As(0) and Fe. U and Fe are not correlated (Denecke et al., 2007). The linear correlation between As(0) and Fe shows that both components must be incorporated into the same mineral, implying the presence of arsenopyrite in the sample. This is confirmed by the observed similarity between As K XANES for arsenopyrite and that observed in As(0)-rich portions of the sediment. Further indication of the presence of arsenopyrite is seen in elemental distribution maps recorded with a high lateral resolution, where an As-rich boundary layer or rim surrounding framboidal Fe nodules is observed. Uranium occurs in immediate vicinity of these As-rich boundary layers.

From these results, a hypothesis for one of the driving mechanisms for uranium-enrichment by secondary uranium(IV) minerals in the sediment is elaborated. The arsenopyrite in the sediment reduced the mobile, groundwater-dissolved U(VI) to less-soluble U(IV), thereby immobilising the uranium in the sediment. As a consequence,

As(V) was formed. Uranium, therefore, is associated with As(V). These findings are consistent with that from extended SE analysis described above.

4 Geochemical conditions in the clay/lignite horizon

The Ruprechtov groundwaters are generally low mineralised, with ionic strengths in the range of $2 \cdot 10^{-3}$ and $2 \cdot 10^{-2}$ mol/l. Groundwaters from the clay/lignite horizon are of the Ca-HCO_3-type, whereas groundwaters from the granite are from the Ca-SO_4-type. The geochemical conditions in the clay/lignite horizon are further characterised by low Eh-values and pH-values between 7 and 8 (Figure 9), whereas the granite waters are more oxidising, with pH-values slightly below 7. These conditions are reflected by low U concentrations in the range of app. $5 \cdot 10^{-10}$-$5 \cdot 10^{-9}$ mol/l in the water from clay/lignite horizons and concentrations up to $5 \cdot 10^{-8}$ mol/l in the granite water. Geochemical calculations with PHREEQC show that U concentrations in the clay/lignite horizon are likely controlled by amourphous uraninite (Noseck and Brasser, 2006).

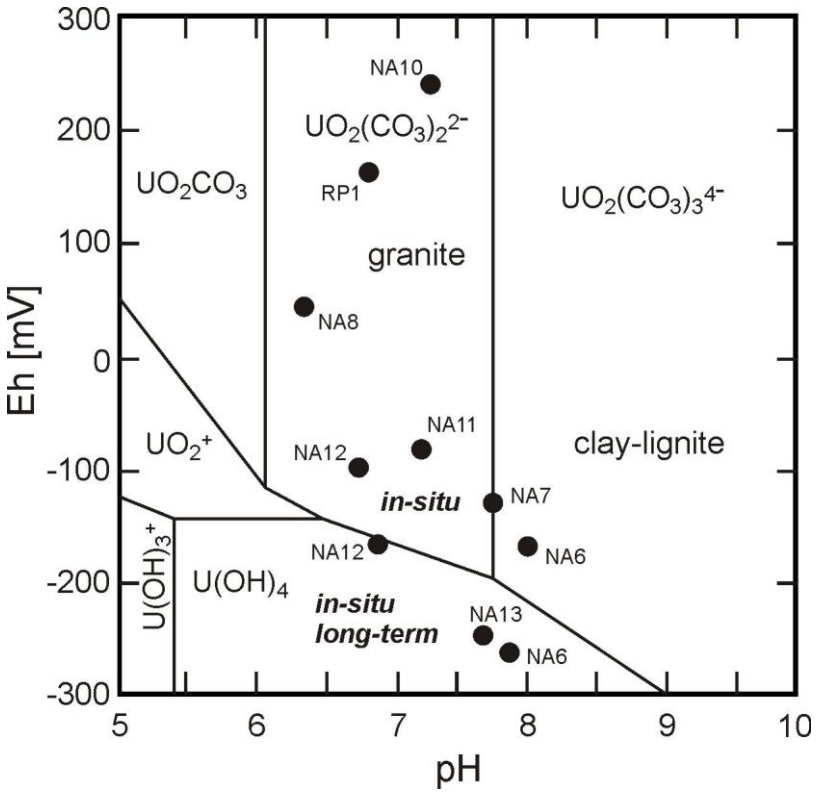

Fig. 9: pH-Eh-phase diagram of aqueous uranium species The dots represent groundwater measurements and illustrate the differences in the geochemical environment between granite and the clay/lignite horizon.

Laboratory data suggest that indigenous sulphur-reducing bacteria, extracted from samples taken at the site, helped maintain the redox potential at a level promoting reduction of U(VI) to U(IV) (Abdelous et al., 2008). It seems that the bacteria have most likely played a role during formation of sulphide minerals, such as pyrite, which are frequently observed in the clay/lignite layers at the site. The reduction of sulphates to sulphides resulted in the formation of pyrite. Figure 10 is an image of framboidal pyrite, whose shape suggests mineral growth by activity of microbes.

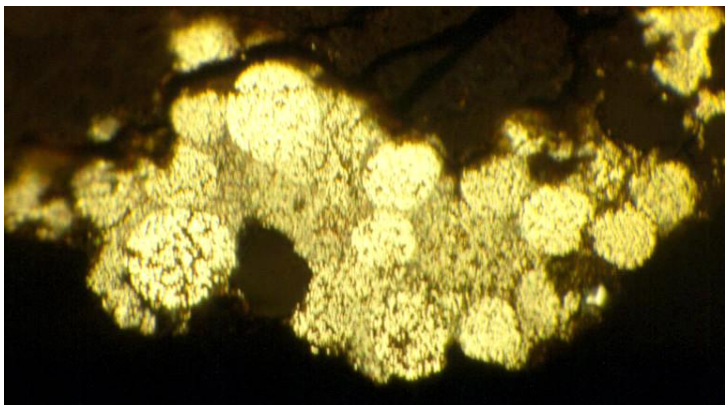

Fig. 10: Microphotograph of framboidal pyrite in the clay/lignite horizon.

5 Integration of results: Uranium enrichment scenario

Integration of all available information from our multi-method analyses, combined with current knowledge of the geological development of the site (Noseck and Brasser, 2006) results in the following scenario for U enrichment at the Ruprechtov site. Detrital input of U-bearing minerals (monazite, zircon, xenotime) predate the kaolinisation of the granite and is older than 30 Ma. During the Lower Oligocene and Miocene (30-16 Ma), the major volcanic activity occurred and deposited tuffaceous material in the basins. The alteration of granite to kaolin, i.e. by reaction of CO_2 with feldspars, and the argillisation of the tuffaceous material took place during this period. Microbial activity in the clay/lignite horizon led to the reduction of dissolved sulphate by sulphate-reducing bacteria, thereby leading to the formation of pyrite nodules. Sorption of As and subsequent formation of arsenopyrite occurred on the surface of the pyrite nodules. In this period, CO_2-rich water likely initiated U release from accessory minerals in the granite by formation of soluble uranyl-carbonate complexes. Uranium transported into

the clay/lignite horizon accumulated there by reduction of U(VI) to U(IV). One important reaction, which could be traced back until today, was the reduction of U(VI) by thin arsenopyrite layers on pyrite nodules formed by microbial sulphate reduction. Probably, microbial degradation of organic matter in the clay/lignite horizon caused phosphate release into the groundwater. This process is likely still active today (Noseck et al., 2007). The increased phosphate concentrations caused the precipitation of U as secondary phosphate minerals, e.g. ningyoite. Secondary uraninite might have formed at later stages of the geological history at conditions of lowered U concentrations, where saturation of ningyoite was no longer maintained.

The U series disequilibria results show that transport and immobilisation of U in the clay/lignite layers continued following the major input of U during the Tertiary. This, more recently enriched U seems to occur partially in the U(VI) state. However, we have not yet been able to identify the form of this U. We assume that it occurs adsorbed on clay or organic material.

The potential impact of these processes on AR in the sediment and groundwater in the clay/lignite horizon is illustrated in Figure 11. We assume that at the time of major U input during the late Tertiary (> 10 Ma), the AR in the infiltrating groundwater was unity, as it is today. Inflowing U(VI) was reduced at that time in the clay/lignite horizon and precipitated as secondary mineral phases. Therefore, the immobile U(IV) phase formed had the same ratio of unity.

Due to α-recoil related processes over a time frame of several million years, selective leaching of ^{234}U decreases the AR in the stable secondary U(IV) phase. The preferred mobilisation of ^{234}U for ^{238}U also leads to an AR increase in the pore-water and in the groundwater-bearing layers, with low flow velocity in the clay/lignite horizon. The AR in the pore-water and groundwater-bearing layers is also affected by slow inflow of water from the infiltration area, containing U with AR around 1. Typical AR values in the clay/lignite horizon are in the range between 2 and 4. Similar values are found in the more accessible U fractions in the immobile phase, which have been more recently accumulated in the clay/lignite horizon.

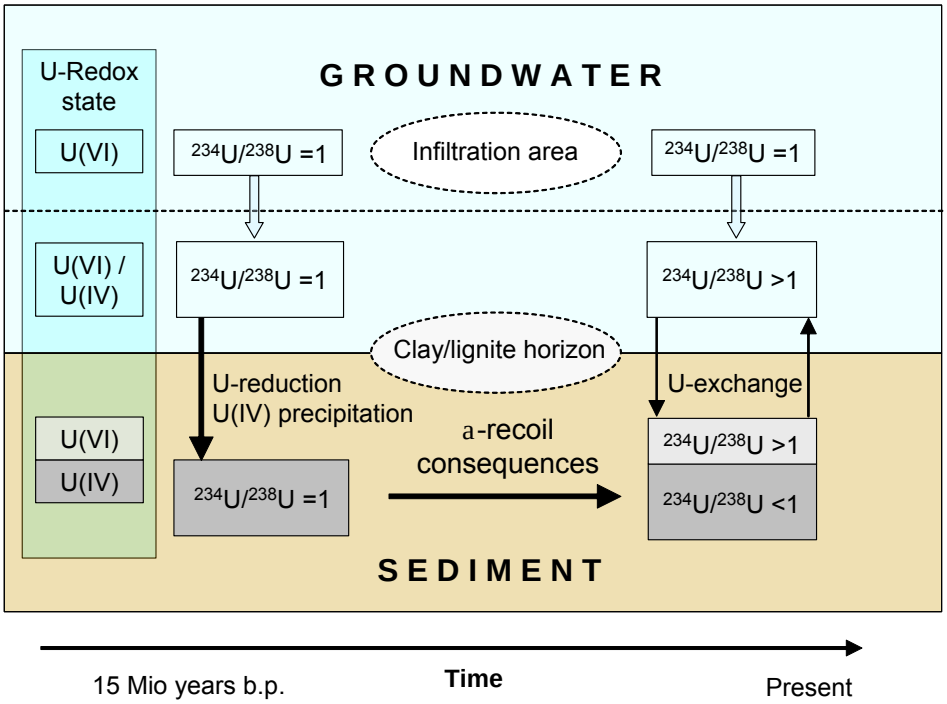

Fig. 11: A model for the development of the $^{234}U/^{238}U$ AR in the groundwater-sediment-U system in the clay/lignite horizon. The uranium redox state in each component is shown in the boxes on the left. ARs (boxes) in dissolved and immobile phases in the clay/lignite horizon are affected by inflow of water from the infiltration area (open arrows), mobilisation/immobilisation processes and consequences of α–recoil processes (closed arrows) during the very long time frames (see text).

6 Conclusions and outlook

The paper shows the great potential of combining macroscopic and microscopic methods to provide insight into the U enrichment processes at the Ruprechtov site, and at similar sites elsewhere. Microscopic methods aided in identifying important mineral phases and their origin, i.e. primary minerals of detrital origin or secondary minerals. Detailed X-ray spectroscopic investigations with a micro-focussed beam identified U as a tetravalent phosphate or sulphate mineral phase, in good agreement with ASEM and electron-microprobe results. Furthermore, the spatial distribution of elements and element correlations, i.e. Fe with As(0) and U with As(V), have revealed one important immobilisation mechanism of U(VI) by reduction to U(IV) on arsenopyrite layers formed on pyrite surfaces.

The results from microscopic methods are supported by cluster analysis of sequential extraction results, demonstrating the correlation of U with As and P. Furthermore, U(IV)/U(VI)-separation and SE, coupled with analysis of AR in each phase, identified that the major part of U occurs in the tetravalent state, in agreement with results from spectroscopic methods. It was established that the U(IV) phase remained stable over geological times under the reducing conditions in the clay/lignite horizon. Additionally, an easier accessible fraction of U(VI) was identified in the clay/lignite horizon, which was formed more recently.

To separate U(IV) and U(VI), a wet chemical method was applied for the first time to the samples from Ruprechtov site. The results are very promising, but the quantification of U(IV) and U(VI) phases using the separation method needs to be assessed, to ascertain if possible redox disturbances are caused by the U dissolution. A systematic study aimed to compare U(IV)/U(VI)-separation and SE methods with homogenised samples is under way. In addition, the effect that Fe has on the redox state of U during the sample dissolution will be investigated.

7 Acknowledgement

This work was financed by the German Federal Ministry of Economics and Technology (BMWi) under contract no 02 E9995, by RAWRA and Czech Ministry of Trade and Industry (Pokrok 1H-PK25), and by the European Commission within the integrated project FUNMIG.

8 References

Abdelous, A., Grambow, B., Andres, Y., Noseck, U., 2008. Uranium in argillaceous sediments: sorption/desorption processes and microbial effects. Submitted to Environ. Sci. Technol.

Denecke, M.A., Somogyi, A., Janssens, K., Simon, R., Dardenne, K., Noseck, U., 2007. Microanalysis (micro-XRF, micro-XANES and micro-XRD) of a Tertiary sediment using synchrotron radiation. Microscopy Microanal. 13(3), 165-172.

Denecke, M.A., Havlová, V., 2006. Element Correlations Observed in Ruprechtov Tertiary Sediments: Micro-Focus Fluorescence Mapping and Sequential Extraction. Proceedings of the 2nd Annual FUNMIG Workshop, Stockholm, Sweden 21.11-23.11.2006.

Denecke, M.A., Janssens, K., Proost, K., Rothe, J., Noseck, U., 2005. Confocal micro-XRF and micro-XAFS studies of uranium speciation in a Tertiary sediment from a waste disposal natural analogue site. Environ. Sci. Technol. 39(7), 2049-2058.

Ervanne, H., Suksi, J., 1996. Comparison of Ion-Exchange and Coprecipitation Methods in Determining Uranium Oxidation States in Solid Phases. Radiochemistry 38, 324-327.

Förster, H.-J., 1998a. The chemical composition of REE–Y–Th–U-rich accessory minerals from peraluminous granites of the Erzgebirge–Fichtelgebirge region, Germany. Part I: The monazite-(Ce) – brabantite solid solution series. Amer. Mineral. 83(3–4), 259–272.

Förster, H.-J., 1998b. The chemical composition of REE–Y–Th–U-rich accessory minerals from peraluminous granites of the Erzgebirge–Fichtelgebirge region, Germany. Part II: Xenotime. Amer. Mineral. 83(11–12), 1302–1315.

Hammer, Ø., Harper, D.A.T., Ryan, P.D. 2001. PAST: Paleontological Statistics Software Package for Education and Data Analysis. Palaeontologia Electronica 4. http://palaeo-electronica.org/2001_1/past/issue1_01.htm>.

Havlová V., Laciok A., 2006. Geochemical study of uranium mobility in Tertiary argillaceous system at Ruprechtov site, Czech Republic. Czech Journal of Physics 56, Suppl. D81.

Miller, B., Hooker, P., Smellie, J., Dalton, J., Degnan, P., Knight, L., Noseck, U., Ahonen, L., Laciok, A.,Trotignon, L., Wouters, L., Hernán, P., Vela, A., 2006. Network to review natural analogue studies and their applications to repository safety assessment and public communication (NAnet). Synthesis Report. EUR 21919.

Noseck, U., Rozanski, K., Dulinski, M., Laciok, A., Brasser, Th., Hercik, M., Havlova, V., Buckau, G., 2007. Characterisation of hydrogeology and carbon chemistry by use of natural isotopes – Ruprechtov site, Czech Republic. Appl. Geochem. (in prep.).

Noseck, U., Brasser, Th., 2006. Application of transport models on radionuclide migration in natural rock formations - Ruprechtov site. Gesellschaft für Anlagen- und Reaktorsicherheit (GRS) mbH, GRS-218, Braunschweig.

Noseck, U., Brasser, Th., Raijlich, P., Laciok, A., Hercik, M., 2004. Mobility of uranium in Tertiary argillaceous sediments - a natural analogue study. Radiochim. Acta 92, 797-803.

Percival J.B., 1990. Clay mineralogy, geochemistry and partitioning of uranium within the alternative halo of Cigar Lake uranium deposit, Saskatchewan, Canada. Carleton University, Ottawa, PhD Thesis.

Suksi, J., Rasilainen, K., Pitkänen, P., 2006. Variations in the $^{234}U/^{238}U$ activity ratio in groundwater – A key to characterise flow system? Physics and Chemistry of the earth 31(10-14), 556-571.

Tessier, A., Campbell, P.G.C., Bosson, M., 1979. Sequential extraction procedure for the speciation of particulate trace metals**.** Anal. Chem. 51, 844-851.

Thiel, K., Vorwerk, R., Saager, R., Stupp, H.D., 1983. ^{235}U fission tracks and ^{238}U-series disequilibria as a means to study recent mobilisation of uranium in Archaean pyritic conglomerates. Earth Planet Sci. Lett. 65, 249-262.

A.12 Carbon chemistry and groundwater dynamics at natural analogue site Ruprechtov, Czech Republic: Insights from environmental isotopes

Ulrich Noseck[*1], Kazimierz Rozanski[2], Marek Dulinski[2], Václava Havlová[3], Ondra Sracek[4], Thomas Brasser[1], Mirek Hercik[3], Gunnar Buckau[5]

[1]Gesellschaft für Anlagen- und Reaktorsicherheit (GRS) mbH, Theodor-Heuss-Str. 4, 38122 Braunschweig, Germany
[2]AGH - University of Science and Technology, Faculty of Physics and Applied Computer Sciences, Al Mickiewicza 30, 30-059 Kraków, Poland
[3]Nuclear Research Institute Řež plc (NRI), 250 68 Řež, Czech Republic
[4]Ochrana podzemních vod (OPV s.r.o.; Protection of ground water Ltd), Bělohorská 31, 169 00 Praha 6, Czech Republic
[5]Forschungszentrum Karlsruhe, Institut für Nukleare Entsorgung, P.O. Box 3640, 76021 Karlsruhe, Germany

*Corresponding author: Email ulrich.noseck@grs.de; Fax +49-531-8012200

Abstract

Hydrological, geochemical and environmental isotope data from groundwater wells at Ruprechtov natural analogue site are evaluated to characterize the flow pattern and the C chemistry in the system. The results show that water flow in the Tertiary sediments is restricted to 1 to 2 m thick zones in the so-called clay/lignite horizon with two different infiltration areas in the outcropping granites in the western and south-western part of the investigation area. Generally the flow system is separated from the underlying granite by a kaolin layer up to several tens of metres thick. Differences in stable isotope signatures in the northern part of the site indicate very local connections of both flow systems via fault zones. The observed increase of $\delta^{13}C$ values and decrease of ^{14}C activities in dissolved inorganic C during evolution of the groundwater from the infiltration area to the clay/lignite horizon was modelled using simple open- and closed-system models as well as an inverse geochemical model (NETPATH), which included changes in other geochemical parameters. The results from both types of models provided some insights into timescales of groundwater flow, but mainly revealed that additional sources of C are active in the system. These are very likely biodegradation of dissolved and sedimentary organic C (DOC and SOC) as well as the influx of endogenous CO_2. The occurrence of microbial degradation of SOC in the clay/lignite layers is indicated by the increase of biogenic DIC, DOC, and phosphate concentrations. The impact of microbial SO_4 reduction on this process is confirmed by an increase of $\delta^{34}S$ values in dissolved SO_4^{2-} from the infiltration area to the clay/lignite horizon with an enrichment factor of 11 ‰. The very low DOC concentrations of 1 to 5 mg C/L in the clay/lignite horizon with an organic matter content up to 50 % C is probably caused by very low availability of organic matter to the processes of degradation and DOC release, demonstrated by extraction experiments with SOC.

1 Introduction

Natural analogue studies contribute to the safety aspect for radioactive waste repositories in deep geological formations. They provide a better understanding of mobilisation and immobilisation processes of naturally occurring radionuclides in complex geological systems over extended periods of time. The Ruprechtov site, located in the north-western part of the Czech Republic, has been investigated from this perspective. It represents an analogue for potential migration processes in similarly structured overburden of salt domes, which are foreseen as potential host rocks for radioactive waste repositories such as the Gorleben site in Germany. Especially the occurrence of layers with a high content of organic material at the Ruprechtov site is of interest, because in the overburden of the Gorleben site lignite-rich horizons act as a source for humic colloids, which might facilitate radionuclide transport (Buckau et al., 2000a).

A prerequisite for better understanding of radionuclide migration at the site identified as a natural analogue is a thorough characterisation of the hydrogeological conditions, including time scales of groundwater flow in the area. Therefore, during recent years a comprehensive drilling programme was implemented at the Ruprechtov site (Noseck and Brasser, 2006). The characterisation of the groundwater flow regime at the site was based on determination of the hydraulic properties of the sedimentary layers, water-level measurements, analyses of major and trace elements as well as environmental isotope concentrations in groundwater. Furthermore, isotopic data were used to obtain a better insight into the complex C chemistry at the site. This sets up the basis for understanding the features and processes responsible for generation of dissolved organic matter, e.g. humic colloids.

A flow pattern for the Ruprechtov aquifer system has already been described by Noseck et al. (2004). The present contribution is a continuation of this work. For current evaluation of the system more drilling data and a substantially larger set of isotope data were available.

2 Geology of the study area

The Tertiary Sokolov basin, where the Ruprechtov site is located, was filled with tuffitic material by major volcanic activity during the Oligocene and Miocene. These tuffs are now argillized and denominated as pyroclastic sediments. At the Ruprechtov site, the basin is surrounded and underlain by Carboniferous granitic rocks, which have been intensively kaolinized in their upper part. Kaolin layers reach thicknesses of several tens of meters and in general represent low-permeability aquitards in the system. It is supposed that the kaolinisation process occurred mainly during the Miocene, after coverage with tuffitic material (Noseck and Brasser, 2006). The basal Staré-Sedlo

Formation (or equivalent rocks) fills depressions on the basement top and is overlain by the so-called volcano-detritic formation, which is mainly composed of volcanogenic series and intercalated lignite seams. The argillized lignite seams consist of up to 50 % organic matter and are associated with sandy material in many boreholes. Therefore, this layer is denoted as the clay/lignite-sand horizon. Uranium enrichment is observed within the lower part of and slightly below the lignite seams. A simplified geological cross-section is shown in Figure 1.

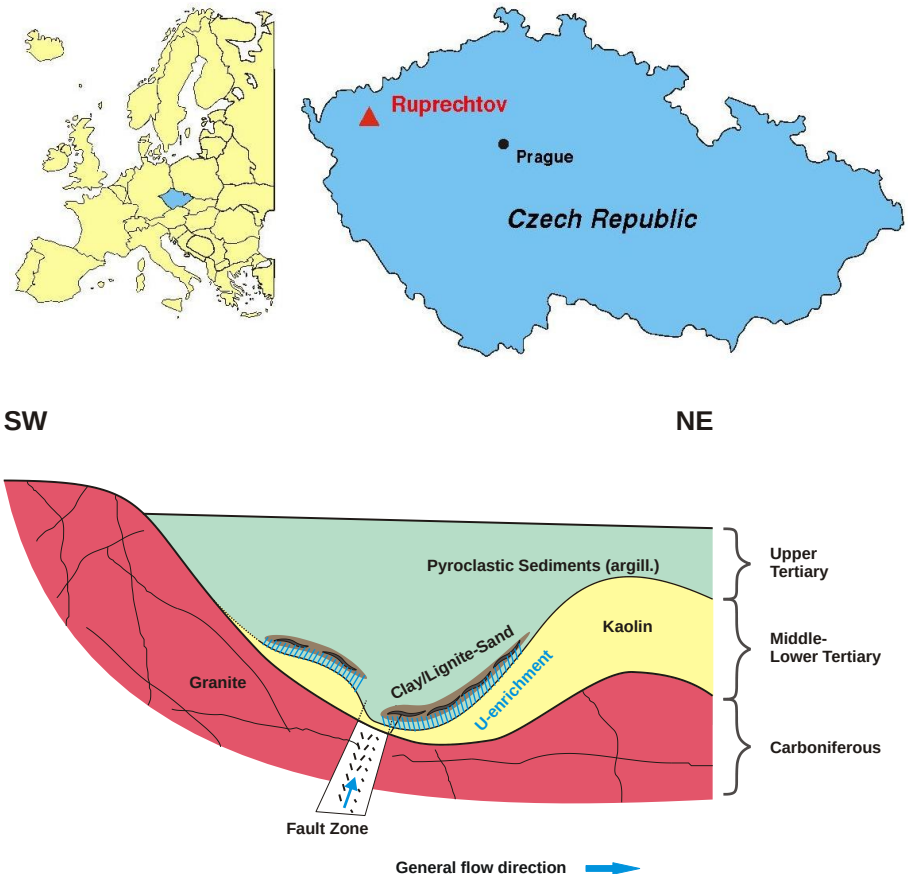

Fig. 1. Location of the Ruprechtov site in the Czech Republic (top) and simplified geological cross section of the Tertiary basin at Ruprechtov site (bottom)

An important feature of the kaolin/pyroclastics-interface is its strong morphology and substantial differences in kaolin thickness. The interface reveals a complex structure with elevations and depressions, where the greatest kaolin thicknesses forms elevated regions and lowest thicknesses of only a few meters coincide with depressions. The occurrence of fault zones in this area is known from a previous geological survey and their positions correlate with the morphological depressions (Noseck and Brasser, 2006). Therefore, areas with very low kaolin thickness might represent a connection of different groundwater systems in the granite and Tertiary sediments.

3 Material and methods

3.1 Hydrogeology

Altogether 12 wells have been drilled and lined in the study area in order to sample and characterize groundwater flow. Seven additional boreholes, which were drilled within the framework of kaolin exploration at the site, became available for this study. These additional boreholes are equipped with relatively long screens which may lead to the mixing of water originating from different water-bearing horizons. The location of sampled boreholes is indicated in Figure 2.

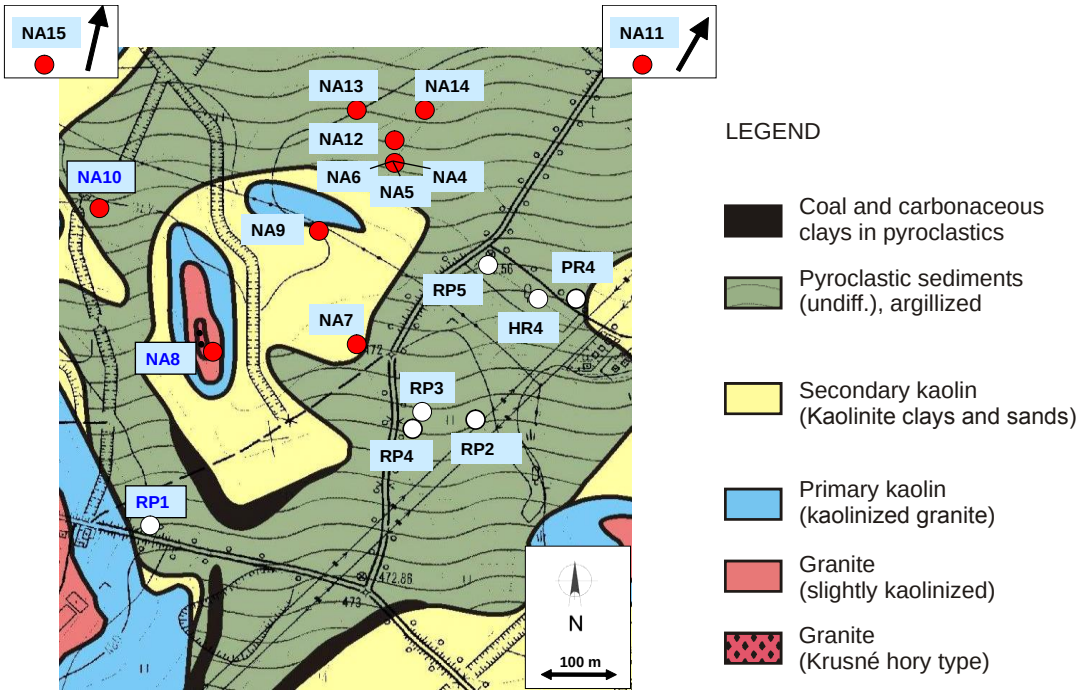

Fig. 2. The location of boreholes at Ruprechtov site, shown on the background of the geologic map. Dark (red) dots indicate research boreholes drilled in the framework of this study. White dots indicate boreholes which were drilled for other purposes and made available for this study. Figure is based on topographic map, which also shows e.g. roads and drainage channels.

Hydraulic conductivities have been determined by laboratory experiments performed on selected drill cores and by on-site pumping tests. Laboratory experiments have been performed according to DIN 18130, T1 (1998) with constant pressure head. Deionized water was used as fluid. For interpretation of on-site pumping tests the methods of Theis and Cooper-Jacob have been applied (Todd, 1980).

3.2 Water chemistry

Samples were obtained with a bladder pump and then filtered through 0.45 μm filters and for most analyses acidified with ultrapure HCl in the field. Concentrations of major

and trace elements were determined using an X-series ICP-MS with quartz controlled 27 MHz ICP generator and high performance quadrupole mass analyzer. Silicon concentration was determined with an IRIS Intrepid XUV ICP-OES. The respective analytical uncertainties (one standard deviation) are in the order of 0.5 % for major elements and <5 % for trace elements and silicon. Chloride was determined by argentometric titration, alkalinity was determined by titration with HCl using the Gran plot to determine end-point, and SO_4^{2-} was determined by ion chromatography. DIC was measured by conversion to CO_2 with H_3PO_4 followed by infrared detection with a TOC/TN 1200 analyser. For DOC analyses the sample was firstly acidified with H_3PO_4 to pH 2 in order to degas DIC. Then DOC was converted to CO_2 by combustion with O_2 and determined using infrared detection with the TOC/TN 1200 analyser. Phosphate and NO_3^- concentrations were determined by photometry. For CH_4 determination groundwater was sampled using special vials in order to prevent air intrusion. After gas - water equilibration in the vial under laboratory conditions CH_4 was determined using gas chromatography with a ThermoFinnigan TRACE GC 2000 with FID and ECD detection and a Supelco capilary chromatography column Carboxen 1006 Plot 30 m x 0.53 mm.

Field parameters (pH, Eh, temperature) were measured by an in-situ probe directly in the sampled boreholes, and in the laboratory. The chemical analyses were performed at Gesellschaft für Anlagen- und Reaktorsicherheit (GRS) mbH and at the Technical University Braunschweig. The results are reported in Table 1.

3.3 Environmental isotopes

Environmental isotope analyses of different types of groundwater samples were performed to characterize in more detail the flow regime and C chemistry of the Ruprechtov aquifer system. Stable isotope ratios ($^2H/^1H$ and $^{18}O/^{16}O$) were determined in near-surface waters to identify typical local infiltration waters. Additionally, ^3H concentrations in water, $^{14}C/^{12}C$ and $^{13}C/^{12}C$ isotope ratios in DIC and DOC pools, as well as $^{34}S/^{32}S$ isotope ratios in dissolved SO_4^{2-}, have been determined in groundwater samples from several wells.

The isotope ratios $^2H/^1H$, $^{18}O/^{16}O$, $^{13}C/^{12}C$ and $^{34}S/^{32}S$ are reported as per mil. deviations (δ^2H and $\delta^{18}O$, $\delta^{13}C$ and $\delta^{34}S$) from the respective isotope ratio of the internationally accepted standards (VSMOW, VPDB, VCDT), as given below for the $^{18}O/^{16}O$ ratio:

$$\delta^{18}O = \left[\frac{(^{18}O/_{16}O)_{sample}}{(^{18}O/_{16}O)_{standard}} - 1 \right] \cdot 1000$$

The respective analytical uncertainties (one standard deviation) are in the order of 0.1 ‰ for $\delta^{18}O$ and $\delta^{13}C$, 0.2 ‰ for $\delta^{34}S$ in the case of NA6/NA7 and 0.3 ‰ in the case of all other wells and 1.0 ‰ for $\delta^{2}H$. The concentration of ^{3}H is reported in Tritium Units (TU). One TU corresponds to the ratio $^{3}H/^{1}H = 10^{-18}$. The analytical uncertainty of the reported ^{3}H concentrations is in the order of 0.5 TU. The ^{14}C concentration is reported in percent modern carbon (pmc) and the quoted analytical uncertainty is in the order of 0.5 pmc and 0.3 pmc, for radiocarbon content in DIC and DOC, respectively.

The ^{3}H and stable isotope composition of water, as well as ^{14}C content and $\delta^{13}C$ values of DIC pool were determined at the Isotope Laboratory at AGH University of Science and Technology, Krakow, Poland. Deuterium and ^{18}O content in water samples were determined using the established techniques: Zn reduction for $\delta^{2}H$ and CO_2-equilibration for $\delta^{18}O$ (Coleman et al., 1982; Epstein and Mayeda, 1953). Tritium content in water samples was measured using electrolytic enrichment and liquid scintillation spectrometry, whereas the radiocarbon content of the DIC pool was determined using benzene synthesis combined with liquid scintillation spectrometry.

For determination of $^{14}C/^{12}C$ ratios in DOC 2L groundwater samples were filtered with a 0.45 µm silver filter, evaporated to 50 mL at 0.1 bar and acidified to pH 2 to remove DIC. The samples were then freeze-dried, combusted at 900°C in a quartz capsule with CuO and Ag wool and afterwards reduced to graphite with H_2 and Fe catalyser at 600°C. Analysis of ^{14}C and ^{12}C was done by accelerator mass spectrometry. Results were converted to percent modern carbon (pmc) units.

The analyses of $^{34}S/^{32}S$-ratios in dissolved SO_4 were performed following the technique of Coleman and Moore (1978), in which SO_2 gas is released by combustion with excess Cu_2O and silica, at 1125°C. Liberated gases were then analysed on a VG Isotech SIRA II mass spectrometer.

The analyses of $\delta^{13}C$ in SIC followed the methodology of McCrea (1950). Degassed samples were decomposed in 100 % H_3PO_4 in vacuum at 25°C. Liberated gases were analysed using a Finnigan Mat 251 mass spectrometer working in a continuous flow regime. The $\delta^{13}C$ content in DOC was analysed from the evaporated residuum, deprived of carbonates and bicarbonates, that was acidified with 100 % H_3PO_4. Liberated gases were analysed using a Finnigan Mat 251 mass spectrometer.

The results of the isotope analyses are summarized in Table 2. Table 2 also contains information on the depth of the screened horizon in the sampled boreholes as well as on the lithology and hydraulic conductivity of the water-bearing layers. For NA4, NA5 and NA6 boreholes, analyses from 3 consecutive sampling campaigns were available.

Table 1. Physical and chemical parameters of groundwater samples collected in the Ruprechtov aquifer system during sampling campaign in May 2004. All concentrations are expressed in mg/L. Eh-values are expressed in mV.

	NA4	NA5	NA6	NA7	NA8	NA9	NA10	NA11	NA12	NA13	NA14	NA15	RP1	RP2	RP5
T[°C]	9.60	9.00	9.80	9.10	9.00	7.30	8.40	9.80	9.10	9.90	9.20	9.40	9.70	9.60	9.10
pH1	n.a.	n.a.	8.00[1)]	8.00[1)]	6.20[1)]	7.19[1)]	7.40	6.89	6.65	7.65	6.85	7.29	6.81[1)]	7.72[1)]	7.00[1)]
pH2	6.78	7.05	7.80[1)]	7.05[1)]	6.45[1)]	6.83[1)]	6.95	7.04	6.68	7.41	7.00	7.09	6.75[1)]	7.35[1)]	6.89[1)]
pH3	6.75	7.04	7.57	7.49	6.15	6.97	6.67	7.11	6.73	7.66	6.94	6.71	6.40	7.70	6.93
Eh1	n.a.	n.a.	-280[2)]	-35[1)]	48[1)]	324[1)]	240	-91	-160[2)]	-252[2)]	-59	58	149[1)]	-3.8[1)]	133[1)]
Eh2	6	-10	-115[1)]	-107[1)]	143[1)]	355[1)]	485	65	15	25	120	245	363[1)]	25[1)]	160[1)]
Al	0.20	0.26	0.22	0.33	0.10	0.15	n.a.	n.a.	n.a.	n.a.	n.a.	n.a.	0.14	0.21	0.25
Ca	51.00	68.90	48.00	86.85	26.24	28.03	40.40	65.60	44.70	54.60	48.70	31.60	31.00	47.10	43.70
Fe	1.87	0.99	0.73	0.13	1.32	0.91	0.37	5.45	2.27	0.83	0.10	0.31	0.34	2.89	1.16
K	13.10	12.30	12.05	6.50	1.40	2.70	8.40	18.90	9.70	16.50	14.60	10.80	2.90	10.30	11.20
Mg	23.60	29.35	18.60	17.90	4.00	5.30	8.40	28.90	19.80	21.70	20.80	12.50	8.80	23.80	21.40
Na	23.30	45.25	37.20	16.40	10.90	14.10	15.50	91.20	20.10	35.80	39.50	25.30	13.40	41.80	19.20
Si	10.30	7.80	7.40	4.40	15.05	18.70	13.00	7.70	15.90	8.00	12.60	11.60	16.80	3.30	9.90
Cl	3.90	8.80	3.60	6.60	4.30	0.60	5.90	10.40	4.30	10.10	13.60	4.00	20.70	26.40	5.54
SO_4	19.80	31.50	49.50	28.20	59.10	11.80	40.80	178.60	22.90	22.90	30.80	40.10	19.80	55.00	14.80
PO_4[2)]	0.19	0.47	0.2	0.72	0.3	0.08	0.16	0.30	0.04	0.14	0.21	0.10	0.35	0.11	0.15
CO_2	40.71	43.60	6.70	9.60	31.70	8.60	24.50	40.60	63.00	10.50	32.80	13.80	44.40	1.00	20.50
NO_3	0.80	0.40	1.20	1.10	1.70	1.10	7.20	1.40	0.30	1.00	2.30	3.50	3.20	2.50	2.20
HCO_3	330.50	469.30	291.80	332.10	44.20	163.50	159.40	379.00	269.20	349.00	316.60	186.70	117.00	277.00	279.00
CH_4	0.634	0.097	0.072	0.007	n.a.	n.a.	0.003	0.011	0.028	0.04	0.022	0.004	n.a.	n.a.	n.a.

pH1: measured in-situ; pH2: measured on-site; pH3: measured in laboratory (T=20°C); Eh1: measured in-situ, Eh2: measured on-site

[1)] sampling campaign from May 2003

[2)] long-term value

Table 2. Depth of screened horizons, lithological units and environmental isotope data for boreholes in the Ruprechtov aquifer system sampled between 2003 and 2006. The table shows also DIC, DOC and SO_4^{2-} concentrations in the analysed groundwater samples.

Well No.	Screen horizon [m]	Lithology	k [m/s]	$\delta^{18}O$ [‰]	$\delta^{2}H$ [‰]	Tritium [TU]	^{14}C DIC [pmc]	^{14}C DOC [pmc]	$\delta^{13}C$ DIC [‰]	$\delta^{13}C$ DOC [‰]	$\delta^{34}S$ SO_4^{2-} [‰]	DIC [mg/L]	DOC [mg/L]	SO_4^{2-} [mg/L]
NA4	34.5 – 36.5	clay/lignite, U	1.52E-06	-9.78	-68.0	<0.5	3.2	40.0	-11.0	-26.6	24.63	74.2	4.22	19.8
NA5	19.3 - 21.3	U	5.47E-08	-8.98	-61.9	<0.5	5.3	n.a.	-10.9	-25	n.a.	90.8	n.a.	31.5
NA6	33.4 - 37.4	clay/lignite, U	5.62E-07	-9.27	-64.6	0.6	13.1	n.a.	-12.4	-26.8	23.5	60	3.27	49.5
NA7/1	15.5 - 19.5	kaolin	1.88E-07	-8.96	-61.5	<0.5	n.a.	n.a.	n.a.	n.a.	n.a.	61.7	3.88	28.2
NA7/2	10.5 - 11	clay/lignite, U	4.40E-05	-9.00	-61.1	<0.5	39.4	n.a.	-16.1	-27.3	20.4	60.8	n.a.	12.3
NA8	8.5 - 24	granite	2.00E-06	-9.22	-62.9	1.1	71.9	64.6	-21.9	-27.8	-8.5	14.5	3.01	59.1
NA9	4.4 - 10	kaolin	3.26E-06	-8.95	-60.8	<0.5	72.1	n.a.	-20.5	-27.1	n.a.	37.1	n.a.	11.8
NA10	19.5 - 27.5	granite	2.86E-08	-8.89	-61.5	1.6	54.6	n.a.	-16.2	-26.4	0.2	33.8	1.99	40.8
NA11	33.2 - 39	clay/lignite, U	6.50E-06	-9.00	-65.5	1.5	7.8	n.a.	-9.6	n.a.	n.a.	82.4	n.a.	178.6
NA12	36.5 - 39.3	clay/lignite, U	3.80E-07	-8.87	-61.9	<0.5	26.5	70.0	-16.0	-25.6	20.11	67	3.69	22.9
NA13	42.2 - 48	clay/lignite, U	2.30E-09	-9.24	-65.9	1.5	n.a.	44.3	n.a.	-27.2	n.a.	68.8	2.32	22.9
NA14	67.6 - 77.6	granite	2.75E-08	-9.33	-64.9	0.6	9.8	n.a.	-12.8	n.a.	16.43	69.1	n.a.	30.8
NA15	28.8 - 31.6	granite	1.19E-07	-9.88	-70.9	<0.5	11.8	n.a.	-13.7	n.a.	n.a.	39.4	n.a.	40.1
RP1	5 - 18	granite	3.37E-07	-9.52	-66.9	<0.5	21.0	n.a.	-16.8	n.a.	3.48	33.4	1.36	19.8
RP2	25 - 43	clay/lignite, U	2.78E-06	-9.81	-69.0	1.1	16.8	n.a.	-13.2	-26.6	n.a.	52.4	1.83	55.0
RP3	25 - 48	clay/lignite, U	2.25E-05	-9.60	-68.2	1.0	13.3	n.a.	-15.3	-26.6	n.a.	59.7	n.a.	24.6
RP5	30 - 58	clay/lignite, U	5.08E-08	-9.75	-68.4	<0.5	6.4	n.a.	-11.7	n.a.	n.a.	58.1	n.a.	14.8
HR4	46.5 - 95	granite	n.a.	-9.31	-64.3	1.2	29.9	n.a.	-14.5	-26.2	n.a.	n.a.	n.a.	n.a.
PR4	5 - 32	clay/lignite, U	n.a.	-9.00	-63.7	9.7	n.a.	n.a.	n.a.	n.a.	n.a.	n.a.	n.a.	n.a.

Data are single values from measuring campaigns in 2003, 2004 and 2006, respectively. Exceptions are $\delta^{18}O$, $\delta^{2}H$ and ^{3}H data for wells NA4, NA5, NA6 and RP5 and ^{14}C values in DIC for wells NA4 and NA5, which are averages of 2 or 3 analyses, respectively.

4 Results and discussion

4.1 Hydrology

Laboratory experiments on selected drill cores as well as on-site determination of hydraulic conductivities (pumping tests) revealed that only distinct water bearing layers exist with k-values of 10^{-5} m/s to 10^{-8} m/s and thicknesses of about 1 to 2 m only, mainly in the vicinity of the clay/lignite-sand layer. In contrast, the pyroclastic sediments and the underlying kaolin have a lower hydraulic conductivity, with typical k-values of 10^{-10} m/s to 10^{-11} m/s. The k-values for the different wells are shown in Table 2. As indicated above, fracture zones and areas with very low thickness of underlying kaolin might represent hydraulic connections between clay/lignite-sand layers and granite.

4.2 Hydrogeochemistry

The chemical conditions of the site are characterized by low mineralized waters with ionic strengths in the range from 0.003 mol/L to 0.02 mol/L. The pH-values vary in the range 6.2 to 8 and the Eh-values from 435 mV to -280 mV. More oxidising conditions with lower pH-values are found in the near-surface granite waters of the infiltration area. In the clay/lignite horizon conditions are more reducing with Eh-values as low as -280 mV. The Eh-values measured directly by in-situ probe are significantly lower than those measured on-site in pumped water (cf. Table 1). The latter method is more susceptible to disturbances by contact with atmosphere, which is probably responsible for the observed differences in Eh values.

Groundwater from nearly all boreholes of the clay/lignite horizon is of Ca-HCO_3-type. The exceptionally high Na and SO_4 concentrations in NA11 are probably an artefact of contamination by drilling fluid. The waters from the infiltration area in granite (NA8, NA10 and RP1) as well as water from borehole NA12 with significantly lower alkalinity and Ca concentration are defined as Ca-SO_4-type water. All DOC values are in a range between 1 mg/L and 5 mg/L. In a number of boreholes from the clay/lignite horizon CH_4 concentrations of over 0.01 mg/L (up to 0.7 mg/L) were detected.

In order to identify the most important factors controlling the groundwater geochemistry a principal component analysis (PCA) was performed by the program PAST (Hammer et al., 2001).

The results show that most information is covered by two components: Principal Component 1 (PC1) accounts for 80.6 % and Principal Component 2 (PC2) accounts for 15.3 % of the variability in the data set. PC1 is well defined and has a highly positive loading for HCO_3, positive loadings for Ca, Na, and Mg and a highly negative loading

for the redox potential, i.e. samples with low Eh are covered by this component. It represents a geochemically evolved reducing groundwater, similar to the water from the clay/lignite horizon with increased concentrations of cations and with high concentration of HCO_3^-. PC2 is not that well defined and has a positive loading for Si, highly negative value for HCO_3 and negative values for Na, and Mg. This component represents immature ground water, probably dominated by the dissolution of silicates close to recharge areas in the granitic formation.

The results of PCA are illustrated in Figure 3 indicating a progressive geochemical evolution from the left to the right. Wells from infiltration areas NA10 through RP1, NA9 and NA8 have relatively low values of PC1. On the other hand, clay/lignite wells NA12, NA13, NA11, NA4, NA14, NA5, and especially NA6, and NA7 have high values of PC1. This is consistent with decreasing Eh values and increasing HCO_3 concentrations in the same direction.

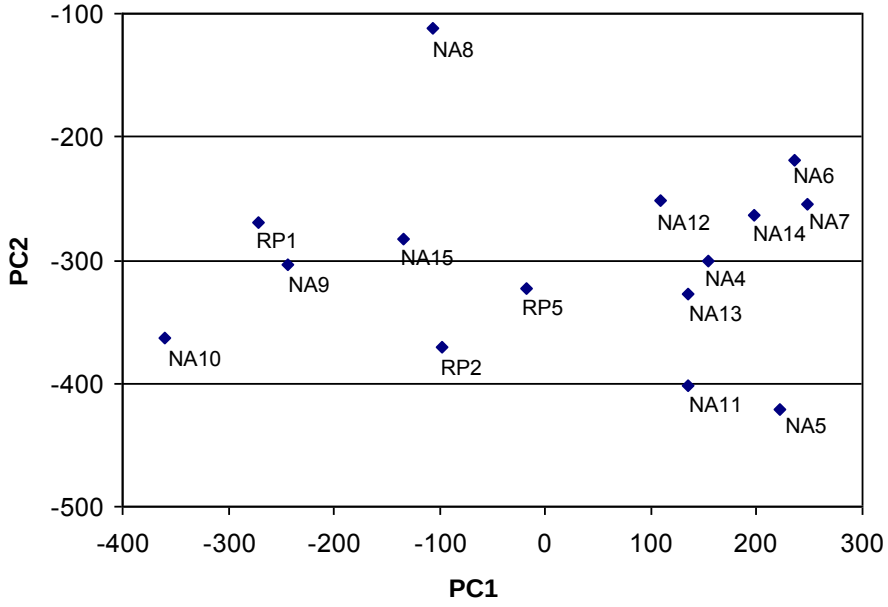

Fig. 3. Results of Principal Component Analysis: plot of PC1 vs. PC2 (see discussion in the text).

Groundwater in most of the analysed wells reaches saturation with respect to carbonate minerals. This is shown in Figure 4 where calculated saturation indices for several carbonate minerals are presented. Only groundwater samples in the boreholes NA8, RP1, NA12 and NA9 are undersaturated with respect to carbonate-bearing minerals. Calculations have been performed with PHREEQC (Parkhurst and Appelo, 1999) and thermodynamic database NAPSI_290502(260802) (Hummel et al., 2002).

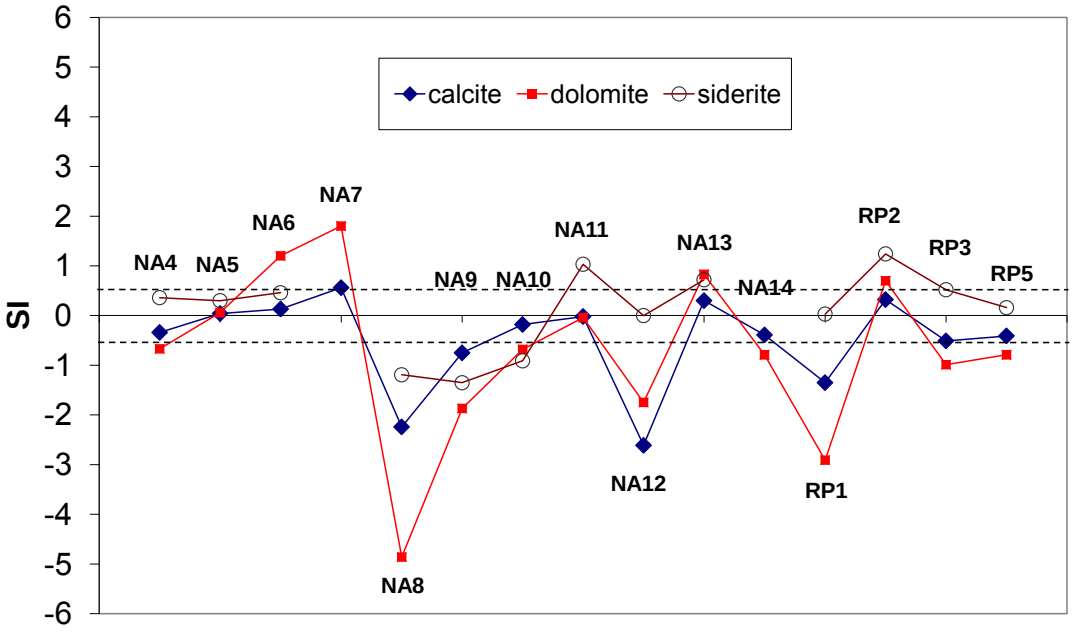

Fig. 4. Saturation indices (SI) for carbonate-bearing minerals in selected groundwater samples from Ruprechtov site. Horizontal lines indicate SI ranges where equilibrium is assumed.

4.3 Isotopes of water and flow pattern

Tritium is absent in the majority of the analysed boreholes, indicating the pre-bomb age of groundwater. Some traces of ^{3}H were found in NA8, NA10, NA11, NA13, RP2, RP3 and HR4. The highest concentration of ^{3}H (9.7 TU), comparable with the current concentration of ^{3}H in local precipitation, was found in borehole PR-4.

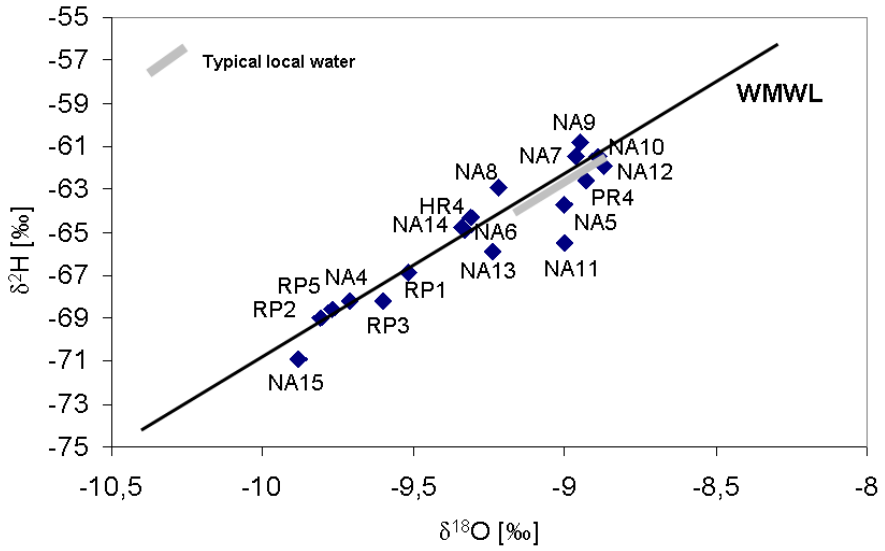

Fig. 5. Stable isotope composition of the analysed groundwater samples in the Ruprechtov aquifer system. Bold grey line denotes isotope signature of local, recent infiltration waters.

Deuterium and ^{18}O contents in the analysed wells are presented on Figure 5. It is apparent that stable isotope composition of the analysed water samples varies in a rather broad range: $\delta^{18}O$ changes from approximately -9.8 ‰ to -8.8 ‰. In general, the data points cluster around the world meteoric water line (WMWL). The range of $\delta^{2}H$ and $\delta^{18}O$ values in recent local infiltration waters have been determined on the basis of isotope analyses of representative water samples in the study area (Noseck et al., 2002). This range is marked on Figure 5 by the bold, grey line. A number of data points on Figure 5 reveal more negative $\delta^{2}H$ and $\delta^{18}O$ values when compared to local, recent infiltration waters, suggesting the influence of the altitude and/or the climatic effect.

Spatial distribution of $\delta^{2}H$ and $\delta^{18}O$ values is shown in Figure 6. In general, the analysed waters can be divided into two groups, isotopically heavier groundwater in the NW region of the study area (marked with a white frame) and isotopically light groundwater in the SE region (marked with a grey frame). The waters in the NW region can be further subdivided into a group with $\delta^{18}O$ values between -8.8 ‰ and -9.0 ‰ and a group with $\delta^{18}O$ values between -9.2 ‰ and -9.4 ‰.

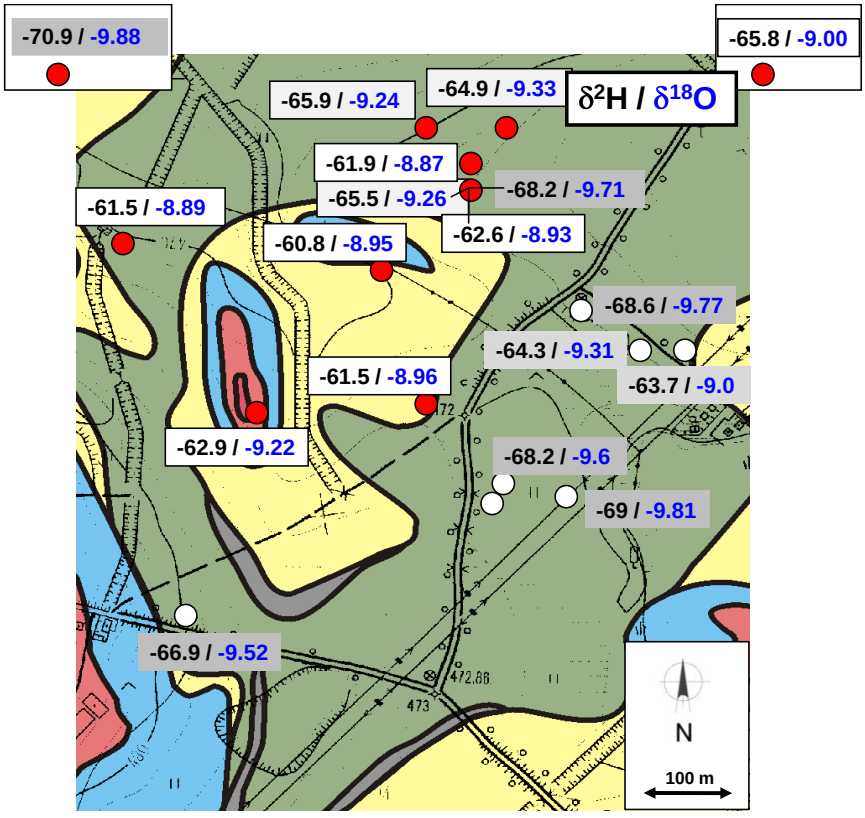

Fig. 6. Spatial distribution of $\delta^{2}H$ and $\delta^{18}O$ values in groundwater samples representing the Ruprechtov aquifer system.

The distribution of hydraulic heads measured in April 2004 is shown in Figure 7. The data indicate a hydraulic gradient from SW to NE. The boreholes sampling water from granite are marked in a white frame, all other values are given in light a grey frame. Three western wells (NA8, NA10 and RP1) represent groundwater from near-surface granite. They contain measurable amounts of ^{3}H but differ significantly in stable isotope composition. Whereas NA10 and NA8 reflect signatures of recent local waters (cf. Fig. 5), water from RP1 is isotopically lighter. The most probable explanation of the differences in stable isotope composition among those wells is that water from RP1 originates from an infiltration area which is elevated by about 200 to 300 m when compared to the other two wells.

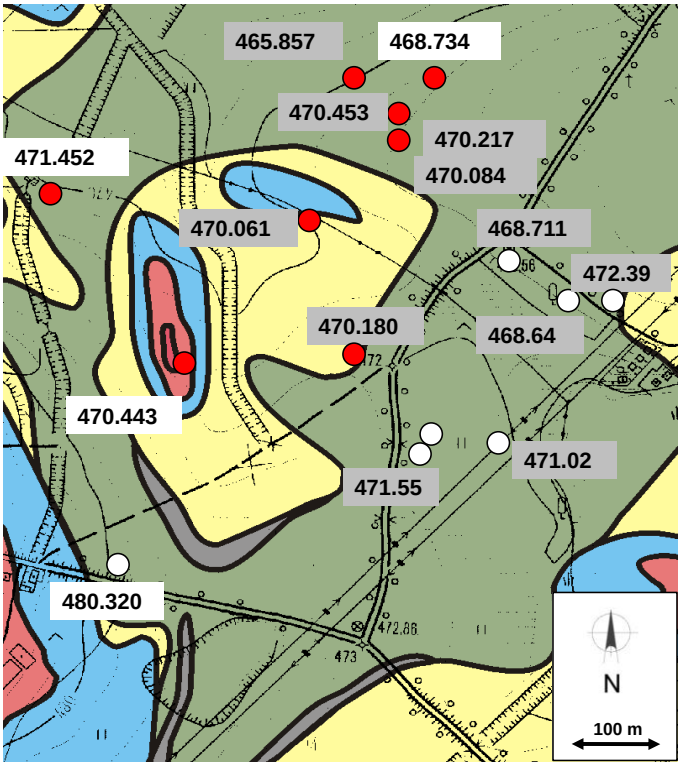

Fig. 7. Hydraulic heads in the Ruprechtov aquifer system based on measurement in April 2004.

Several boreholes in the south-eastern region of the study area (RP2, RP3, RP5) reveal similar stable isotope signatures as RP1 borehole. This suggests hydraulic connection between RP1 and the SE region of the study area. PR4 and HR4 located in the eastern part of the study area are older drillings which are not well documented. The elevated $\delta^{18}O$ values measured in those wells might be caused by admixture of surface water. This is very likely, particularly for PR4, where the filter horizon covers the depth interval from 5 m to 32 m. A strong indication for such admixture of surface water is provided by elevated ^{3}H content in those wells (9.7 TU and 1.2 TU in PR4 and HR4, respectively).

Water samples originating from near-surface horizons (boreholes NA9, NA7 and NA5) reveal stable isotope ratios similar to NA10, indicating hydraulic connections to the infiltration area in the NW of the study area.

Boreholes located in the northern part of the study area reveal a relatively large range of δ^2H and $\delta^{18}O$ values. NA12 shows similar values to NA10, suggesting hydraulic connection to the western infiltration area. A cluster of 3 wells (NA4, NA5, NA6) shows isotopically depleted water in the deeper horizon (NA4 and NA6, screened from ca. 33 m to 37 m), suggesting an elevated recharge area, whereas NA5 screened between 19 m and 21 m, falls into the range of recent local infiltration (cf. Fig. 5). Other boreholes in this region (NA13 and NA14) seem to represent mixtures of isotopically depleted water and local infiltration water. NA13 shows some traces of ^3H, which is rather unexpected for the deep horizon sampled by this well.

The water in the deeper granite (NA14) may represent a mixture of water originating in the north-western infiltration area and water infiltrated in the south-western area. Additionally, there seems to be a hydraulic connection between the north-western infiltration area and the water-bearing horizons in the northern area of the Tertiary (NA12, NA13, NA6). Since those wells are located in a region of low kaolin thickness, where fault zones occur, local connections between water-bearing horizons in the Tertiary and underlying granite are likely. Therefore, groundwater in this region might represent a mixture of underlying granite water and infiltration water from the north-western infiltration area.

Boreholes NA15 and NA11 are more than 1000 m away from the study area. Due to the complex, heterogeneous geological structure, including fault zones and the irregular morphology of the Tertiary basement, it is difficult to judge if and how those wells are hydraulically connected with the area under consideration.

The different lines of evidence discussed above provided the basis for the conceptual model of groundwater flow pattern in the studied Ruprechtov aquifer system. The model is shown in Figure 8. The general direction of groundwater flow is from SW to NE, with a local infiltration area in the outcrops of granite.

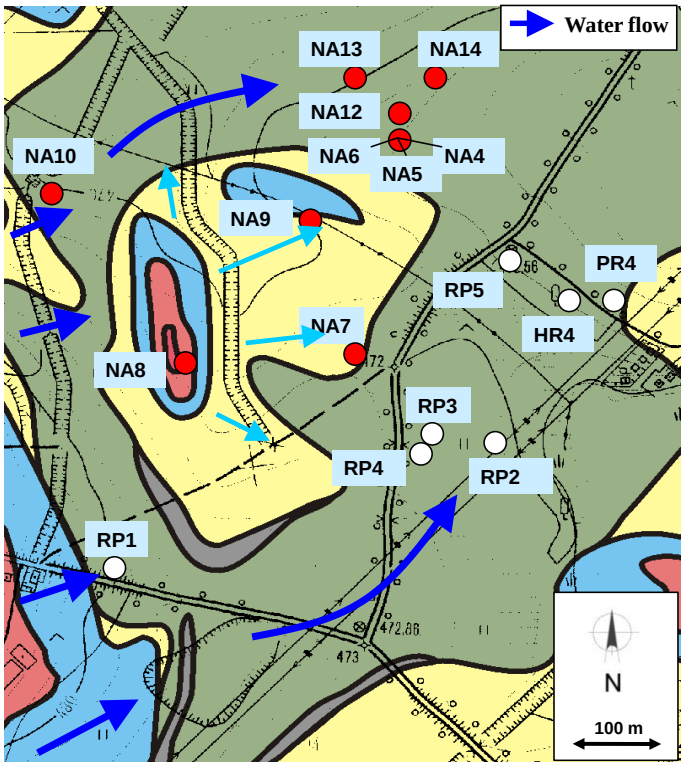

Fig. 8. Conceptual model of groundwater flow pattern in the studied Ruprechtov aquifer system

4.4 Isotopes of carbon

Isotopes of C were determined in the Ruprechtov aquifer system in order to obtain additional information on the time scales of groundwater flow and to characterize water mixing processes as well as chemical reactions within the C system. The isotope measurements comprised both DIC and DOC pools in groundwater.

Radiocarbon activity and $\delta^{13}C$ values of DIC have been determined for 16 boreholes. $\delta^{13}C$ values of the DOC pool were obtained for 12 wells while ^{14}C activity in DOC was determined only in 4 wells. It is apparent from Table 2 that ^{14}C activities and $\delta^{13}C$ values of DIC cover a wide range of values, from 72.1 to 3.2 pmc and from -21.9 ‰ to -10.4 ‰, respectively. The ^{14}C activity found in the DOC pool range from ca. 40 to 70 pmc, while $\delta^{13}C_{DOC}$ values change only slightly, between ca. -25.0 ‰ and -27.8 ‰.

The radiocarbon content of the analysed groundwater samples has been plotted in Figure 9 as a function of respective $\delta^{13}C$ values. A broad, inverse relationship between radiocarbon content of the DIC pool and its $\delta^{13}C$ values is apparent, with high concentrations of radiocarbon associated with the most negative $\delta^{13}C$ values. While the ^{14}C activities and $\delta^{13}C$ values observed in NA8 and NA9 (ca. 72 pmc and -21 ‰) are expected for fresh infiltration water from the recharge zone devoid of carbonates, C isotope composition of DIC in NA10 and RP1 boreholes located on major directions of groundwater flow (cf. Fig. 8) indicates that those waters have already evolved

chemically and isotopically (cf. discussion below). Although measured ^{14}C activities in the DIC pool (cf. Table 2) can be converted to uncorrected groundwater "ages" (Noseck and Brasser, 2006), it is obvious that C isotope values should be interpreted in the context of geochemical evolution of the DIC pool, taking into account possible addition and/or removal of isotopes of C from the system via precipitation/dissolution reactions. As expected, the observed ^{14}C activities of the DOC pool are located to the right hand side of the regression line in Figure 9 and can be converted to ages of organic matter sources.

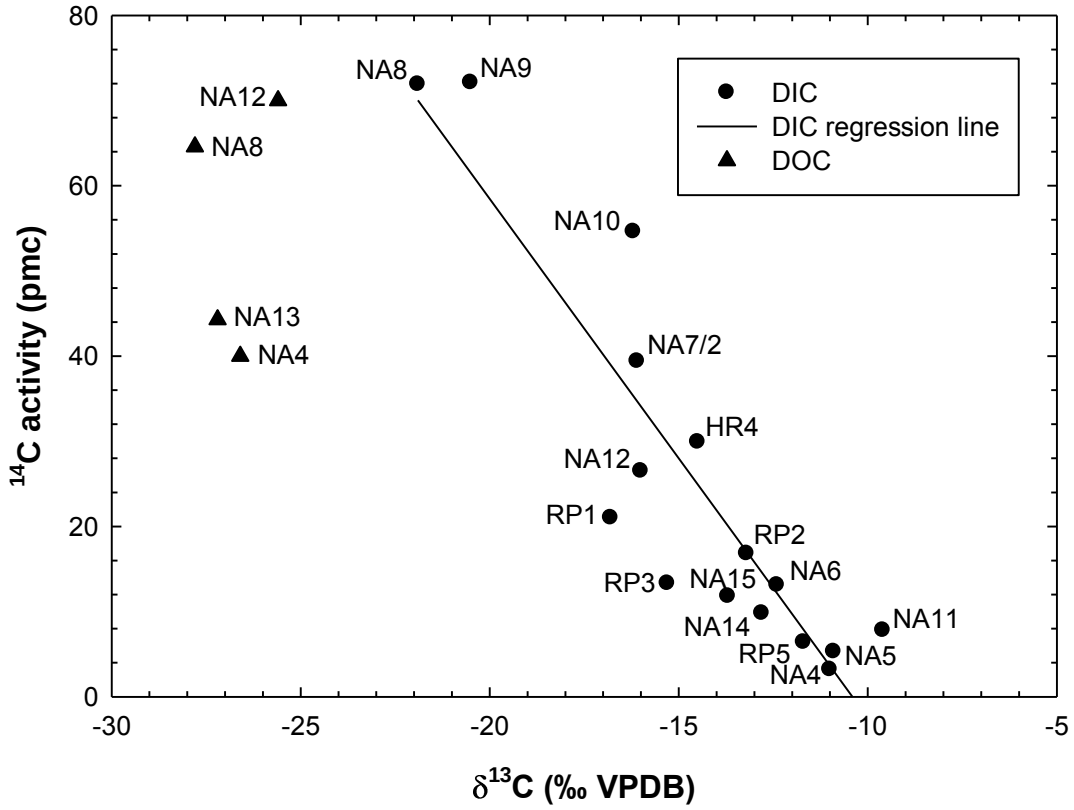

Fig. 9. Radiocarbon activity [pmc] versus $\delta^{13}C$ values of DIC and DOC pool in the sampled boreholes of the Ruprechtov aquifer system.

The following processes influencing ^{14}C activities and $\delta^{13}C$ values in DIC should be considered in the context of the present study: (i) dissolution of sedimentary inorganic C (SIC), (ii) microbial degradation of dissolved and/or sedimentary organic C (DOC and SOC, respectively), (iii) input of endogenous CO_2.

Sedimentary inorganic C from the Tertiary formation is free of radiocarbon and its $\delta^{13}C$ values are expected to be about 0 ‰. This is confirmed by analyses of $\delta^{13}C$ in siderite from boreholes RP5 and NA5 showing values of 1.8 ‰ and 2.6 ‰, respectively. Dissolution of SIC leads to reduced activities of ^{14}C and gradual increase of $\delta^{13}C$ values of the DIC pool. The $\delta^{13}C$ value of SOC pool is expected to be around -25‰ to -27 ‰. This is underpinned by analyses of two samples from Tertiary SOC in

core material from RP2 showing values of -26.6 ‰ and -24.9 ‰, respectively (Noseck and Brasser, 2006). Although SOC in the Tertiary is obviously free of radiocarbon, the dissolved organic C originating in the soil zone may contain significant amounts of ^{14}C, depending on the age of organic matter from which the dissolved fractions (HA, FA, hydrophilic acids) were derived. The endogenous CO_2 is free of radiocarbon and, according to the literature, its $\delta^{13}C$ values vary from -6 ‰ to -3‰. In the Eger rift region, approximately 30 km SW of the study area, Weise at al. (2001) found $\delta^{13}C$ values of endogenous CO_2 equal to be around -2.7 ‰.

The evolution of the C isotope composition of the DIC pool in the infiltrating water recharging the given groundwater system can be addressed using two contrasting conceptual models (e.g. Deines et al., 1974; Clark and Fritz, 1997): (i) the open-system model assuming that the pore water in the unsaturated zone is in continuous contact with an infinite reservoir of soil CO_2 of constant parameters (partial pressure, C isotope composition) during the process of dissolution of the mineral carbonate phase, (ii) the closed-system model where the infiltrating water first equilibrates with the soil CO_2 reservoir and then moves to the region where dissolution of mineral phase(s) takes place, without contact with the CO_2 reservoir. Both models lead to very different C isotope composition of the DIC pool, particularly with respect to the radiocarbon content, and to the different size of the DIC pool in the infiltrating water.

These two simple models have been used as a first, semi-quantitative step in the interpretation of C isotope data gathered in the framework of this study. They also provide a general conceptual framework in which the C isotope data can be linked to the size of the DIC pool. The ^{14}C activities and $\delta^{13}C$ values measured in the sampled boreholes were plotted as a function of the size of the DIC reservoir (Fig. 10a and b). Superimposed on that are different trend lines predicted by the simple models mentioned above.

The trajectories marked in Figure 10 by black lines (solid and dashed) indicate the initial evolution of the C isotope composition of the DIC pool. First, soil CO_2 of prescribed characteristics (partial pressure 0.01 atm, ^{14}C activity equal to 100 pmc, $\delta^{13}C$ equal to -24 ‰) dissolves gradually in the infiltrating water until saturation with respect to $CaCO_3$ (^{14}C activity equal to 0 pmc, $\delta^{13}C$ value equal to +2 ‰) is reached. The saturation points are marked by stars. From those points on, the solution was allowed to evolve further under closed-system conditions (grey solid and dashed lines) by adding new C in the form of CO_2, devoid of ^{14}C. Two different $\delta^{13}C$ values of this additional C were considered: -27 ‰ and -16 ‰. The first value corresponds to CO_2 derived from decomposition of SOC, the second one representing a 1:1 mixture of biogenic CO_2 ($\delta^{13}C$ of -27 ‰) and endogenous CO_2 with a $\delta^{13}C$ value of around -3 ‰.

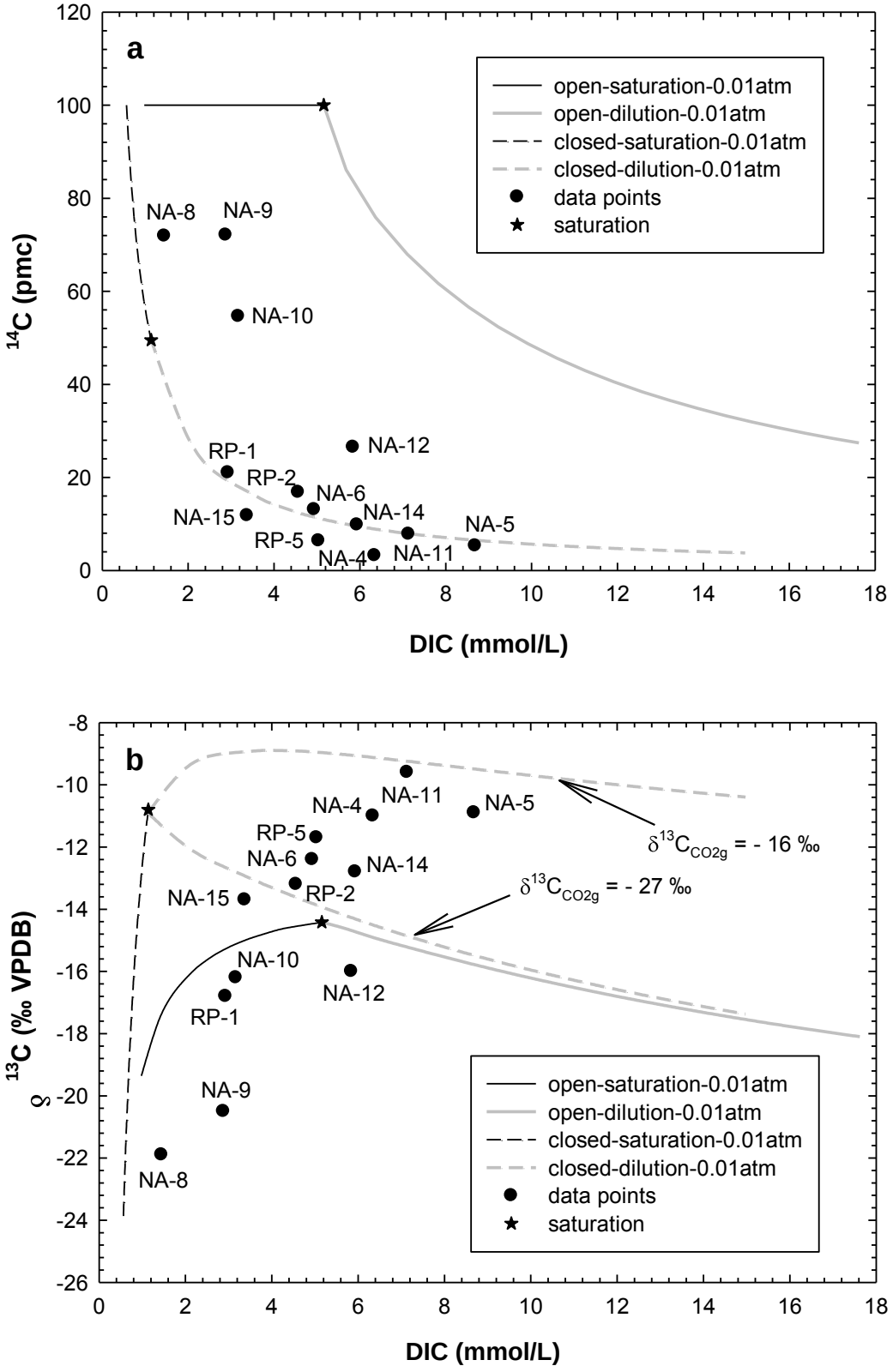

Fig. 10. Carbon isotope evolution of the DIC reservoir under open- and closed-system conditions. Stars indicate saturation of the solution with respect to $CaCO_3$. Subsequent evolution of the DIC reservoir (grey lines), resulting from input of additional C, was calculated via consecutive equilibrium stages with a solid carbonate phase (see text for details).

As seen in Figure 10a, the ^{14}C data cluster around the closed-system trend lines with two-step addition of C to the solution. Some data points are located either to the right-hand side (NA8, NA9, NA10, NA12) or below (NA15, RP5, NA5, NA4) the trend line. The ^{13}C data (Fig. 10b) provide additional constraint on the process of adding additional C to the system. The majority of data points are located between the trend lines representing two different $\delta^{13}C$ values of gaseous CO_2 entering the solution: -27 ‰ and -16 ‰. While $\delta^{13}C$ values observed in well RP2 reflects the dominating contribution of CO_2 from decomposition of organic matter, for borehole NA11 they suggest that both sources of CO_2 are represented in approximately equal proportions.

Groundwater in boreholes NA8, NA9, NA12 and RP1 is undersaturated with respect to carbonate minerals (cf. Fig. 4). Well NA8 characterized by the lowest mineralization is situated in granitic rocks. Well NA9 has a considerably higher HCO_3^- concentration when compared to NA8 and slightly higher concentrations of main cations, with reduced concentrations of NO_3^- and SO_4^{2-} ions. Similar ^{14}C activities and $\delta^{13}C$ values in both waters suggest that oxidation of DOC in the unsaturated zone contributed additional C to the solution shifting these data points to the right-hand side of the trend lines shown in Figure 10. Carbon isotopes from well RP1 are difficult to interpret. While the ^{14}C activity falls on the line representing the closed-system model, its $\delta^{13}C$ value indicates rather an open-system model. Well NA12 shows the highest carbonate content among the discussed group of wells. The measured ^{14}C activities and $\delta^{13}C$ values suggest a significant admixture of C probably originating from decomposition of organic matter depleted in ^{14}C, combined with dissolution of carbonates.

The position of data points representing wells NA15, RP5, NA5 and NA4 below the trend line in Figure 10a could be interpreted in terms of water age. The distance between the trend line and the given data point (between ca. 1.3 and 5.9 pmc) can then be converted to radiocarbon age. The resulting ages would be in the order of 1.8 – 8.6 ka.

Although the discussion of C isotope data in the context of simple models presented above gives interesting insights with respect to sources of C in the solution and possible age effects, it does not provide a full description of the chemical and isotope evolution of groundwater in the studied system as the trend lines shown in Figure 10 represent geochemical evolution of a hypothetical solution under prescribed boundary conditions. Such description can be accomplished only in the framework of fully fledged geochemical models.

4.4.1. Inverse modelling

Inverse modelling was carried out using the NETPATH code (Plummer et al., 1994). NETPATH is an interactive computer program allowing simulation of chemical and

isotopic mass-balance reactions between two prescribed points (wells) in a given aquifer system. If sufficient isotopic data are available, Rayleigh-type calculations can be performed to predict the C isotopic composition and to derive the groundwater age at the end-point. As a result of NETPATH modelling, multiple hypotheses with respect to geochemical evolution and the resulting age of the DIC pool usually emerge. They may be further used to constrain the groundwater ages.

Two pairs of wells were selected for model calculations using the NETPATH code: NA10-NA12 and RP1–RP2. They are located along the flow lines originating in two hypothetical infiltration areas, in the SW and NW of the study area, respectively (cf. Fig. 8).

Four groups of models (N1, N2, N3 and N4) were tested using the NETPATH code. Configuration of constraints and phases used in the modelling is summarized in Table 3.

Table 3. Groups of NETPATH models. 'X' sign means that given constraints and phases are applied.

	Group N1	Group N2	Group N3	Group N4
Constraints:				
C, S, Ca, Mg, K, Fe, RS	X	X	X	X
Na	X	X	X	
Cl	X	X	X	
^{13}C		X	X	X
Phases:				
CH_2O (diss.), calcite (diss.), CO_2 gas (diss.), dolomite (diss.), goethite (diss.), gypsum (diss.), Mg/Na exchange, pyrite, siderite, sylvite	X	X	X	X
Halite	X	X	X	
Exchange			X	X

The initial C isotope composition of the phases was the same for all tested models: $\delta^{13}C$ (dolomite, calcite, siderite) = 2.0 ‰, $\delta^{13}C(CO_2$ gas) = -3.0 ‰, $\delta^{13}C(CH_2O)$ = -27.0 ‰. Calcite, dolomite, siderite and gaseous CO_2 were assumed to be radiocarbon-free. Two different values of radiocarbon activity in the SOC pool were assumed in the model calculations: 0 and 60 pmc.

The results of the modelling exercise are summarized in Figure 11 which shows ^{14}C activities calculated by the NETPATH code for the end-point wells (RP2 and NA12), starting from the values observed in the initial wells (RP1 and NA10, respectively). The models which gave $\delta^{13}C$ values inconsistent with the observed ones (groups N1 and N2) were not included in Figure 11. Each bar shown in Figure 11 represents a group of 2 to 6 chemically different models fulfilling the constraints outlined in Table 3 and leading to similar ^{14}C activities in the end-point well. Models within the given group differ in

proportions between individual fluxes of C (endogenous CO_2, DOC/SOC, calcite/dolomite) and minerals entering the solution or being precipitated during chemical evolution of water. They also differ with respect to the extent of Ca, Mg/Na cation exchange reactions.

No reliable models could be found within N1 and N2 groups. The calculated values of $\delta^{13}C$ for N1 and N2 groups were significantly different from those measured in wells RP2 and NA12. This disagreement suggests that Ca/Na exchange is an important process for the chemical evolution of the solution between initial and final wells.

The assumption that additional C delivered to the solution is free of radiocarbon (open bars in Fig. 11) leads to calculated ^{14}C activities in the end-point wells (RP2, NA12) significantly lower than the measured ones, creating 'negative' ages in the range between -5.5 and -23 ka for RP2 and -2.3 and -8.6 ka for NA12.

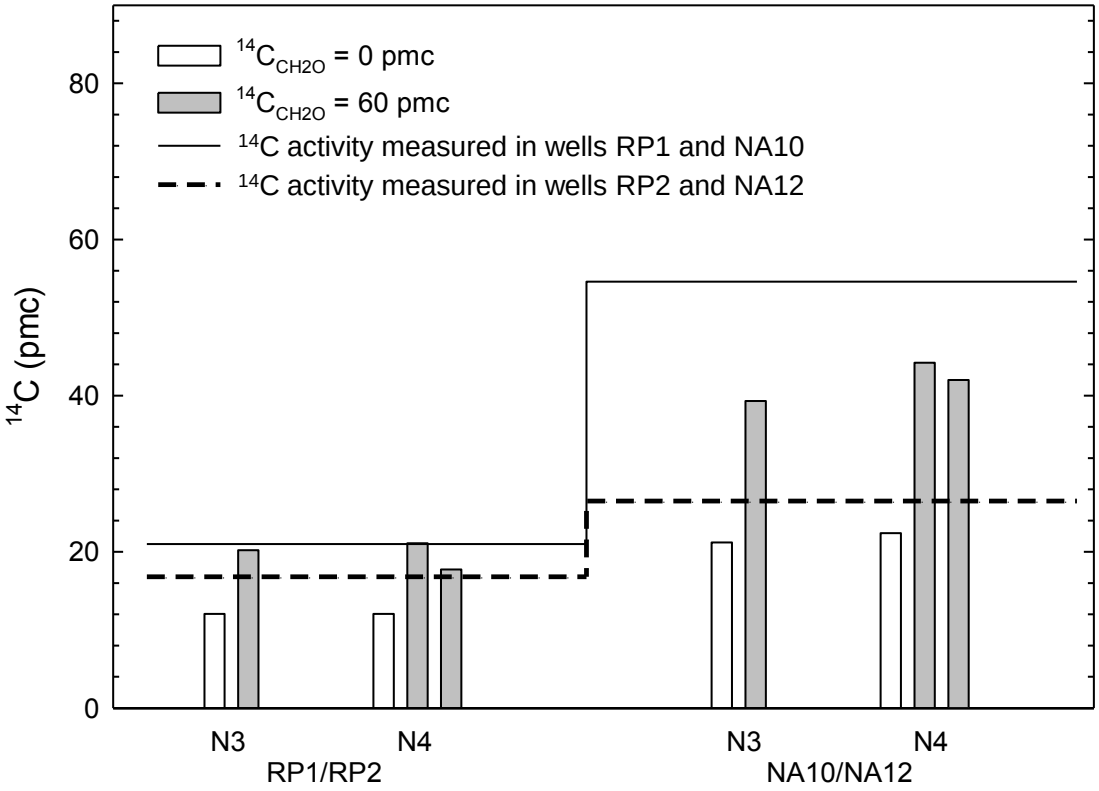

Fig. 11. Comparison of measured and modelled radiocarbon activities in wells RP2 and NA12. Geochemical modelling was performed using NETPATH code (see text for details).

The second set of models (heavy bars in Fig. 11) was calculated assuming that additional biogenic C added to the solution has a ^{14}C activity equal 60 pmc. The calculated radiocarbon activities in the end-point wells are generally higher than the measured ones. The differences between measured and calculated activities, when converted to groundwater ages, yield values between 0.45 and 1.9 ka for RP2 and 3.2 to

4.2 ka for NA12. It should be noted that 3 out of 5 models for RP2 and 4 out of 6 models for NA12 fulfil the chemical and isotope constraints (group N4 in Table 3) without assuming an additional source of C in the solution in the form of endogenic CO_2.

4.4.2. Role of microbial degradation of SOC

Further information on evolution of the DIC pool is derived from isotopic characterisation of DOC. Generally, the concentration of DOC in groundwater from the Ruprechtov site is low, with values from 1 to 5 mg C/L, with only slightly elevated values in water from the clay/lignite horizon when compared to granite. First DOC characterisation of water from the clay/lignite horizon by MALDI-TOF-MS indicated lower molecular organic matter substances with characteristics of fulvic acids (Havlova, 2006). The DOC concentrations were much lower than those observed in the overburden from the Gorleben site (concentrations up to 200 mg C/L), despite the fact that clay/lignite layers in the Ruprechtov site contain up to 50 % SOC.

In Gorleben aquifers the conversion of sedimentary organic matter by microbial reduction with release of DOC and DIC plays an important role (Buckau et al., 2000a). A schematic presentation with major elements of this mineralisation process is shown in Figure 12.

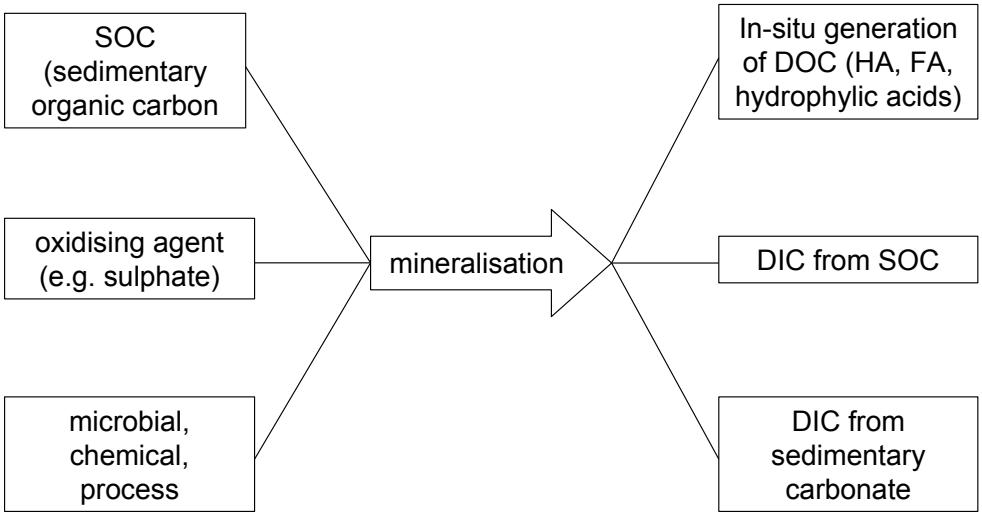

Fig. 12. Conceptual description of the mineralisation of sedimentary organic C (Buckau et al., 2000a).

The conditions for microbial degradation of SOC by SO_4 reduction in the clay/lignite layer in the Ruprechtov aquifer system are fulfilled. The SO_4 is available in all boreholes and its concentrations vary between 10 and 60 mg/L (cf. Table 1). Also, the

existence of SO_4-reducing bacteria in the clay/lignite layer has been demonstrated through analyses of sediments from borehole NA4 (Abdelouas et al., 2009).

Mineralisation by the oxidation of SOC and subsequent formation of DOC and DIC as shown in Figure 12 is accompanied by the reduction of electron acceptors like SO_4^{2-}, i.e. the decrease in concentrations of these species coupled with increasing DOC. Such a trend, with respect to SO_4 concentration, can be observed in groundwaters from granite and clay lignite horizons (Figure 13). On the other hand, an increasing trend is evident for phosphates, which are released in this process. This is in agreement with observations from the Gorleben site, where phosphate concentration rises with increasing DOC concentration in groundwater. It is an indicator that SOC oxidation is microbially mediated. Microbes metabolize SOC, by reducing sulphates and/or nitrates and releasing originally SOC-bound phosphates into the solution.

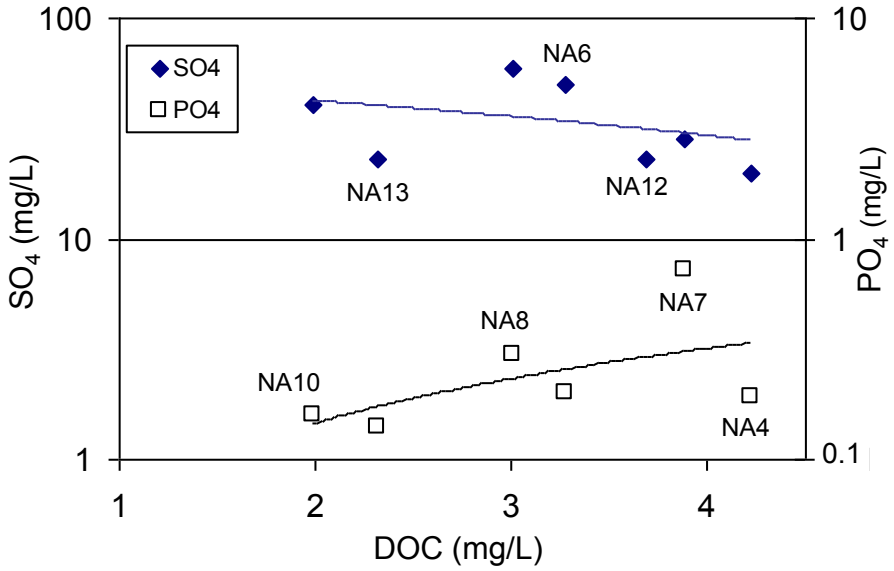

Fig. 13. Concentrations of SO_4^{2-} and PO_4^{3-} with trend lines for selected Ruprechtov wells from the western and northern area as a function of dissolved organic C concentration.

The $\delta^{13}C$ values of DOC are in a range between -25 ‰ and -27.8 ‰. This is in agreement with expected values around -27 ‰ for DOC formed by degradation of C-3 cycle plants (Clark and Fritz, 1997). In earlier analyses significantly higher $\delta^{13}C$ values in two boreholes, i.e. NA4 (-16.9 ‰ and -22.9 ‰) and NA12 (-23.7 ‰) have been found. The increase of $\delta^{13}C$ values, especially for NA4 within 3 a, indicates an initial contamination with organic C with higher $\delta^{13}C$ value caused by drilling. Therefore, it is assumed that the lowest values measured most recently (August 2006) are most reliable.

The ^{14}C activity values of the DOC pool were only available for 4 boreholes. Wells NA4, NA12 and NA13 were chosen because they represent water from the clay/lignite

horizon and NA8 is located in the infiltration area around the granite outcrop (cf. Fig. 1). The ^{14}C activity of dissolved organic C (humic and fulvic acids) under forest prior to nuclear atmospheric testing is expected to be around 50-60 pmc (Buckau et al., 2000b). If degradation of Tertiary sedimentary organic material in the clay/lignite layers is occurring, ^{14}C activity in DOC in the clay/lignite layers should be reduced. Assuming that the value of approximately 65 pmc in NA8 is typical for infiltration water (although NA8 is not the major source for water from clay/lignite layers) the lower values of 40 and 44 pmc found in the two boreholes in clay/lignite layers (NA4 and NA13) would support the hypothesis of DOC formation due to the degradation of SOC, assuming groundwater in those wells is not several thousand years old. If the observed decrease of ^{14}C activity were to be entirely due to radioactive decay of ^{14}C, the resulting apparent ages would be in the order of 3.1 to 3.9 ka, in broad agreement with the results of NETPATH geochemical modelling for well NA12 which is situated close to wells NA4 and NA13. However, the ^{14}C activity of DOC found in NA12 (app. 70 pmc) is even higher than that in NA8 possibly indicating some contamination of unknown origin. Unfortunately, no reliable value could be obtained for borehole NA10 from the western infiltration area

Additional insights into possible in-situ degradation of SOC can be gained from S isotope analyses of dissolved SO_4^{2-}. Assuming a simple organic compound, complete SO_4 reduction can be written as

$$SO_4^{2-} + 2\ CH_2O \ = \ H_2S + 2HCO_3^-.$$

In the presence of Fe the reaction product (H_2S) will be fixed as mono-sulphide and afterwards transformed to pyrite. Microbial SO_4 reduction is accompanied by isotope fractionation. The lighter isotope ^{32}S is preferentially metabolized by the microbes leaving residual SO_4 in the solution enriched in ^{34}S, whereas $\delta^{34}S$ values in precipitated sulphides decrease (Clark and Fritz, 1997).

The results of $\delta^{34}S$ analyses of dissolved SO_4 are shown in Figure 14a. For wells NA10 and RP1 representing NW and SW infiltration areas (dashed circle), the $\delta^{34}S$ values are low and vary between 0.2 and 3.5 ‰. Water from the local infiltration area in granite around NA8 is different, with an even lower $\delta^{34}S$ value of -8.45 ‰. Waters from the clay-lignite horizon (solid circle) show higher $\delta^{34}S$ values, in the range between 16.4 ‰ and 24.6 ‰. Substantial $\delta^{34}S$ enrichment of dissolved SO_4 in these boreholes is a strong indication that SO_4 reduction occurs in the clay/lignite layers. Figure 14b shows an increase of $\delta^{13}C$ in DIC with increasing $\delta^{34}S$ values. This observation supports the mechanism assumed in the conceptual model in Figure 12, i.e. that the formation of DIC by degradation of sedimentary organic matter goes together with additional formation of DIC by dissolution of SIC (Buckau et al., 2000a).

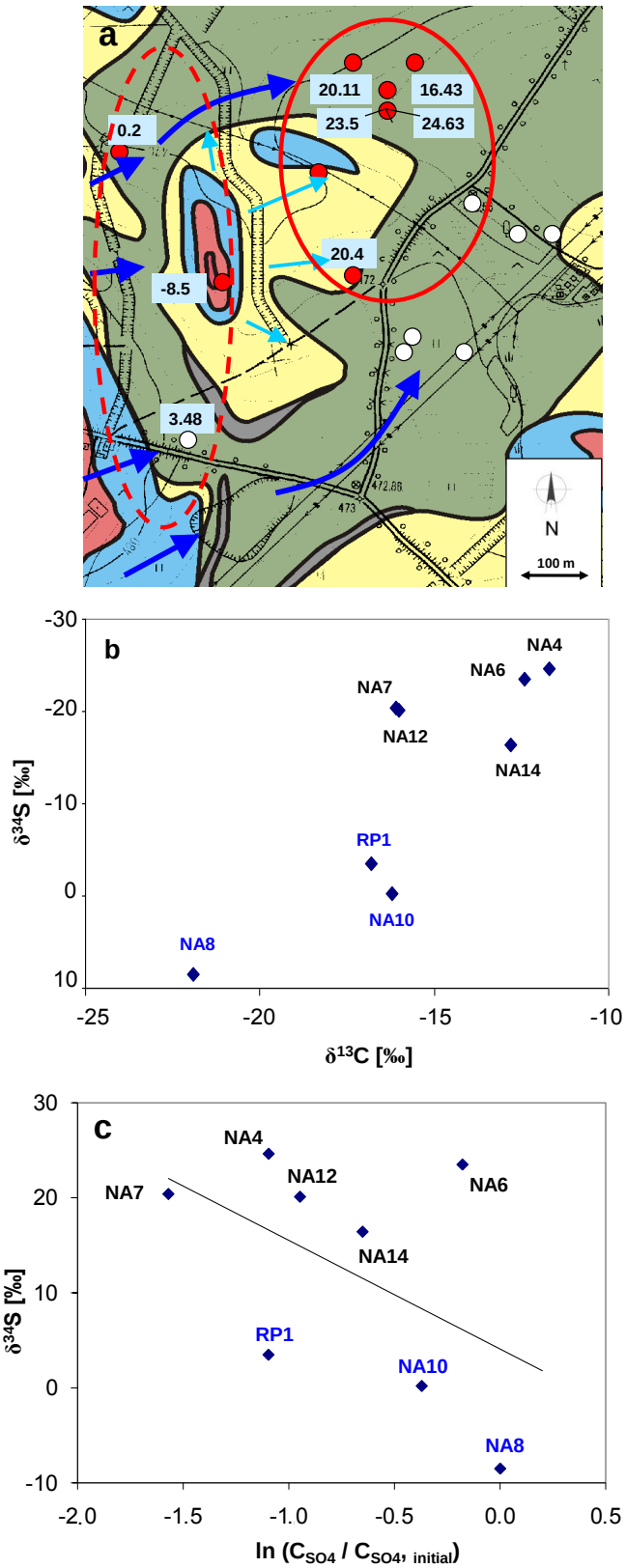

Fig. 14. (a) Distribution of $\delta^{34}S$ in different boreholes at Ruprechtov site, (b) $\delta^{34}S$ versus $\delta^{13}C$, and (c) $\delta^{34}S$ versus $\ln(C_{SO4} / C_{SO4,\ initial})$. For further explanation see the text.

A similar enrichment in the heavy S isotopes has been observed in numerous studies e.g. in groundwater from the "Niederrheinische Bucht", where δ^{34}S-values of dissolved SO_4 of between 1 ‰ and 49.5 ‰ were observed by Schulte et al. (1997). They found δ^{34}S values systematically increasing with depth, with the highest values in deep reducing water in the vicinity of lignite layers, where SO_4 reduction occurs.

With the initial SO_4 concentration in the infiltration area and the concentration after SO_4 reduction in the clay lignite horizon an enrichment factor ε can be derived from the Rayleigh equation

$$\varepsilon = \frac{\delta^{34}S_{SO4} - \delta^{34}S_{SO4,initial}}{\ln \frac{C_{SO4}}{C_{SO4,initial}}}.$$

Based on the data from all wells shown in Figure 14 an enrichment factor of 11.4 ‰ was calculated as a best fit of the straight line in Figure 14c. Compared to other investigations, this value is relatively low, but not unusual for bacterial SO_4 reduction. Enrichment factors in a similar range between 9 ‰ and 11 ‰ have been observed, e.g. in studies by Strebel et al. (1989), Spence et al. (2001), and Knöller et al. (2004).

The results of δ^{34}S analyses provide a strong indication that microbial reduction of SO_4 occurs in the clay/lignite horizon using sedimentary organic C as electron donor. However, this process only slightly increases the DOC content in the water-bearing layers in the clay lignite horizon, with concentrations up to 5 mg C/L. First analyses of SOC from the clay lignite horizon indicate that the composition of the sedimentary organic matter plays an important role. Extraction by the alkali method (dissolution and precipitation) according to IHSS scheme (Cervinka et al., 2007) indicates that low concentration of dissolved organic matter in the Ruprechtov system is caused mainly by low availability of organic matter for degradation. Only a small fraction of SOC is extractable/releasable to the groundwater. After alkaline extraction more than 50 % of the organic matter remains in the residual fraction. An additional reason for low DOC content might be the strong sorption properties of clay layers that could fix humic acids on the sediment matrix (Wang and Xing, 2005). Sorption experiments to investigate this effect in groundwater-sediment samples from the clay-lignite horizon at Ruprechtov site are under way.

5 Conclusions

Environmental isotopes were used to characterize C chemistry and dynamics of groundwater flow at the nuclear waste repository natural analogue in the Ruprechtov aquifer system in the north-western part of the Czech Republic. The results so far reveal rather complex hydrogeological conditions, with infiltration areas in the outcropping

granites in the western and southern part and preferential water flow in layers only a few metres thick, which do not represent a continuous aquifer, but rather distinct areas of increased permeability. In general, active water flow is confined to the Tertiary formation and the underlying granite, which are separated by a kaolin layer of variable thickness. There are strong indications for local connections of the flow systems in the underlying granite and in the Tertiary sediments in the northern part, where the kaolin thickness is very small and the existence of fault zones is confirmed.

Modelling of C isotope data with the aid of simple models (open- and closed-system) as well as inverse geochemical modelling performed with the aid of the NETPATH code highlights the need for additional sources of C in the system to properly explain the observed chemical and isotope evolution of the DIC reservoir. The most probable sources of this additional C include the biodegradation of dissolved and sedimentary organic C as well as the influx of endogenous CO_2.

There are strong indications that microbial reduction of SO_4 contributes to the formation of DOC and biogenic DIC in the clay/lignite layers. These are, in particular, the increase of $\delta^{34}S$ in dissolved SO_4^{2-} and an increase of biogenic DIC and phosphate with increasing DIC concentration along the potential flow path of groundwater in the system.

Environmental isotope data, combined with the chemical composition of water and geochemical modelling also allowed some insights into timescales of groundwater flow. They helped to identify potential infiltration areas and major directions of groundwater flow. The presence of ^{3}H in some wells (e.g. NA8, NA10) points to the contribution of recent infiltration occurring after the 1950s. The modelling of chemical and isotope evolution of the DIC pool with the NETHPATH code also yielded some information on apparent groundwater ages in the system. For the most probable scenario of this evolution, assuming that the additional C added to the solution is devoid of radiocarbon, the inverse modelling yields negative radiocarbon ages of the DIC pool suggesting a short transition time for groundwater. In the second scenario (^{14}C activity of the additional C equal to 60 pmc), the resulting age differences between investigated pairs of wells are between 0.45 and 1.900 ka for RP1/RP2 and 3.2 to 4.2 ka for NA10/NA12, pointing to groundwaters ages in similar ranges. This scenario, although being rather unlikely, indicates that when some ^{14}C is present in the additional C being added to the solution, originating for instance from the decomposition of dissolved organic C of soil origin, the calculated age differences between the modelled pairs of wells will grow. The overall evidence currently in hands suggests however that groundwater in the Ruprechtov aquifer system is most probably not older than ca. 1 ka.

Acknowledgements
This work was financed by the German Federal Ministry of Economics and Labour (BMWA) under contract nos 02 E 9551 and 02 E 9995, by RAWRA and the Czech Ministry of Trade and Industry (Pokrok 1H-PK25) and by the European Commission within the integrated project FUNMIG. The contribution of AGH was partly supported by statutory funds of the AGH University of Science and Technology (project no. 11.11. 220.01). Comprehensive rewiews by N. Plummer and P. Swart significantly improved the manuscript.

References

Abdelouas, A., Grambow, B., Andres, Y., Noseck, U., 2009. Uranium in argillaceous sediments: sorption/desorption processes and microbial effects. Environ. Sci Technol., inpress.

Buckau, G., Artinger, R., Geyer, S., Wolf, M., Fritz, P., Kim, J.I., 2000a. Groundwater in-situ generation of aquatic humic and fulvic acids and the mineralization of sedimentary organic carbon. Appl. Geochem. 15, 819-832.

Buckau, G., Artinger, R., Geyer, S., Wolf, M., Fritz, P., Kim, J.I., 2000b. ^{14}C dating of Gorleben groundwater. Appl. Geochem. 15, 583-597.

Cervinka, R.; Havlova, V.; Noseck, U.; Brasser, Th., Stamberg, K., 2007. Characterisation of organic matter and natural humic substances extracted from real clay environment. Proc. 3rd. Annual Workshop Proc. 6TH EC FP - FUNMIG IP, Edinburgh 26th – 29th November 2007.

Clark, I.D., Fritz, P., 1997. Environmental Isotopes in Hydrology. Lewis Publishers, Boca Raton, New York.

Coleman, M.L., Moore, M.P., 1978. Direct reduction of sulfates to sulfur dioxide for isotopic analysis. Anal. Chem. 50, 1594-1595.

Coleman, M.L., Shepherd, T.J., Durham, J.J., Rouse, J.E.. Moore, G.R., 1982. Reduction of water with zinc for hydrogen isotope analysis. Anal. Chem. 54, 993-995

Deines, P., Harmon, R.S., Langmuir, D., 1974. Stable carbon isotope ratios and the existence of a gas phase in the evolution of carbonate ground waters. Geochim. Cosmochim. Acta 38, 1147-1164.

DIN 18130 (en), 1998. Soil - investigation and testing; Determination of the coefficient of water permeability - Part 1: Laboratory tests (DIN 18130-1:1998-05), Beuth-Verlag, Berlin-Wien-Zürich

Epstein, S., Mayeda, T., 1953. Variation of ^{18}O content of waters from natural sources. Geochim., Cosmochim. Acta 4, 213-218.

Hammer, O., Harper, D.A.T., Ryan, P.D., 2001. Past: paleontological statistics software package for educational and data analysis. Paleontol. Electron 4, 9-178.

Havlova, V., 2006. Pers. Comm. October 2006.

Hummel,W., Berner, U., Curti, E., Thoenen, T., Pearson, F.J., 2002. Nagra/PSI Chemical Thermodynamic Data Base Version 01/01 (Nagra/PSI TDB 01/01) NAPSI_290502.DAT. Last Modified 26-Aug-2002.

Knöller, K., Fauville, A., Mayer, B., Strauch, G., Friese, K., Veizer, J., 2004. Sulfur cycling in an acid mining lake and its vicinity in Lusatia, Germany. Chem. Geol. 204, 303-323.

McCrea, J. M., 1950. On the isotopic chemistry of carbonates and a paleotemperature scale. J. Chem. Phys. 18, 849-857.

Noseck, U., Brasser, Th., 2006. Radionuclide transport and retention in natural rock formations – Ruprechtov site. Gesellschaft für Anlagen- und Reaktorsicherheit, GRS-218, Köln.

Noseck, U., Brasser, Th., Raijlich, P., Hercik, M., Laciok, A., 2004. Mobility of uranium in tertiary argillaceous sediments – a natural analogue study. Radiochim. Acta 92, 797-801.

Noseck, U., Brasser, Th., Pohl, W., 2002. Tertiäre Sedimente als Barriere für die U-Th-Migration im Fernfeld von Endlagern. Gesellschaft für Anlagen- und Reaktorsicherheit, GRS-176, Köln.

Parkhurst D. L., Appelo C. A. J., 1999. User's Guide to PHREEQC (Version 2) – A Computer Program for Speciation, Batch-Reaction, One-Dimensional Transport, and Inverse Geochemical Calculations. U.S. Geol. Surv., Water-Resour. Invest. Rep.99-4259.

Plummer L. N., Prestemon E. C., Parkhurst D. L., 1994. An interactive code (NETPATH) for modelling NET geochemical reactions along a flow PATH. Version 2.0: U.S. Geological. Survey, Water-Resour. Invest. Rep. 94-4169.

Schulte, U., Strauß, H., Bergmann, A., Obermann, P., 1997. Isotopenverhältnisse der Schwefel und Kohlenstoffspezies aus Sedimenten und tiefen Grundwässern der Niederrheinischen Bucht. Grundwasser 3, 103-110.

Spence, M.J., Bottrell, S.H., Thornton, S.F., Lerner, D., 2001. Isotopic modelling of the significance of bacterial sulphate reduction for phenol attenuation in a contaminated aquifer. J. Contam. Hydrol. 53, 285-304.

Strebel, O., Böttcher, J., Fritz, P., 1989. Use of isotope fractionation of sulfate-sulfur and sulfate-oxygen to assess bacterial desulfurication in a sandy aquifer. J. Hydrol. 121, 155-172.

Todd, D.K., 1980: Groundwater Hydrology. John Wiley & Sons, New York.

Wang, K., Xing, B., 2005. Structural and sorption characteristics of adsorbed humic acid on clay minerals. J. Environ. Qual. 34, 342-246.

Weise, S. M., Bräuer, K., Kämpf, H., Strauch, G., Koch, U., 2001. Transport of mantle volatiles through the crust traced by seismically released fluids: A natural experiment in the earthquake swarm area Vogtland/NW Bohemia, Central Europe. Tectonophys. 336, 137-150.

A.13 Investigation of far-field processes in sedimentary formations at a natural analogue site - Ruprechtov

Ulrich Noseck[1], Vaclavá Havlová[2], Radek Cervinka[2], Juhani Suksi[3], Melissa Denecke[4], Wolfgang Hauser[4]

[1]GRS, Germany
[2]NRI, Czech Republic
[3]University of Helsinki, Finland
[4]FZK-INE, Germany

Summary

The analogue study at Rurpechtov site aimed at in-depth understanding of the behaviour of uranium and organic matter in a natural sedimentary system similar to overlying strata of salt domes but also other host rock formations for radwaste disposal. By application of a set of different microscopic and macroscopic analytical methods the complex immobilisation mechanism for uranium and the long-term stability of the immobile U(IV) phases were shown. Sedimentary organic carbon (SOC) is microbially degraded in the lignite rich layers, but DOC concentrations are relativley low, since only a very small fraction of SOC seems to be accessible. Beside increase of process understanding another important contribution of this study to the Safety Case consists in further development and testing of methods for colloid analysis, sample characterisation on µ-scale, and evaluation of environmental isotope signatures.

1. Introduction

In component RTDC5 of the integrated EC project FUNMIG the far field of the host rock formation salt is subject of the investigations. In contrast to the two other host-rock components RTDC3 (clay) and RTDC4 (granite) RTDC5 is a natural analogue study. The study is performed at Ruprechtov site in Czech Republic and represents an analogue for potential migration processes in a similarly structured overburden of a salt dome but also in other geological formations, which are foreseen as potential host rocks for radioactive waste repositories.

Results from site characterisation were already available before this study, e.g. [1]. Within the FUNMIG project specific questions have been addressed, to receive an in-depth understanding of the evolution of the natural system and the key processes involved in uranium immobilisation as well as the behaviour of organic matter. Emphasis was put into characterisation of the immobile uranium phases, their long-term stability and the processes controlling mobility of uranium in the system. The second major issue comprised the behaviour of colloids and organic matter in the system, i.e. to better understand the interrelation between sedimentary organic carbon (SOC) and dissolved organic carbon (DOC) and its impact on the mobility of uranium.

The Ruprechtov site, located in the north-western part of the Czech Republic, is geologically situated in a Tertiary basin [1]. The study area is characterised by a granitic body, which partly

crops out in the west and in the south (see Figure 1) and is widely kaolinised in varying thicknesses (up to several tens of metres) on its top in the central part. The horizon of major interest is the so-called clay/lignite layer, a zone of 1-3 m thickness at the interface of kaolin and overlaying pyroclastic sediments (in 20 to 50 m depth), with high content of SOC, areas of uranium enrichment and partly aquiferous. This layer does not represent a continuous aquifer, but rather distinct areas. As indicated in Figure 1 the general groundwater flow direction in the water bearing zones in the Tertiary is from southwest to northeast. Infiltration area is supposed to be in the outcropping granite in the western and south-western part, represented by the boreholes NA10, NA8 and RP1.

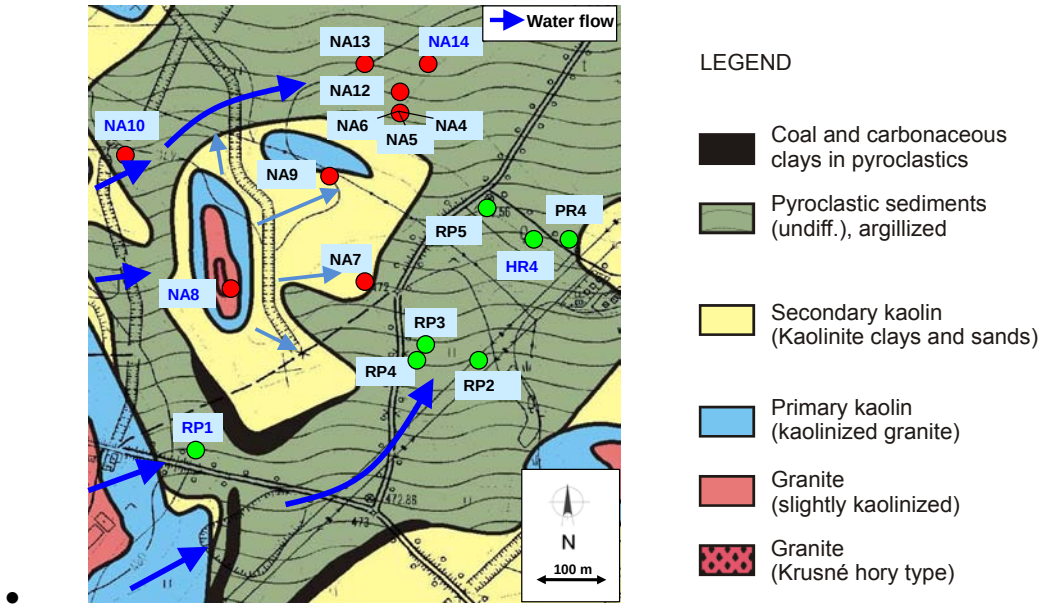

Figure 1: Geological sketch of Ruprechtov site with location of the boreholes [2].

2. Methodology

As described above the investigations in RTDC5 are a natural analogue study, where specific questions are addressed, reflected by the following three work packages. The methodology for each work package is briefly described.

Colloid characterisation: A borehole groundwater sampling system and a mobile laser-induced breakdown detection equipment (LIBD) for colloid detection, combined with a geo-monitoring unit has been further developed and applied to characterise the natural background colloid concentration in groundwaters of the Ruprechtov natural analogue site [3]. To minimise artefacts during groundwater sampling the contact to atmospheric oxygen has been excluded by use of steel sampling cylinders opening and closing by remote control. The groundwater samples collected in this way are transported to the laboratory where they were eluted from the cylinders under original hydrostatic pressure without contact to oxygen. Behind the LIBD detection cell the system consists of in-series connected detection cells for pH, Eh, electrical conductivity, and oxygen content.

Characterisation of immobile uranium phases: Different microscopic and macroscopic methods have been applied to selected samples to characterise the immobile uranium phases. These methods comprise µ-XRF and µ-XAFS spectroscopy, sequential extraction, U(IV)/U(VI) separation with $^{234}U/^{238}U$ ratio determination. Detailed information can be found in [4]. In addition, sorption

experiments have been performed and exchangeable uranium determined by isotope exchange with ^{233}U, e.g. [9], [13]. µ-XRD and µ-XAFS were applied the first time to natural samples and the method was further developed within the FUNMIG project.

Real system analyses: This work package comprised the integration of results from both other work packages and available information from site characterisation. Moreover, analyses of specific environmental isotopes, in particular $\delta^{34}S$ in dissolved sulphates as well as $\delta^{13}C$ and ^{14}C in DOC have been performed. Additional work was carried out on characterisation of DOC and SOC (integration with RTDC2). DOC was characterised by IR and MALDITOF spectroscopy, whereas extracted humic substances were characterised using elementary analysis, ash and moisture content, UV-Vis spectroscopy, FTIR spectroscopy and acidobasic titrations. Details can be found in [5].

3. Results

3.1 Colloids

As described above part of the work was dedicated to method-development and qualification. During the project a new mobile geomonitoring system including a system for the laser-induced breakdown detection of colloids (LIBD) was developed [3]. It was successfully applied to the detection of colloids in natural groundwater samples from Ruprechtov site and other sites in Sweden.

It could be shown that colloid concentrations down to µg/l are detected with the special sampling technique. By comparison with in-situ probe measurements in several boreholes it was also demonstrated that reducing conditions with minimal access of atmosphere oxygen are maintained. In-situ experiments in granite demonstrated that colloid generating processes like redox changes (e.g. in EDZ) and/or mechanical erosion can increase the natural colloid background by up to several orders of magnitude.

The LIBD determined natural background colloid concentrations found at Ruprechtov are compared with data of studies performed in Äspö (Sweden) and Grimsel (Switzerland). A comprehensive representation of colloid concentrations in different water samples as determined by LIBD as a function of the respective ionic strength is given in Figure 2 [3]. Increasing ionic strength usually forces colloid aggregation which is reflected in lower colloid concentration in the respective groundwater.

In the Ruprechtov groundwater samples the ionic strength varies in the range of $2 \cdot 10^{-3}$ to $1.1 \cdot 10^{-2}$ mol/l without any significant influence on the measured colloid concentration. The broad bandwidth of detected colloid concentrations in groundwater of ionic strength <100 mmol/l (Grimsel, Ruprechtov) suggests that different parameters besides ionic strength as e.g. pH and/or groundwater velocity may control the actual colloid concentrations. However, the studies suggest that an ionic strength of 100 mmol/l represents some kind of upper limit: colloids may persist in groundwater with ionic strengths below this value for considerable time scales and variable colloid concentrations. At ionic strengths above 100 mmol/l natural aquatic colloid stability is effectively decreased. As a consequence, for groundwater samples from Äspö and simulated NaCl solutions a clear dependency of the maximum colloid concentrations with the salinity of the solution is found.

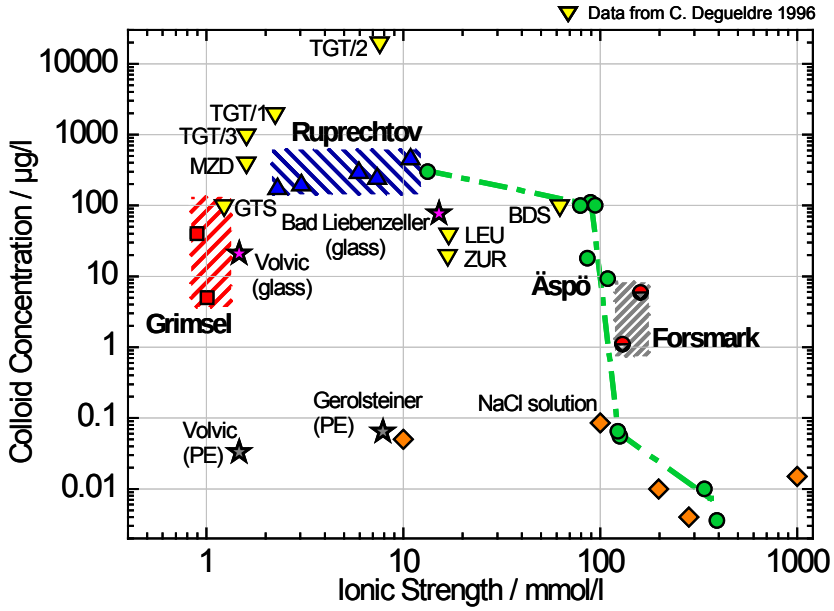

Figure 2: Comparison of colloid concentration in different types of natural groundwater, mineral water and synthetic NaCl-solution versus ionic strength. For details see [3]

3.2 Characterisation of immobile uranium phases

The application of macroscopic and microscopic methods provided detailed insight into the U enrichment processes at the Ruprechtov site. Confocal µ-XRF and µ-XANES notably contributed to the identification of uranium immobilisation processes. In good agreement with results from other spectroscopic methods like ASEM and electron-microprobe µ-XANES identified U as U(IV) [6]. As demonstrated in Figure 3 (left), the shape and intensities show the average valence state of the sampled volume to be U(IV). All three curves do not show the multiple scattering feature 10-15 eV above the white line (WL) characteristic for U(VI) nor do they show a significant decrease in the WL intensity, which would be expected for U(VI) as be seen in the schoepite spectrum.

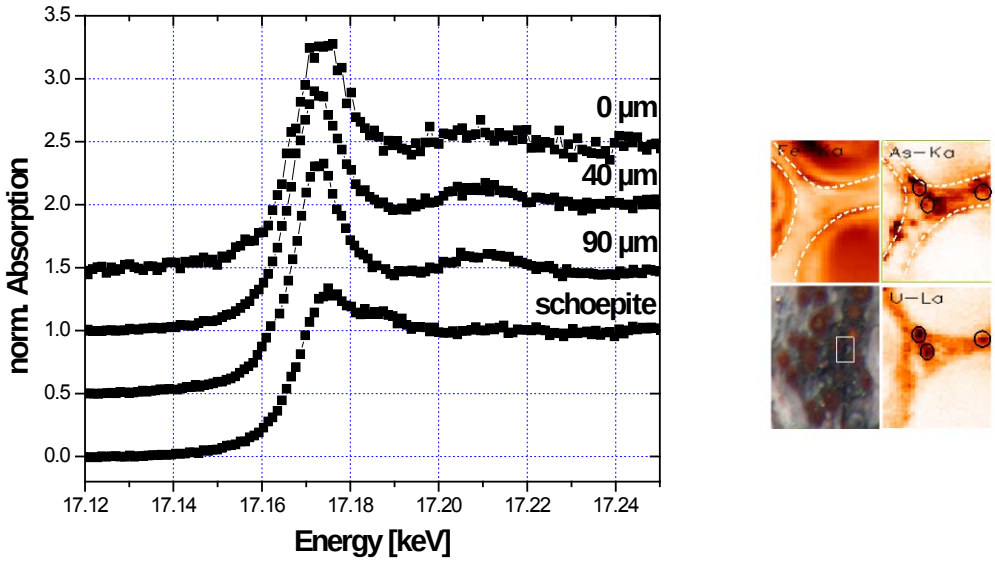

Figure 3: Results from µ-XANES (left) and µ-XRD (right) of a sample from borehole NA4 [6,7].

By µ-XANES it was also shown that As exists in two oxidation states, As(0) and As(V). The analyses of a number of tomographic cross-sections of elemental distributions recorded over different sample areas show a strong positive correlation between U and As(V). By further development of the method, using new planar compound refractive lens (CRL) array at the Fluoro-Topo-Beamline at the synchroton facility ANKA of the Forschungszentrum Karlsruhe, a higher spatial resolution (focus beam spot size of 2 x 5 μm^2 (V x H)) was achieved. The high resolution made it possible for the first time to discern an As-rich boundary layer surrounding Fe(II)-nodules, see Figure 3, right [7]. This suggests that an arsenopyrite mineral coating of framboidal pyrite nodules is present in the sediment. Uranium occurs in direct vicinity of the As-rich layers. In conclusion of these results a driving mechanisms for uranium-enrichment by secondary uranium(IV) minerals in the sediment was suggested. Mobile, groundwater-dissolved U(VI) was reduced on the arsenopyrite layers to less-soluble U(IV), which formed U(IV) mineral phases. As(0) was oxidised to As(V). Uranium, therefore, is associated with As(V).

The results from microscopic methods are supported by cluster analysis of sequential extraction results. They also indicate that U occurs in the tetravalent state, since major part of uranium is extracted in the respective steps for U(IV) forms and the residual fraction [4]. By cluster analyses, performed to identify possible correlations between elements, a strong correlation of U with As and P was found (see Figure 4), supporting the mechanism postulated above and the existence of uranium phosphate mineral ningyoite identified by SEM-EDX.

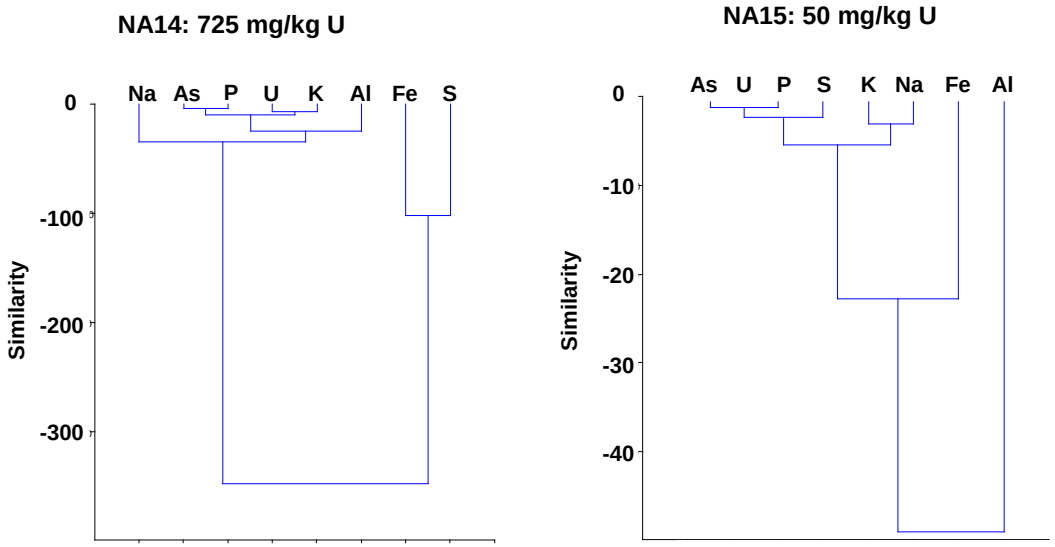

Figure 4: Cluster analyses for extended SE results of samples from the boreholes NA14 and NA15

In order to separate U(IV) and U(VI), a wet chemical method [9] was applied for the first time to Ruprechtov samples. A major result is that uranium in all samples consists of both U(IV) and U(VI) [4]. Results from all analyses are summarised in Table 1. The extraction did not dissolve all uranium. The content of uranium in this insoluble phase is denoted as U(res). In all phases the $^{234}U/^{238}U$ activity ratio was determined, which is denoted as AR. The AR differs significantly in the U(IV) and U(VI) phases, with ratios <1 in the U(IV) phase and ratios >1 in the U(VI) phase in nearly all samples. The AR of the U(res) phase is, with exception of NA12, similar to that observed in the U(IV) phase. Different (higher) AR in the NA12 residue may indicate involvement of different U compounds in the sample material, i.e. U(IV) and insoluble U(res) represent different compounds. Taking into account the higher stability of U(IV) phases we assume that insoluble uranium exists as a stable mineral phase in oxidation state IV. Most uranium in all samples is U(IV), with contents between 50 and 90 wt.%. The highest U(IV) fraction is found in NA6-37.

Table 1. Amount of uranium and $^{234}U/^{238}U$-activity ratios (ARs) in the different phases from uranium separation [4]

sample	**U** [ppm]	**U(IV)**		**U(VI)**		**U(res, IV)**		**U(IV) total**
		[%]	$^{234}U/^{238}U$	[%]	$^{234}U/^{238}U$	[%]	$^{234}U/^{238}U$	[%]
NA6 35a	356±7	28.7	0.54±0.01	41.9	1.42±0.02	29.5	0.65±0.01	58.1
NA6 35b	468±9	45.9	0.56±0.01	33.3	1.69±0.03	20.7	0.64±0.02	66.7
NA6 35c	369±8	23.3	0.47±0.01	47.4	1.16±0.02	29.3	0.67±0.01	52.6
NA6 37a	37.3±2	73.7	0.79±0.03	15.7	2.66±0.07	10.6	0.73±0.01	84.3
NA6 37b	47.5±1,5	66.2	0.52±0.01	9.0	3.37±0.15	24.8	0.86±0.02	91.0
NA6 37c	35.7±2	51.3	0.58±0.01	19.8	2.56±0.08	28.9	0.71±0.04	80.2
NA11 a	52.5±2,2	4.2	0.44±0.02	34.1	0.94±0.01	61.7	0.55±0.02	65.9
NA11 b	53.6±2,5	6.1	0.39±0.02	49.6	0.94±0.02	44.3	0.67±0.02	50.4
NA12 a	27.2±1,4	3.9	0.26±0.02	47.5	1.31±0.04	48.6	1.22±0.03	52.5
NA12 b	31.4±2,1	4.2	0.13±0.02	57.4	1.25±0.04	38.4	1.04±0.03	42.6
NA13 a	216±7	5.4	0.53±0.02	46.8	1.15±0.02	47.8	0.55±0.01	53.2
NA13 b	230±9	1.6	0.58±0.03	46.2	1.15±0.02	52.2	0.53±0.01	53.8
NA14 b	317±10	13.3	0.87±0.02	68.8	1.28±0.02	18.0	0.44±0.01	31.2
NA14 c	354±11	25.4	0.88±0.02	39.6	1.11±0.01	41.5	0.54±0.01	58.5

That U(res) and U(IV) exhibit in nearly all samples an AR below one is a strong indicator for their long-term stability. AR values significantly below unity are caused by the preferential release of ^{234}U, which is facilitated by α-recoil process and subsequent ^{234}U oxidation. In order to attain low AR values of approx. 0.2 in the U(IV) phase, it must have been stable for a sufficiently long time, i.e. no significant release of bulk uranium has occurred during the last million years. This is in good agreement with the hypothesis that the major uranium input into the clay/lignite horizon occurred during Tertiary, more than 10 My ago [10].

3.3 Real system analysis

One part of the work comprised the re-evaluation of existing, and the evaluation of new hydrological, geochemical and environmental isotope data from groundwater wells at Ruprechtov site to characterise the hydrogeological flow regime and the carbon chemistry in the system. The existing idea about the flow system in the tertiary sediments was confirmed. Additionally, the complexity of the system was demonstrated [2]. Differences in stable isotope signatures in the northern part of the site indicate very local connections of the flow systems with the flow system in the underlying granite via fault zones.

The chemical conditions of the site are characterised by low mineralised waters with ionic strengths in the range from 0.003 to 0.02 mol/l. The pH-values vary in a range of 6.2 to 8, the Eh-values from 435 mV to -280 mV. More oxidising conditions with lower pH-values are found in the near-surface granite waters of the infiltration area. In the clay/lignite horizon the conditions are strongly reducing with Eh-values as low as -280 mV. The Eh-values measured directly by in-situ probe are significantly lower than those measured on-site in pumped water. The latter method is more susceptible to disturbances by the contact with atmosphere, which is probably responsible for these differences. In order to understand the carbon chemistry and the interrelation between SOC and DOC isotopes of carbon in DIC, DOC and SOC were evaluated. This work is described in detail in

[2]. Here only few major aspects concerning the formation of DOC in the clay/lignite layer are touched.

In Figure 5 on the left the correlation between biogenic DIC and DOC is plotted, assuming that the ^{13}C content of the source water is of inorganic origin with -27 ‰ and additional DIC is of organic origin. Besides data for NA8, which well is probably not strongly connected to the clay/lignite water, the other data follow a line, with increase of biogenic DIC from infiltration waters NA10 and RP1 to the waters from the clay/lignite layer. It is one important indication that in this layer DOC is formed by additional release of DIC, as it is observed at other sites, e.g. 11].

Concerning the mechanism of DOC release important information can be gained from other isotope signatures. A strong indicator for microbial degradation of organic matter by sulphate reduction is the $\delta^{34}S$ signal in dissolved sulphates. Since sulphate reducing bacteria had already been detected at the site, appropriate analyses were performed in groundwater from the infiltration area and from the clay/lignite layers.

The results show that $\delta^{34}S$-values in waters from the clay-lignite layer are in a range between 16.4‰ and 24.6 ‰, i.e. strongly increased compared to the values between -8.5 and 3.48 observed in the wells from the infiltration area (see Figure 5, right). The substantial enrichment of ^{34}S in these boreholes is a clear indication that microbial sulphate reduction occurs in the clay/lignite layers. The microbial sulphate reduction is accompanied by isotope fractionation. The lighter isotope ^{32}S is preferentially metabolised by the microbes leaving residual sulphate in the solution enriched in ^{34}S, which is observed here. With the initial sulphate concentration in the infiltration area and the concentration after sulphate reduction in the clay lignite an enrichment factor ε can be calculated by use of the Rayleigh equation. Based on the data from all wells shown in Figure 5 and the corresponding sulphate concentrations an enrichment factor of 11‰ was calculated [2]. Compared to other investigations this value is comparably low, but not unusual for bacterial sulphate reduction. Enrichment factors in a similar range between of ~10 ‰ have been observed e.g. in [12].

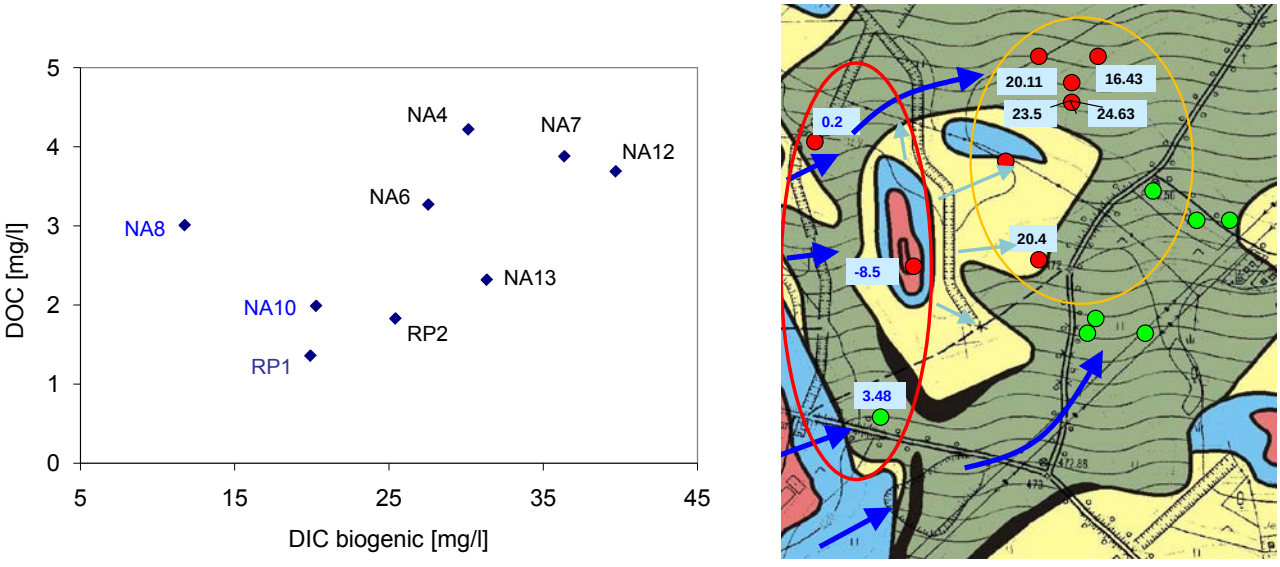

Figure 5: Correlation of biogenic DIC with DOC (left) and $\delta^{34}S$ values in boreholes from the infiltration area (red circle) and clay/lignite layers(yellow circle) [2]

In order to better understand the interrelation between SOC and DOC, in particular to understand the relatively low DOC concentrations below 5 mg C/l in the water from clay/lignite layer compared to other sites with SOC-bearing sediments [11], a more detailed analysis of SOC from selected samples of clay/lignite layers have been performed. This work represents a strong link between RTDC5 and RTDC2. SOC was characterised in detail by

- micropetrographical methods,
- application of different extraction schemes,
- degradability experiments, and
- interaction experiments of humic acids with natural clay samples.

The micropetrographical study showed that the sedimentary organic matter at Ruprechtov site is generally formed by slightly dispersed matter with low degree of coalification, which only reaches brown coal or lignite degree. The main components of detritic and xylodetritic coal samples and clay-lignite samples are mineral admixtures and huminite of the maceral group [5].

According to the results from SOC characterisation it seems that the low concentration of dissolved organic matter in the Ruprechtov system is mainly caused by the low availability of organic matter to the processes of degradation. Only a very small fraction of SOC is accessible to the groundwater. An additional reason could be the strong sorption properties of the clay that fix humic acids on the sediment matrix. This is indicated in first sorption experiments performed by NRI with standard HA leonardite on the montmorillonite standard SWy-2 and on low TOC clay samples from borehole Na11. The results are shown in Figure 6 and indicate significant sorption of HA on the clay samples with higher sorption values on Ruprechtov samples compared to standard montmorillonite [5].

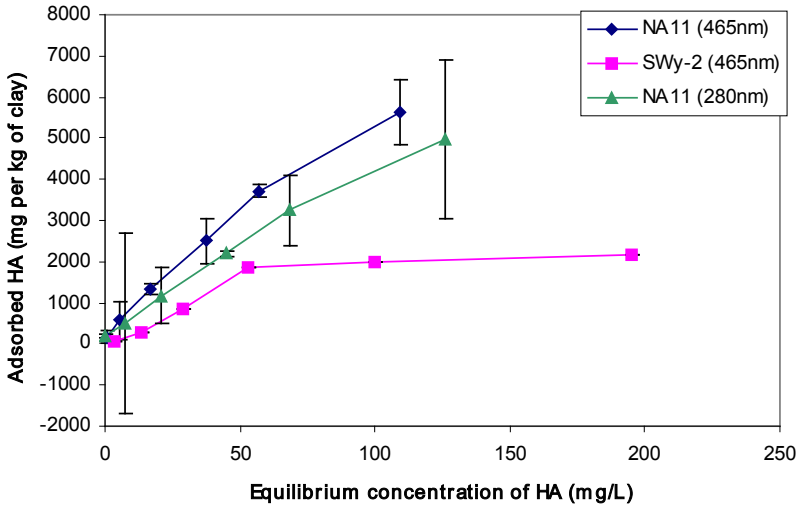

Figure 6: Sorption isotherm of HA on different clay samples

The integration of all results showed that organic matter did not play such an important role by direct interaction with uranium, but SOC contributed and still contributes to maintain reducing conditions in the clay/lignite layers. It can be concluded that SOC within the sedimentary layers was (and to some extent still is) microbially degraded. By this process DOC is released, providing protons to additionally dissolve SIC [2]. Moreover SO_4^{2-} is reduced leading (and has lead in the geological past) to the formation of iron sulphides, especially pyrite. Reducing conditions, being maintained amongst others by sulphate reducing bacteria, caused the reduction of As, which sorbed onto pyrite surfaces, forming thin layers of arsenopyrite. Uranium U(VI), originally being released

from the outcropping/underlying granite, was reduced to U(IV) on the arsenopyrite surfaces. UO_2 and uranium phosphates were formed by reaction of U(IV) with phosphates PO_4^{3-}, released by microbial SOC degradation. These uranium(IV) minerals have been stable and immobile over geological time frames.

Geochemical calculations with GWB [14] and revised NEA TDB [15] confirmed that U(IV) is the preferential oxidation state in the clay/lignite layers. These calculations also indicate that the redox conditions in the clay/lignite horizon are controlled by the SO_4^{2-}/S^{2-} couple. Uranium concentrations in the clay/lignite layer observed today are determined by amorphous UO_2 and ningyoite. One important issue which could not be clarified is, whether the more accessible U fraction found by U(IV)/U(VI) separation really exists in the hexavalent state or has been oxidised after sampling.

4. Conclusions

This natural analogue study contributed to the Safety Case for the far-field transport in sedimentary layers in different ways. A very important part was the aspect of method development and testing, e.g. colloid sampling under undisturbed conditions, first application to natural samples and further development of µ-XRF and µ-XANES as well as application of modern isotope analyses like $\delta^{34}S$ signatures to identify relevant processes in the field. All these methods are important for characterisation of a potential repository site including lab and field experiments.

Although Ruprechtov site turned out to be rather complex with regard to hydrogeology and geological evolution, the mechanisms for immobilisation of uranium have been identified. By application of a set of different microscopic and macroscopic analytical methods distinct immobile uranium phases have been characterised and their long-term stability was shown. The results further indicate that DOC does not contribute to mobilisation of U because of the relatively low DOC concentration in the clay/lignite layer. DOC is formed by microbial degradation of SOC in the clay/lignite layers but only a very small fraction of SOC seems to be accessible.

In general it was shown that sedimentary layers can provide a strong barrier function for uranium, when specific prerequisites are fulfilled. Under the strongly reducing conditions in the clay/lignite layers at Ruprechtov site, there are no indications for significant uranium release during the last million years. The low uranium concentrations in the groundwater of app. 10^{-9} mol/l are determined by amorphous UO_2 and ningyoite.

5. Acknowledgements

This project has been co-funded by the European Commission and performed as part of the sixth EURATOM Framework Programme for nuclear research and training activities (2002-2006) under contract FI6W-CT-2004-516514, by the German Federal Ministry of Economics and Technology (BMWi) under contract no 02E9995, and by RAWRA and Czech Ministry of Trade and Industry (Pokrok 1H-PK25).

References

[1] Noseck, U., Brasser, Th., Rajlich, P., Laciok, A., Hercik, M., (2004). Mobility of uranium in Tertiary argillaceous sediments - a natural analogue study. Radiochim. Acta 92, 797-803.

[2] Noseck, U., Rozanski, K., Dulinski, M., Havlova, V., Sracek, O., Brasser, Th., Hercik, M., Buckau, G., (2008). Characterisation of hydrogeology and carbon chemistry by use of natural isotopes – Ruprechtov site, Czech Republic. Appl. Geochem. (in prep.).

[3] Hauser, W. Geckeis, H., Götz, R., Noseck, U., Laciok, A. (2005). Colloid Detection in Natural Ground Water from Ruprechtov by Laser-Induced Breakdown Detection.

[4] Noseck,U., Brasser, Th., Suksi, J., Havlova, V., Hercik, M., Denecke, M.A., Förster, H.J., (2008). Identification of uranium enrichment scenarios by multi-method characterisation of immobile uranium phases. J. Phys. Chem. Earth, doi:10.1016/j.pce.2008.05.018.

[5] Cervinka, R., Havlova, V.; Noseck, U.; Brasser, Th.; Stamberg, K., (2007). Characterisation of organic matter and natural humic substances extracted from real clay environment. Annual Workshop Proceedings of the IP Project FUNMIG". Edinburgh 26.-29.November 2007.

[6] Denecke, M.A., Janssens, K., Proost, K., Rothe, J., Noseck, U., (2005). Confocal micro-XRF and micro-XAFS studies of uranium speciation in a Tertiary sediment from a waste disposal natural analogue site. Environ. Sci. Technol. 39(7), 2049-2058.

[7] Denecke, M.A., Somogyi, A., Janssens, K., Simon, R., Dardenne, K., Noseck, U., **(**2007). Microanalysis (micro-XRF, micro-XANES and micro-XRD) of a Tertiary sediment using synchrotron radiation. Microscopy Microanal. 13(3), 165-172.

[8] Ervanne, H., Suksi, J., (1996). Comparison of Ion-Exchange and Coprecipitation Methods in Determining Uranium Oxidation States in Solid Phases. Radiochemistry 38, 324-327.

[9] Havlová, V., Laciok, A.; Vopálka, D.; Andrlík, M. (2006): Geochemical Study of Uranium Mobility in Tertiary Argillaceous System at Ruprechtov Site, Czech Republic. Czechoslovak Journal of Physics, Vol. 56, Suppl. D, 1-6.

[10] Noseck, U., Brasser, Th., 2006. Radionuclide transport and retention in natural rock formations – Ruprechtov site. Gesellschaft für Anlagen- und Reaktorsicherheit, GRS-218, Köln.

[11] Buckau, G., Artinger, R., Geyer, S., Wolf, M., Fritz, P., Kim, J.I., (2000). Groundwater in-situ generation of aquatic humic and fulvic acids and the mineralization of sedimentary organic carbon. Appl. Geochem. 15, 819-832.

[12] Knöller, K., Fauville, A., Mayer, B., Strauch, G., Friese, K., Veizer, J., (2004). Sulfur cycling in an acid mining lake and its vicinity in Lusatia, Germany. Chem. Geol. 204, 303-323.

[13] Vopalka, D., Havlova, V., Andrlik, M. (2008): Characterization of U(VI) behaviour in the Ruprechtov site (CZ). Proc. of the International Conference Uranium Mining and Hydrogeology V, Freiberg, September, 14.-18. 2008.

[14] Bethke, C.M., (2006): The Geochemist's Workbench Release 6.0. Hydrogeology Program, University of Illinois.

[15] Yoshida, Y., Shibata M., (2004): Establishment of Data Base Files of Thermodynamic Data developed by OECD/NEA Part II - Thermodynamic data of Tc, U, Np, Pu and Am with auxiliary species. JNC Technical Report, JNC TN8400 2004-025.

Gesellschaft für Anlagen- und Reaktorsicherheit (GRS) mbH

Schwertnergasse 1
50667 Köln
Telefon +49 221 2068-0
Telefax +49 221 2068-888

Forschungszentrum
85748 Garching b. München
Telefon +49 89 32004-0
Telefax +49 89 32004-300

Kurfürstendamm 200
10719 Berlin
Telefon +49 30 88589-0
Telefax +49 30 88589-111

Theodor-Heuss-Straße 4
38122 Braunschweig
Telefon +49 531 8012-0
Telefax +49 531 8012-200

www.grs.de

ISBN 978-3-939355-30-4